# RECLAMATION

*Managing Water in the West*

**Technical Memorandum No. 86-68210-2018-02**

# West Salt River Valley Basin Study Climate, Hydrology, and Demand Projections

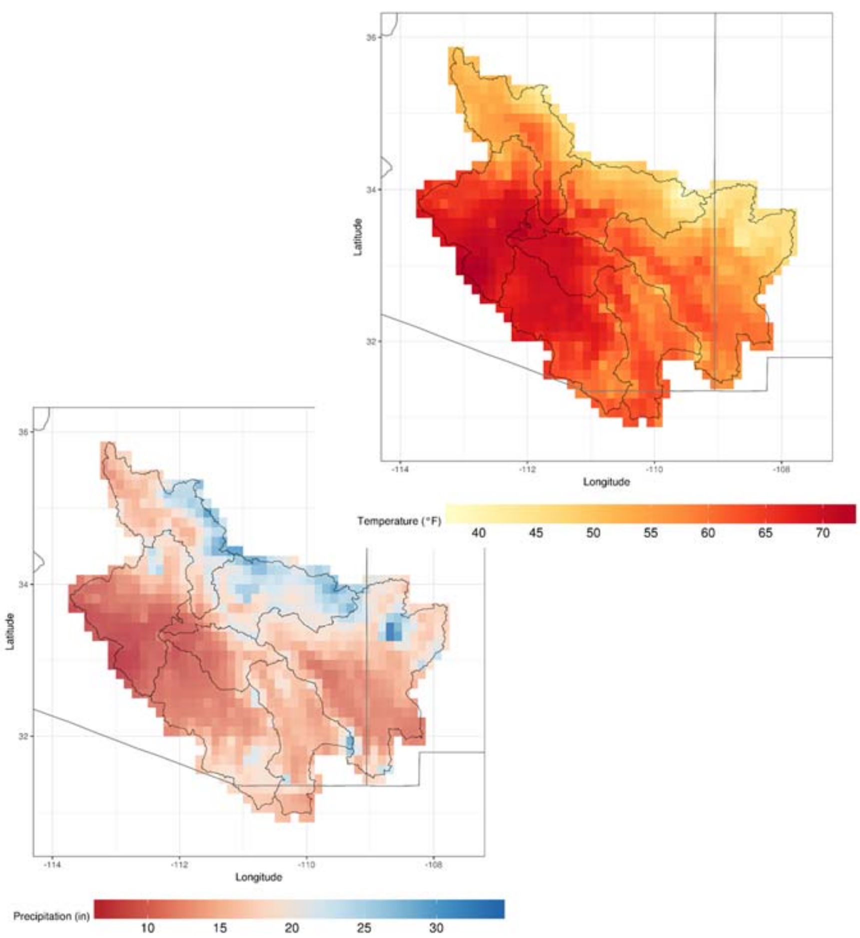


**Department of the Interior**
**Bureau of Reclamation**
**Phoenix Area Office**

**February 2018**

# Mission Statements

The U.S. Department of the Interior protects America's natural resources and heritage, honors our cultures and tribal communities, and supplies the energy to power our future.

The mission of the Bureau of Reclamation is to manage, develop, and protect water and related resources in an environmentally and economically sound manner in the interest of the American public

**BUREAU OF RECLAMATION**
**Technical Service Center, Denver, Colorado**

**Technical Memorandum No. 86-68210-2018-02**

# West Salt River Valley Basin Study
# Climate, Hydrology, and Demand Projections

**Prepared for:**
**Phoenix Area Office**
**Lower Colorado Region**

*Prepared by:*

**Water, Environmental and Ecosystems Division (86-68200)**
**Water Resources Planning and Operations Support Group (86-68210)**

**Tom Pruitt, Civil Engineer**

*Peer reviewed by:*

**Mark Spears, Hydraulic Engineer, Technical Service Center**
**Subhrendu Gangopadhyay, Supervisory Civil Engineer, Technical Service Center**

(page intentionally left blank)

# CONTENTS


Abbreviations and Acronyms ........ v
Chapter 1. Introduction ........ 1
Chapter 2. Current climate conditions ........ 5
Chapter 3. Climate Projections ........ 9
Chapter 4. Deriving Climate Change Scenarios from Climate Projections ........ 11
4.1. Baseline Scenario ........ 11
4.2. Future Climate Change Scenarios ........ 11
Chapter 5. VIC Hydrologic Model Overview ........ 19
Chapter 6. VIC Hydrologic Model Simulations ........ 23
Chapter 7. SAC-SMA Hydrologic simulations ........ 27
7.1. Hydrologic Model Description ........ 27
7.2. Development of weather inputs using the HDe technique ........ 28
7.3. Developing future potential evapotranspiration inputs for SAC-SMA ........ 29
7.4. Hydrologic modeling results ........ 30
Chapter 8. Irrigation Demands ........ 37
8.1. Background ........ 38
8.2. Demands Methodology ........ 39
8.3. Historical Baseline Demands ........ 42
8.4. Future Demands ........ 49
Chapter 9. Summary ........ 51
Chapter 10. Uncertainty ........ 53
10.1. GCMs and Climate Downscaling ........ 53
10.2. Hydrologic Modeling ........ 55
10.3. Demands ........ 56
Chapter 11. References ........ 59
Appendix A. VIC simulated streamflow graphics ........ A-1
Appendix B. Demands Summary Tables ........ B-1


## Figures


Figure Page

1. Map of the West Salt River Valley Basin Study area showing stream locations (blue). Also shown are features (Recharge Analysis Zone and Active Model Boundary) relevant to groundwater modeling for the area. ... 3
2. Map of HUC6 areas (black line) with streams contributing to the study area water supply. Stream locations (filled green circles) and the active groundwater model boundary (red line) from Figure 1 are also shown. ...... 4
3. Spatial distribution of mean annual temperature based on gridded dataset developed by Maurer et al. (2002) for 1950-1999. Grid cells are 1/8° resolution. ........ 6

4. Spatial distribution of mean annual precipitation based on gridded dataset developed by Maurer et al. (2002) for 1950-1999. Grid cells are 1/8° resolution. ........ 7
5. Global temperature change (mean and one standard deviation as shading) relative to 1986–2005 for the SRES scenarios run by CMIP3 and the RCP scenarios run by CMIP5. The number of model projections is given in parenthesis. Source: Figure 2 from Knutti et al (2012). ........ 10
6. Change in mean annual temperature (°F) versus percent change in mean annual precipitation between the 2060s and historical baseline period. Projected changes using statistically downscaled CMIP5 GCM simulations are illustrated. ........ 14
7. Change in mean annual temperature (°F) from the baseline scenario. ........ 17
8. Change in mean annual precipitation (percent) from the baseline scenario. ........ 18
9. Variable Infiltration Capacity Model schematics, including a) spatial discretization and overview, b) snow model algorithm, and c) routing model. ........ 21
10. Monthly average (top) and boxplots (bottom) of simulated streamflow in cubic feet per second (CFS) for the baseline and five HDe climate change scenario simulations for the Gila River site ........ 24
11. Monthly average (top) and boxplots (bottom) of simulated streamflow for the baseline and five HDe climate change scenario simulations for the Hassayampa River site (shown in Figure 1). ........ 25
12. SAC-SMA sub-basins (black outline) and contributing streams (blue lines) to three sites on the Agua Fria, Salt, and Verde Rivers. VIC grid cells at 1/8° resolution (red lines) within the contributing areas are also shown. ........ 31
13. Monthly average (top) and boxplots (middle) of simulated streamflow and monthly ratios (bottom) for SAC-SMA (left panel) and VIC (right panel) simulations for the baseline and five HDe climate change scenario simulations for the Agua Fria River site ........ 33
14. Monthly average (top) and boxplots (middle) of simulated streamflow and monthly ratios (bottom) for SAC-SMA (left panel) and VIC (right panel) simulations for the baseline and five HDe climate change scenario simulations for the Salt River site (shown in Figure 12). ........ 34
15. Monthly average (top) and boxplots (middle) of simulated streamflow and monthly ratios (bottom) for SAC-SMA (left panel) and VIC (right panel) simulations for the baseline and five HDe climate change scenario simulations for the Verde River site (shown in Figure 12). ........ 35
16. HUC8 sub-basins for which agricultural irrigation demand under climate change scenarios results are presented. Note that two HUC8 sub-basins are truncated at the US-Mexico border in this and subsequent maps—consistent with results presented in Reclamation, 2015. ........ 38
17. Reference evapotranspiration equation parameters schematic. ........ 40
18. Dual crop coefficient evapotranspiration concept schematic. ........ 41
19. Spatial distribution of baseline temperature and projected temperature change for different climate scenarios for the 2040-2069 period. The cross-hatched pattern indicates no results available as no crops are likely grown on these HUC-8s. ........ 44

20. Spatial distribution of baseline precipitation and projected precipitation percent change for different climate scenarios for the 2050s (2040-2069 period). .......... 45
21. Spatial distribution of baseline reference evapotranspiration and projected evapotranspiration percent change for different climate scenarios for the 2050s (2040-2069 period). .......... 46
22. Spatial distribution of baseline crop evapotranspiration and projected evapotranspiration percent change for different climate scenarios for the 2050s (2040-2069 period). .......... 47
23. Spatial distribution of baseline net irrigation water requirements (NIWR) and projected NIWR percent change for different climate scenarios for the 2050s (2040-2069 period). .......... 48
A1. Monthly averages of streamflow for the baseline and five HDe climate change scenario simulations for the Agua Fria River site shown in Figure 1. .......... A-3
A2. Monthly averages of streamflow for the baseline and five HDe climate change scenario simulations for the Cave Creek site shown in Figure 1. A-4
A3. Monthly averages of streamflow for the baseline and five HDe climate change scenario simulations for the Centennial Wash site shown in Figure 1. .......... A-5
A4. Monthly averages of streamflow for the baseline and five HDe climate change scenario simulations for the Jackrabbit Wash site shown in Figure 1. .......... A-6
A5. Monthly averages of streamflow for the baseline and five HDe climate change scenario simulations for the New River site shown in Figure 1. . A-7
A6. Monthly averages of streamflow for the baseline and five HDe climate change scenario simulations for the Queen Creek site shown in Figure 1. .......... A-8
A7. Monthly averages of streamflow for the baseline and five HDe climate change scenario simulations for the Salt River site shown in Figure 1.... A-9
A8. Monthly averages of streamflow for the baseline and five HDe climate change scenario simulations for the Santa Cruz Wash site shown in Figure 1. .......... A-10
A9. Monthly averages of streamflow for the baseline and five HDe climate change scenario simulations for the Skunk Creek site shown in Figure 1. .......... A-11
A10. Monthly averages of streamflow for the baseline and five HDe climate change scenario simulations for the Star Wash site shown in Figure 1. .......... A-12
A11. Monthly averages of streamflow for the baseline and five HDe climate change scenario simulations for the Trilby Wash site shown in Figure 1. .......... A-13
A12. Monthly averages of streamflow for the baseline and five HDe climate change scenario simulations for the Vekol Wash site shown in Figure 1. .......... A-14
A13. Monthly averages of streamflow for the baseline and five HDe climate change scenario simulations for the Waterman Wash site shown in Figure 1. .......... A-15

A14. Monthly averages of streamflow for the baseline and five HDe climate change scenario simulations for the Weekes Wash site shown in Figure 1 .......... A-16

## Tables

Table Page

1. Projected change in mean annual basin wide temperature and precipitation for the climate change scenarios based on CMIP5 BCSD projections; historical period, 1950-1999; future period, 2060s (30-year range, 2045-2074). .......... 15
2. Stream locations shown on the map in Figure 2. .......... 23
3. Stream locations shown on the map in Figure 2. .......... 30

B-1. Summary of HUC8 Sub-basin Average Annual Historical Baseline and Projected Future Temperatures and Projected Future Average Annual Change in Temperature .......... B-3
B-2. Summary of HUC8 Sub-basin Average Annual Historical Baseline and Projected Future Precipitation, Projected Future Average Annual Change in Precipitation and Percent Change in Precipitation .......... B-4
B-3. Summary of HUC8 Sub-basin Average Annual Historical Baseline and Projected Future Reference Evapotranspiration (ET), Projected Future Average Annual Change in Reference ET and Percent Change in Reference ET .......... B-5
B-4. Summary of HUC8 Sub-basin Average Annual Historical Baseline and Projected Future Crop Evapotranspiration (ET), Projected Future Average Annual Change in Crop ET and Percent Change in Crop ET .......... B-6
B-5. Summary of HUC8 Sub-basin Average Annual Historical Baseline and Projected Future Net Irrigation Water Requirement (NIWR) Depth, Projected Future Average Annual Change in NIWR Depth and Percent Change in NIWR Depth .......... B-7

# ABBREVIATIONS AND ACRONYMS

| | |
|---|---|
| A1 | CMIP3 Future Greenhouse Gas Middle Emissions Scenario Family |
| A1B | CMIP3 Future Greenhouse Gas Middle Emissions Scenario |
| A2 | CMIP3 Future Greenhouse Gas High Emissions Scenario |
| ASCE | American Society of Civil Engineers |
| B1 | CMIP3 Future Greenhouse Gas Low Emissions Scenario |
| B2 | CMIP3 Future Greenhouse Gas Low Emissions Scenario |
| BCSD | Bias Corrected and Spatially Downscaled |
| CFS | cubic feet per second |
| CMIP | Coupled Model Intercomparison Project |
| CMIP3 | Coupled Model Intercomparison Project Phase 3 |
| CMIP5 | Coupled Model Intercomparison Project Phase 5 |
| CT | Central Tendency |
| DRI | Desert Research Institute |
| ET | Evapotranspiration |
| $ET_c$ | Crop Evapotranspiration |
| $ET_o$ | Reference Evapotranspiration |
| F | Fahrenheit |
| FAO | Food and Agricultural Organization of the United Nations |
| GCM | General Circulation or Global Climate Model |
| GDD | Growing Degree Days |
| HD | Hot Dry |
| HDe | Ensemble-informed Hybrid Delta |
| HUC | Hydrologic Unit Code |
| HUC6 | Six-digit Hydrologic Unit Code Drainage Area |
| HUC8 | Eight-digit Hydrologic Unit Code Drainage Area |
| HW | Hot Wet |
| IPCC | Intergovernmental Panel on Climate Change |
| $K_{cb}$ | Basal Crop Coefficient |
| $K_e$ | Soil Evaporation Coefficient |
| $K_s$ | Stress Coefficient |
| M&I | Municipal and Industrial |
| NIWR | Net Irrigation Water Requirement |
| NRCS | Natural Resources Conservation Service |
| OCS | Oklahoma Climatological Survey |
| OCWP | Oklahoma Comprehensive Water Plan |
| OWRB | Oklahoma Water Resources Board |
| P | Precipitation |
| $P_e$ | Effective Precipitation |

| | |
|---|---|
| PM | Penman Monteith |
| RCP | Representative Concentration Pathways |
| Reclamation | Bureau of Reclamation |
| SAC-SMA | Sacramento-Soil Moisture Accounting |
| SRES | Special Report on Emissions Scenarios |
| STATSGO | NRCS State Soil Geographic Database |
| SYMAP | Synergraphic mapping system |
| T | Temperature |
| Tmax | Maximum Daily Temperature |
| Tmin | Minimum Daily Temperature |
| USDA | U.S. Department of Agriculture |
| USDA-SCS | Soil Conservation Service |
| WD | Warm Dry |
| WW | Warm Wet |
| WWCRA | West-wide Climate Risk Assessments |

# CHAPTER 1. INTRODUCTION

Climate change scenarios for the West Salt River Valley Basin Study (WSRVBS) are based global climate model (GCM) projections available from the World Climate Research Programme's Coupled Model Intercomparison Project (CMIP). The hydrologic analyses were developed based on the CMIP Phase 5 (CMIP5) projections and the CMIP Phase 3 (CMIP3) projections were used for the demands analysis. The CMIP5 climate projections were chosen for hydrology projections in this study because they represent improvements since the CMIP3 effort and over time have become a widely accepted and used climate resource. The CMIP3 projections are used for demand projections, since we are summarizing work from a previous study.

The climate change scenarios for both the hydrologic and demands analyses were developed using the ensemble informed hybrid delta (HDe) method described in Hamlet et al. (2013). For this study, the future period, referred to as the 2060s, is defined by the 30-year range 2045-2074 for the hydrologic analysis and 2040-2069 for the demands analysis. The current period of record used is the 50-year period 1950-1999. The choice of these periods only reflects a representative future planning period and the apparent inconsistency in the definitions of supply and demand periods arises from previous studies relevant to the WSRVBS, specifically the Colorado River Basin Study (Reclamation, 2012), and the Agricultural Water Demands Study (Reclamation, 2015) were leveraged for the WSRVBS. This choice of the 2060s as the future period was identified by the study partners as the planning horizon of interest.

Using the weather data developed for each of the HDe based climate change scenarios, projections of hydrologic fluxes including runoff were estimated using the gridded macro-scale hydrology model VIC (Variable Infiltration Capacity; Liang et al., 1994). Routed streamflow projections for 16 streamflow locations were subsequently developed from the gridded VIC runoff using the routing scheme described in Lohmann et al. (1996). Figure 1 shows the study area and surface water supply sources that are being investigated as part of the WSRVBS.

The region defined by the six-digit Hydrologic Unit Codes (HUC6) with streams contributing to the study area water supply is shown in Figure 2. This includes the Salt, Verde, Agua Fria, Hassayampa, and Gila Rivers as well as other smaller intermittent streams. Reference to the "study area" in this report includes this HUC6 region, since the water supply is dependent upon these streams.

Additional simulations of climate change scenarios for three streamflow sites on the Salt, Verde, and Agua Fria Rivers were also made using a second hydrology model, the Sacramento Soil Moisture Accounting model (SAC-SMA) and results were compared with those from the VIC simulations.

Estimated agricultural irrigation demands under climate projections-based change scenarios for the study area are summarized from a previous study (Reclamation, 2015) that includes estimated changes in crop irrigation demand in eight major river basins across the Western United States. The Reclamation (2015) demands analysis was performed at the 8-digit Hydrologic Unit Codes (HUC8) level. In this study, the hydrologic analysis was done at the HUC6 level and the results are presented and discussed for each HUC6 sub-basin within the WSRVBS study area.

This Technical Memorandum presents the climate, hydrology and demand projections developed for the WSRVBS. Chapter 2 discusses current climate conditions; Chapter 3 describes future climate projections for the 2060s; Chapter 4 describes the development of climate change scenarios; and Chapters 5 and 6 describe the VIC model and simulation results of future hydrology in the study area. A brief description and discussion of simulation results using the SAC-SMA are presented in Chapter 7. The results of irrigation demand projections are discussed in Chapter 8. A brief overall summary of the results is provided in Chapter 9. Chapter 10 discusses uncertainty involved in using and interpreting future climate, hydrology and demand projections.

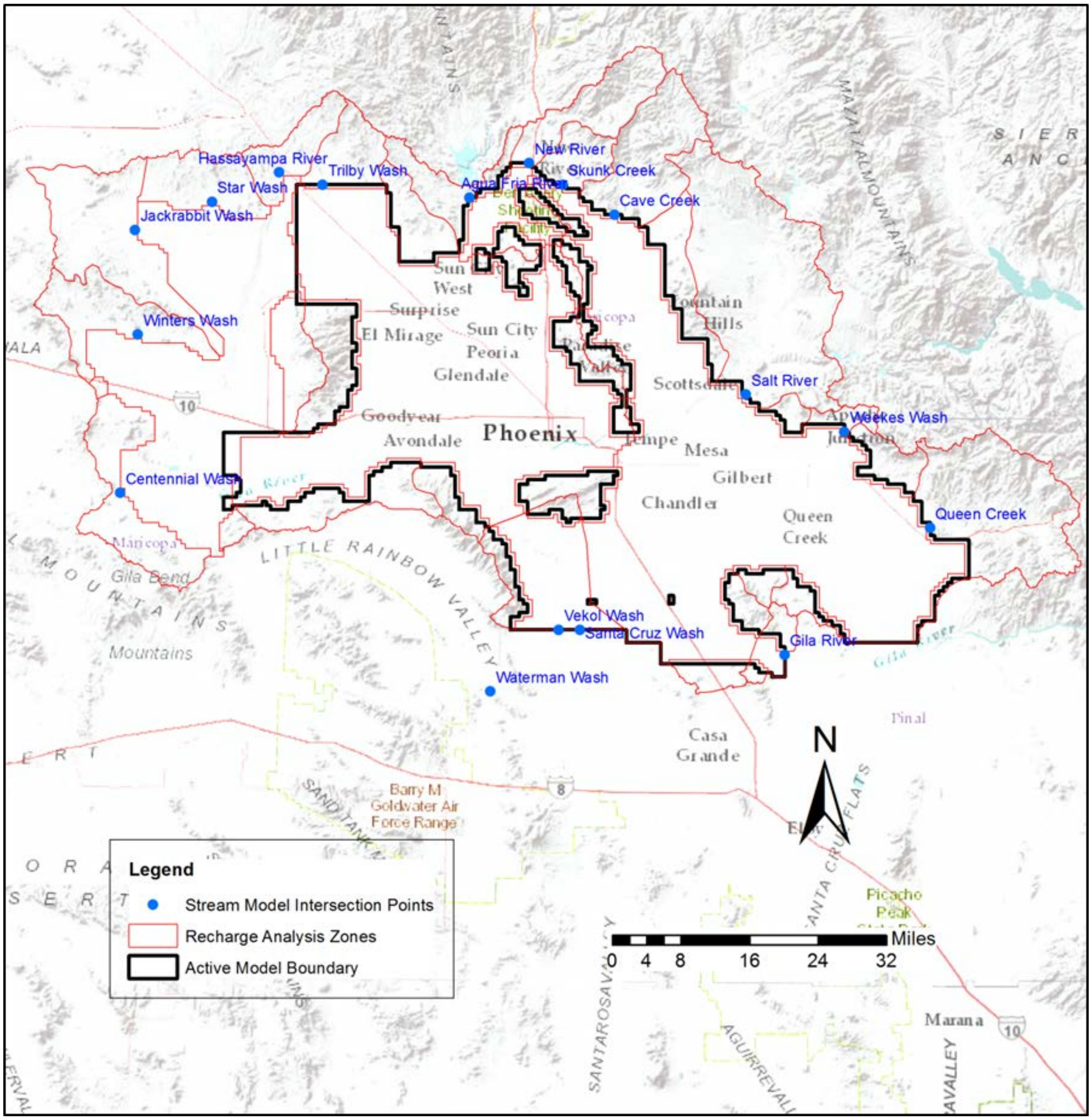


**Figure 1.—Map of the West Salt River Valley Basin Study area showing stream locations (blue). Also shown are features (Recharge Analysis Zone and Active Model Boundary) relevant to groundwater modeling for the area.**

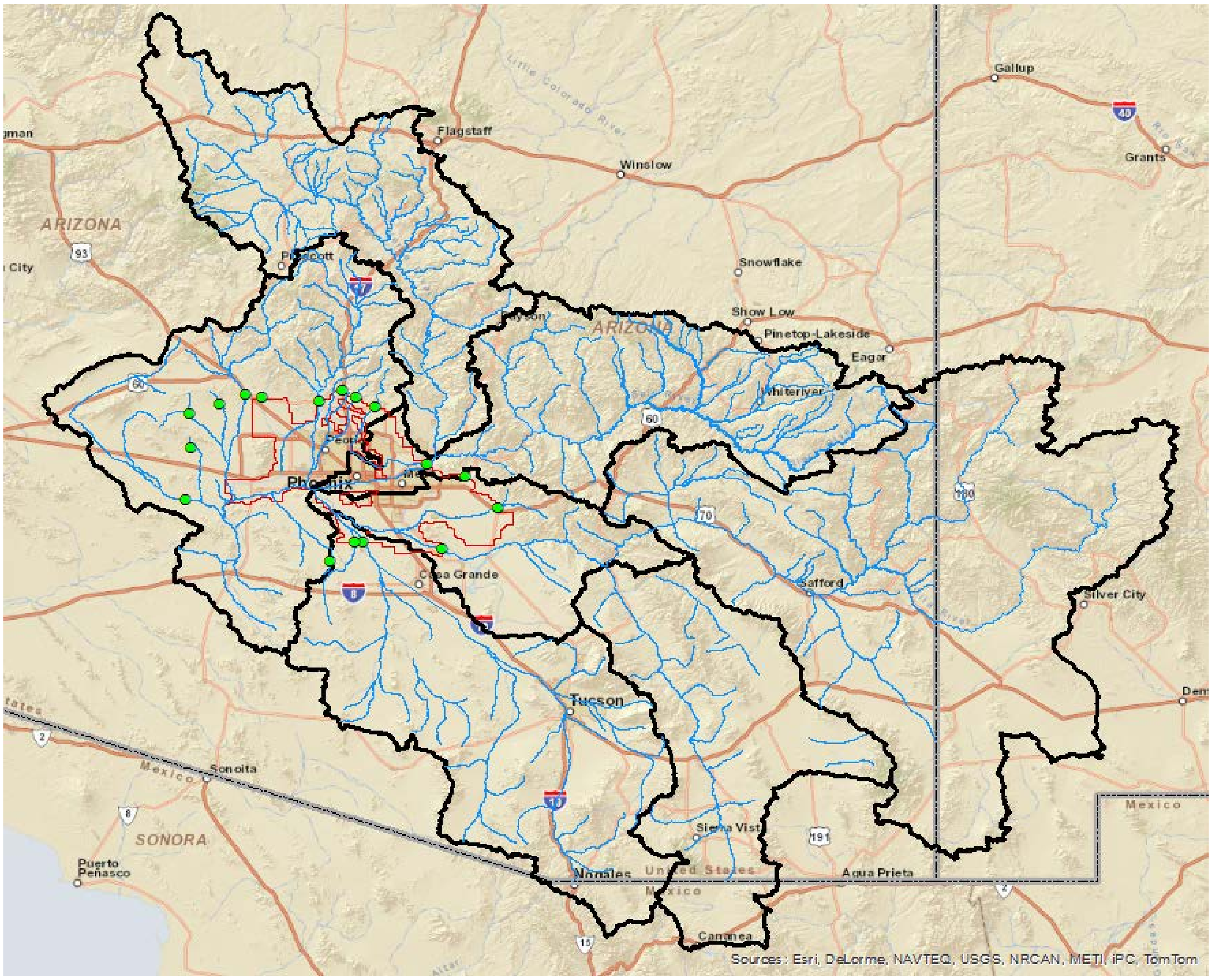


**Figure 2.—Map of HUC6 areas (black line) with streams contributing to the study area water supply. Stream locations (filled green circles) and the active groundwater model boundary (red line) from Figure 1 are also shown.**

# CHAPTER 2. CURRENT CLIMATE CONDITIONS

Current climate conditions over the region (Figures 3 and 4) contributing to the study area water supply were characterized based on the gridded daily precipitation and temperature dataset developed by Maurer et al. (2002). This dataset utilizes daily precipitation and temperature data from the National Weather Service (NWS) Cooperative Observer (Co-Op) network. The station data are processed to remove spatial and temporal inconsistencies and then interpolated to a 1/8° grid (1/8° latitude by 1/8° longitude) covering the continental United States.

The gridded daily precipitation and temperature datasets developed by Maurer et al. (2002) were previously verified by comparison to available station records, other gridded datasets, and by evaluation of hydrologic model simulations with these datasets used as meteorological inputs (Maurer et al. 2002). Results suggest that while the values at a given grid cell typically do not exactly match station records from gauges located within the cell; they do capture the daily, seasonal, and inter-annual variability of station records. In addition, the gridded datasets provide complete and consistent representation of climate conditions that is appropriate for analysis of spatial and temporal variability in climate conditions over large areas.

Figure 3 and 4 show the respective 1950-1999 mean annual temperature and precipitation values for each 1/8° cell in the study area. As illustrated in Figure 3 and 4, climate conditions in the region exhibit warmer and dryer conditions in the southwestern desert portion, with cooler and wetter conditions in the northern and eastern higher elevation portions of the study area. Current mean annual temperature and precipitation values range respectively from 73.0 °F and 6.5 inches in the western desert portion of the region to 37.2 °F and 34.2 inches in the eastern and higher elevation portions of the region. The respective region-wide temperature and precipitation current annual averages are 59.3 °F and 15.9 inches.

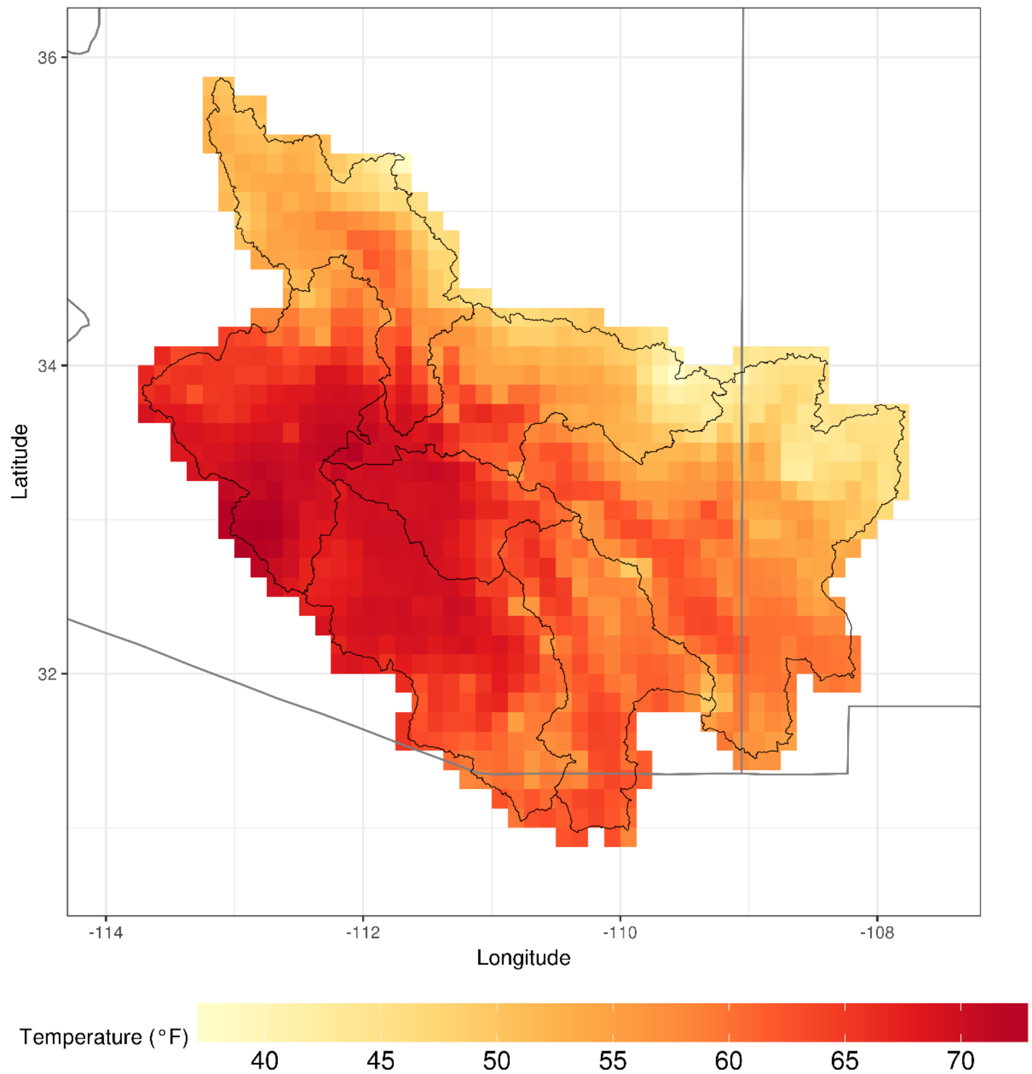


**Figure 3.—Spatial distribution of mean annual temperature based on gridded dataset developed by Maurer et al. (2002) for 1950-1999. Grid cells are 1/8° resolution.**

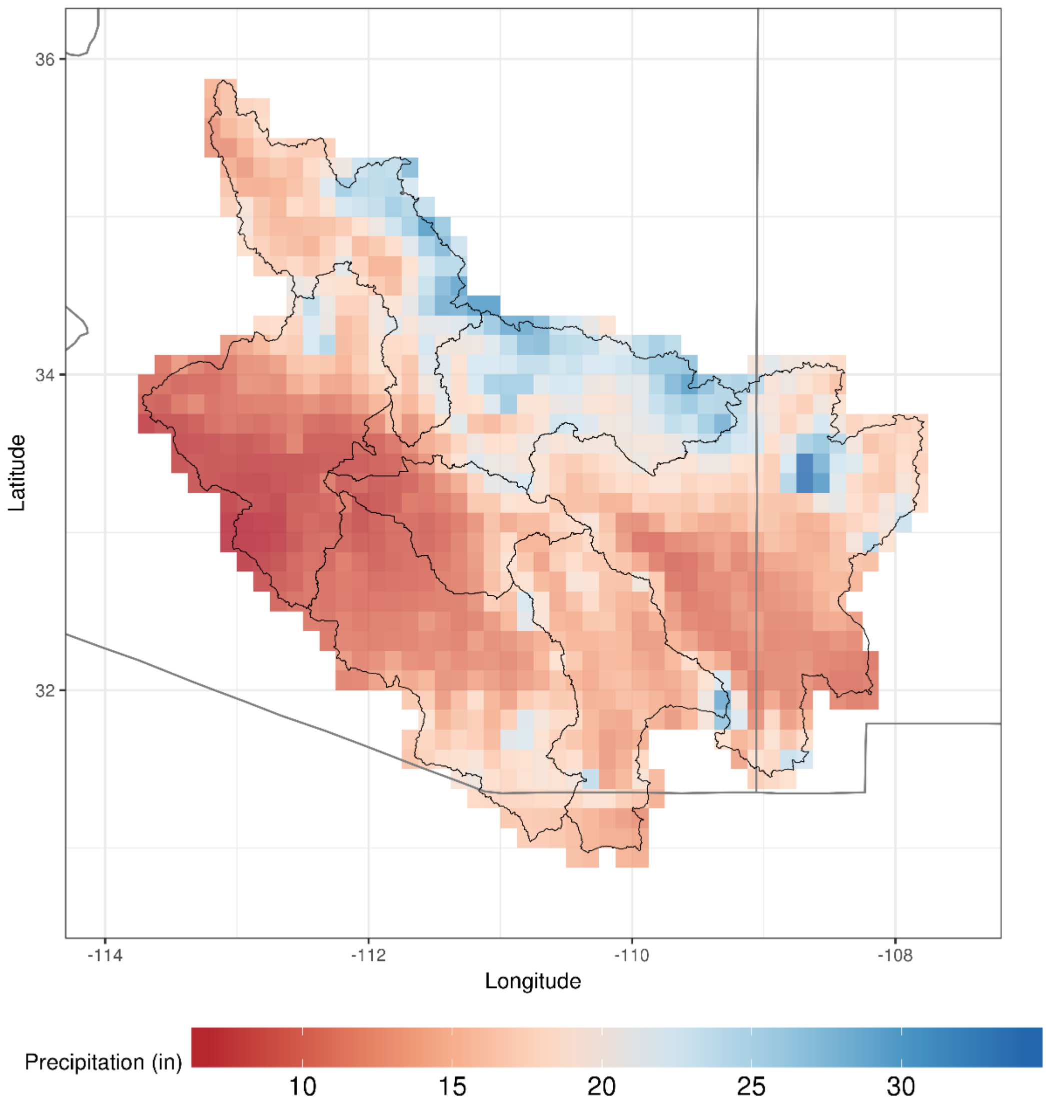


**Figure 4.—Spatial distribution of mean annual precipitation based on gridded dataset developed by Maurer et al. (2002) for 1950-1999. Grid cells are 1/8° resolution.**

(page intentionally left blank)

# CHAPTER 3. CLIMATE PROJECTIONS

Climate projections for the WSRVBS were obtained from an archive of climate and hydrology projections developed by Reclamation in partnership with the U.S. Geological Survey, U.S. Army Corps of Engineers, Lawrence Livermore National Laboratory, Santa Clara University, Climate Central, and Scripps Institution of Oceanography. These projections and associated documentation are available through this downscaled climate and hydrology projections website:http://gdo-dcp.ucllnl.org/downscaled_cmip_projections/dcpInterface.html. The climate projections were statistically downscaled in space from global climate model (GCM) grid resolution to 1/8° latitude by 1/8° longitude. This archive of climate projections is based on GCM simulations compiled by the World Climate Research Programme's Coupled Model Intercomparison Project (CMIP).

Among the available climate and hydrology projections available on the above mentioned website, there are monthly bias-corrected and spatially-disaggregated (BCSD) projections of precipitation and temperature, which are utilized in the WSRVBS. Bias correction generally involves correcting systematic errors in GCM historical simulations based on finer scale observed data. Spatial disaggregation generally involves translating coarse scale GCM simulations to the 1/8° spatial resolution. Projections based on CMIP5 were used in the analysis of future water supply impacts in the West Salt River Valley and are further described below. Both the CMIP Phase 3 (CMIP3) and theCMIP5 projections are briefly discussed below for completeness, and it should be noted that hydrology projections are based on CMIP5 projections and demand projections are based on CMIP3 projections in this study.

CMIP3 projections (Meehl et al., 2007) are summarized in the Fourth Assessment Report by the Intergovernmental Panel on Climate Change (IPCC), completed in 2007 (IPCC, 2007). Generally, climate projections are based on an assemblage of GCM simulations of coupled atmospheric and ocean conditions, with a variety of initial conditions of global ocean – atmosphere system and distinct "storylines" about how future demographics, technology and socioeconomic conditions might affect the emissions of greenhouse gases. There are four families of emissions scenarios (A1, A2, B1 and B2 - described in the IPCC Special Report on Emissions Scenarios [SRES] (IPCC, 2000), in which the scenarios are potential futures based on assumptions of global economic activity and growth. Additionally, there are three subsets to the A1 family (A1F1, A1B, and A1T) based on their technology emphasis with regard to future energy sources with A1B having a balanced emphasis on all energy sources. Projected global warming associated with CMIP3 SRES scenarios available in a downscaled form is shown in the left panel of Figure 5.

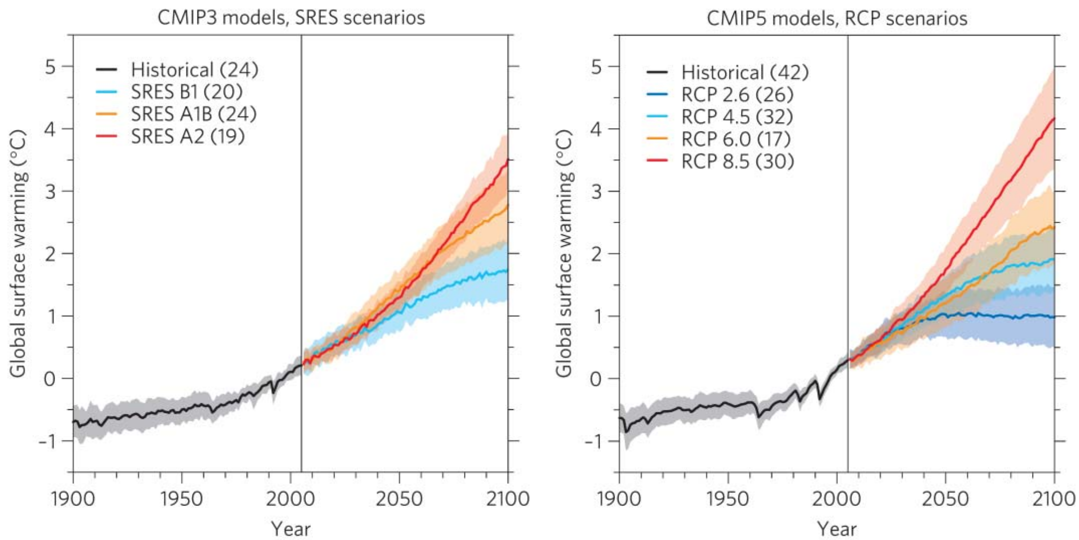


**Figure 5.—Global temperature change (mean and one standard deviation as shading) relative to 1986–2005 for the SRES scenarios run by CMIP3 and the RCP scenarios run by CMIP5. The number of model projections is given in parenthesis. Source: Figure 2 from Knutti et al (2012).**

CMIP5 projections are similar in concept but incorporate improvements in modeling and physical understanding of the Earth system since the CMIP3 effort. The raw CMIP5 model output has been available since early 2011 and has been increasingly used in climate change impacts studies, alongside those from CMIP3. The corresponding IPCC Fifth Assessment Report was completed in 2013. These GCMs rely on greenhouse gas storylines called Representative Concentration Pathways (RCP). Each RCP is representative of a particular amount of radiative forcing (2.6, 4.5, 6.0, and 8.5 Watts per square meter [$W/m^2$] respectively) occurring by the year 2100. The right panel of Figure 5 illustrates projected global warming according to the CMIP5 RCP scenarios. The figure shows that the range of emissions scenarios considered by CMIP5 result in a greater range of projected global warming than by CMIP3 emissions scenarios. The website identified above contains 112 BCSD CMIP3 monthly projections and 231 BCSD CMIP5 monthly projections of precipitation and temperature, among other available hydroclimate data products. Projections based on the four CMIP5 emissions scenarios are available via the website mentioned above and are used as a basis for WSRVBS climate scenarios.

As mentioned previously, the CMIP5 climate projections were chosen for developing the hydrology projections in this study because they represent improvements since the CMIP3 effort and over time have become a widely accepted and used climate resource. The CMIP3 projections are used for demand projections, since we are summarizing work from a previous study (Reclamation, 2015).

# Chapter 4. Deriving Climate Change Scenarios from Climate Projections

To meet the needs of the WSRVBS, five future climate scenarios were developed that would be subsequently used as inputs in impact assessment and reservoir system models to evaluate reliability of water supply for the Basin. First, a baseline climate scenario was developed to represent current climate and hydrologic conditions in the Basin. Five future climate scenarios were then developed to represent the range of projected future climate conditions. For the baseline scenario, climate inputs consist of gridded historical observations of precipitation and temperature for the period 1950-1999. For each future climate scenario, climate-related inputs were developed by perturbing baseline inputs to reflect the projected change in each input variable between the periods 1950-1999 and 2045-2074 corresponding to each of the five selected future scenarios. These future climate scenarios are derived using an ensemble informed hybrid delta (HDe) method (Hamlet et al., 2013; Reclamation, 2010), described in detail below in the future climate change scenarios section.

The following section describes the baseline scenario and development of future climate scenarios for the hydrology analysis using the CMIP5 and the observation-based gridded historical Maurer et al. (2002) datasets. The Reclamation (2015) demands analysis was conducted using the same methods but with the CMIP3 rather than CMIP5 datasets.

## 4.1. Baseline Scenario

The climate baseline scenario is represented by the observation-based gridded historical dataset (Maurer et al., 2002) of precipitation and temperature data for the period 1950-1999. The hydrology and demands baseline scenarios are subsequently developed from this climate data. As conceptualized in this study, the baseline scenario is intended to reflect current climate, hydrologic and demand conditions in the Basin.

## 4.2. Future Climate Change Scenarios

As discussed above, the WSRVBS utilizes climate change scenarios derived using an ensemble informed hybrid delta (HDe) method based on statistically downscaled CMIP5 GCM projections. This method is described in detail below.

The HDe method for developing climate change scenarios involves perturbing baseline historical climate (precipitation and temperature) by change factors computed as the change in precipitation and temperature by month between a chosen future planning horizon and a historical period (Reclamation, 2010). The WSRVBS utilizes an ensemble of statistically downscaled climate projections based on CMIP5 GCMs to estimate percentile specific monthly change factors for both precipitation and temperature.

The HDe method involves defining a climate change scenario based on pooled information from a collection of climate projections. Use of a sufficiently large number of projections pooled together (i.e. projection ensemble), modulates by smoothing (averaging) internal climate variability inherent in each single projection which may be misinterpreted as climate change signal.

The development of HDe climate change scenarios entails two primary steps. These steps include:

1. identifying the climate projections that will inform each of the HDe climate change scenarios, and
2. generation of HDe climate change scenarios using statistical mapping of future projections onto baseline historical gridded observed data.

The first step in the development of HDe climate change scenarios involves identifying the climate projections that will inform each of the scenarios to be considered in the study. Review of climate projections over the WSRVBS region (Figure 2) suggests a warmer future (no projections suggest occurrence of cooling) with a range of drier to wetter conditions, compared to history (1950-1999). As such, ensembles of climate projections that bracket the range of potential futures, from less warm to warmer and drier to wetter conditions, fall into five climate change scenarios. The five HDe scenarios as defined for this study are hot-dry (HD), hot-wet (HW), central tendency (CT), warm-dry (WD) and warm-wet (WW).

For each climate change scenario, change in mean annual temperature (°F) and precipitation (percent) is calculated between the baseline period, 1950-1999, and the future time horizon (2060s defined by the 30-year range 2045-2074) for each 1/8° grid cell within the study area (see Figure 3 and 4). The WSRVBS considers only one future time horizon, the 2060s (2045-2074). Change in mean annual temperature (°F) versus percent change in mean annual precipitation between the 2060s and reference historical period for the 231 CMIP5 projections is used to develop climate change scenarios as discussed below and is shown in Figure 6. Note that there are 231 points representing the total number of available individual GCM projections from the monthly BCSD-CMIP5 archive.

In Figure 6, the dotted black lines represent the median ($50^{th}$ percentile) change values while the solid red lines represent the $10^{th}$ and $90^{th}$ percentile change values. Climate change scenarios are developed by selecting the 10 individual climate projections that fall closest to the intersections of the 10th, 50th, and 90th percentiles of change.[1] The selected projections corresponding to each of the five climate change scenarios are shown in the figure using a range of colors and symbols–(HW=orange, HD=green, WD=blue, WW=purple, CT=yellow). Using only a limited number of climate projections (specifically, 10) to inform a given climate change scenario enables each of the climate change scenarios to be distinct and representative of the defined future conditions (e.g., WW, WD, etc).

Once the climate projections for each of the climate change scenarios have been identified, the second component of the development of HDe scenarios involves generating perturbed historical time series informed by the 10 projections pooled together for each climate change scenario.

[1] The distance between plotted precipitation and temperature change and the 10th, 50th, and 90th percentile change values was computed using the Mahalanobis distance.

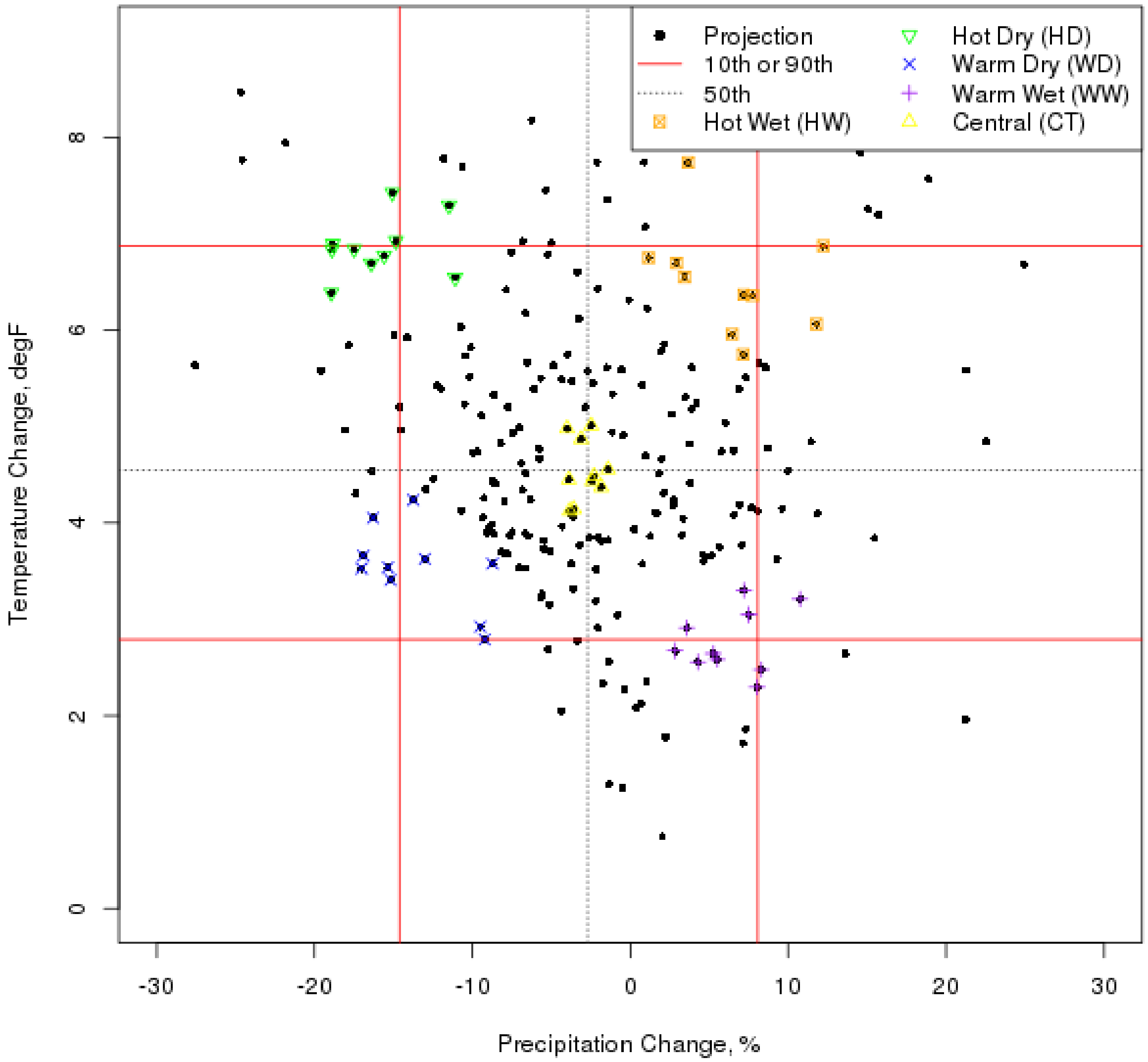


**Figure 6.—Change in mean annual temperature (°F) versus percent change in mean annual precipitation between the 2060s and historical baseline period. Projected changes using statistically downscaled CMIP5 GCM simulations are illustrated.**

Observed baseline gridded monthly precipitation and temperature (Maurer et al., 2002) are mapped, using a quantile mapping technique onto the bias corrected GCM data to produce a set of transformed observations reflecting the future conditions. The entire observed time series of temperature and precipitation at each 1/8° grid cell for the Basin is perturbed in this manner, resulting in a new time series that now has the statistics of the bias corrected GCM data for temperature and precipitation.

Climate change scenarios derived using HDe have several distinguishing features, which have their associated strengths and weaknesses. One weakness of this approach is that, the analysis of climate change impacts is limited to the future time horizons chosen when developing precipitation and temperature change factors. Another weakness is that the scenarios do not explicitly incorporate projected changes in drought variability or sequencing of storm events. The HDe method thus only considers the magnitude changes and no change in sequence from historical events. This however, is one of the key strengths of the HDe approach since the time sequence of projected future storm events matches historical events, facilitating direct comparison between the historical data and future climate scenarios.

Table 1 summarizes projected precipitation and temperature changes using the HDe approach for 2060s. The table includes CMIP5 based projections for the five climate change scenarios described above.

Table 1.—Projected change in mean annual basin wide temperature and precipitation for the climate change scenarios based on CMIP5 BCSD projections; historical period, 1950-1999; future period, 2060s (30-year range, 2045-2074).

| Historical, 1950-1999 | Basin Mean | |
|---|---|---|
| | **Temperature (°F)** | **Precipitation (in)** |
| Baseline | 59.3 | 15.9 |
| **Climate Change Scenarios, 2060s (2045-2074)** | **Projected Change in Basin Mean** | |
| | **Temperature (°F)** | **Precipitation (%)** |
| Hot Dry (HD) | + 6.9 | - 12.9 |
| Hot Wet (HW) | + 6.6 | + 10.0 |
| Central Tendency (CT) | + 4.6 | - 0.6 |
| Warm Dry (WD) | + 3.6 | - 10.2 |
| Warm Wet (WW) | + 2.8 | + 8.8 |

The spatial distributions of the change from the baseline for the five scenarios are shown in Figure 7 and 8 for mean annual temperature and mean annual precipitation, respectively.

(page intentionally left blank)

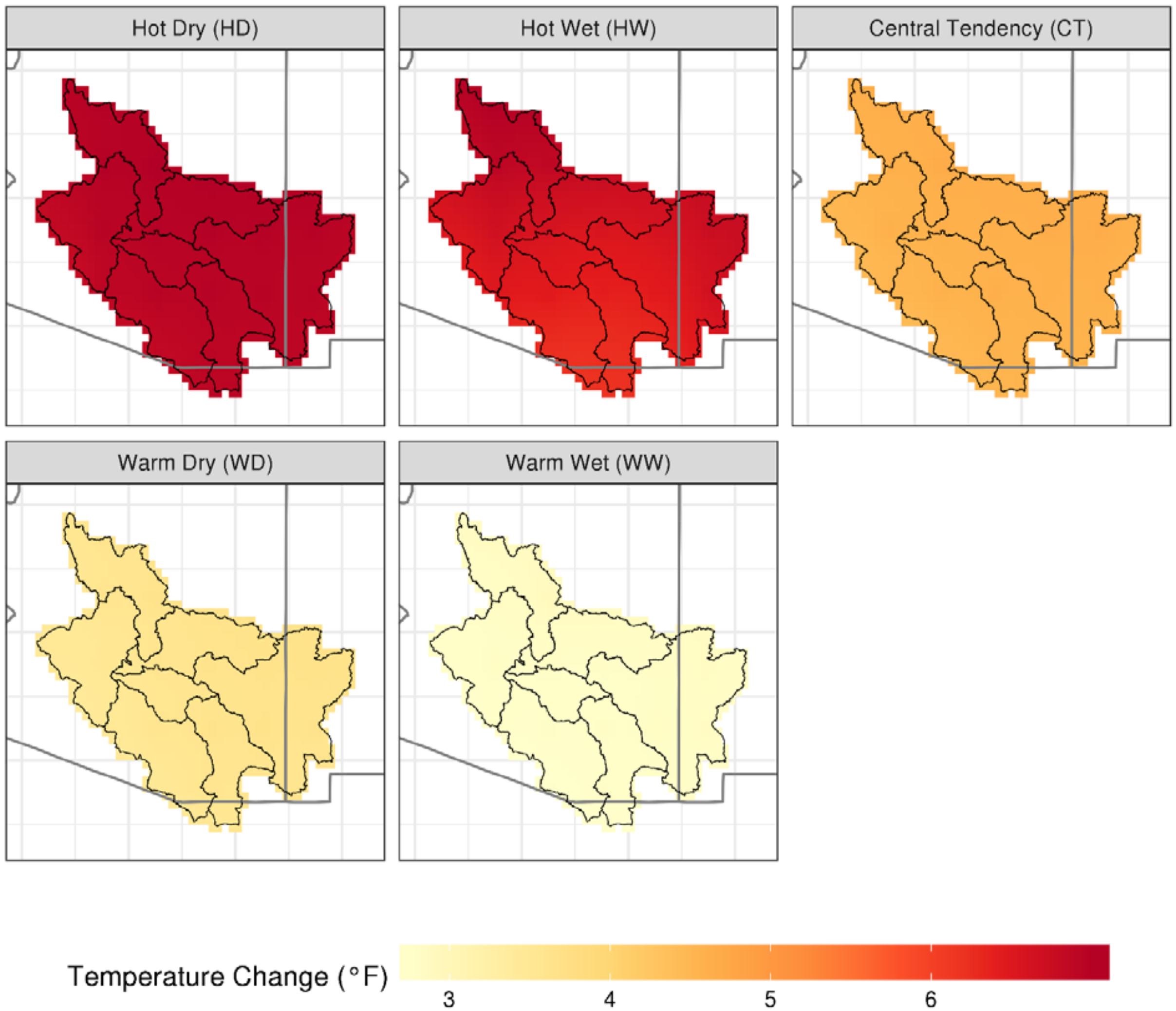


**Figure 7.—Change in mean annual temperature (°F) from the baseline scenario.**

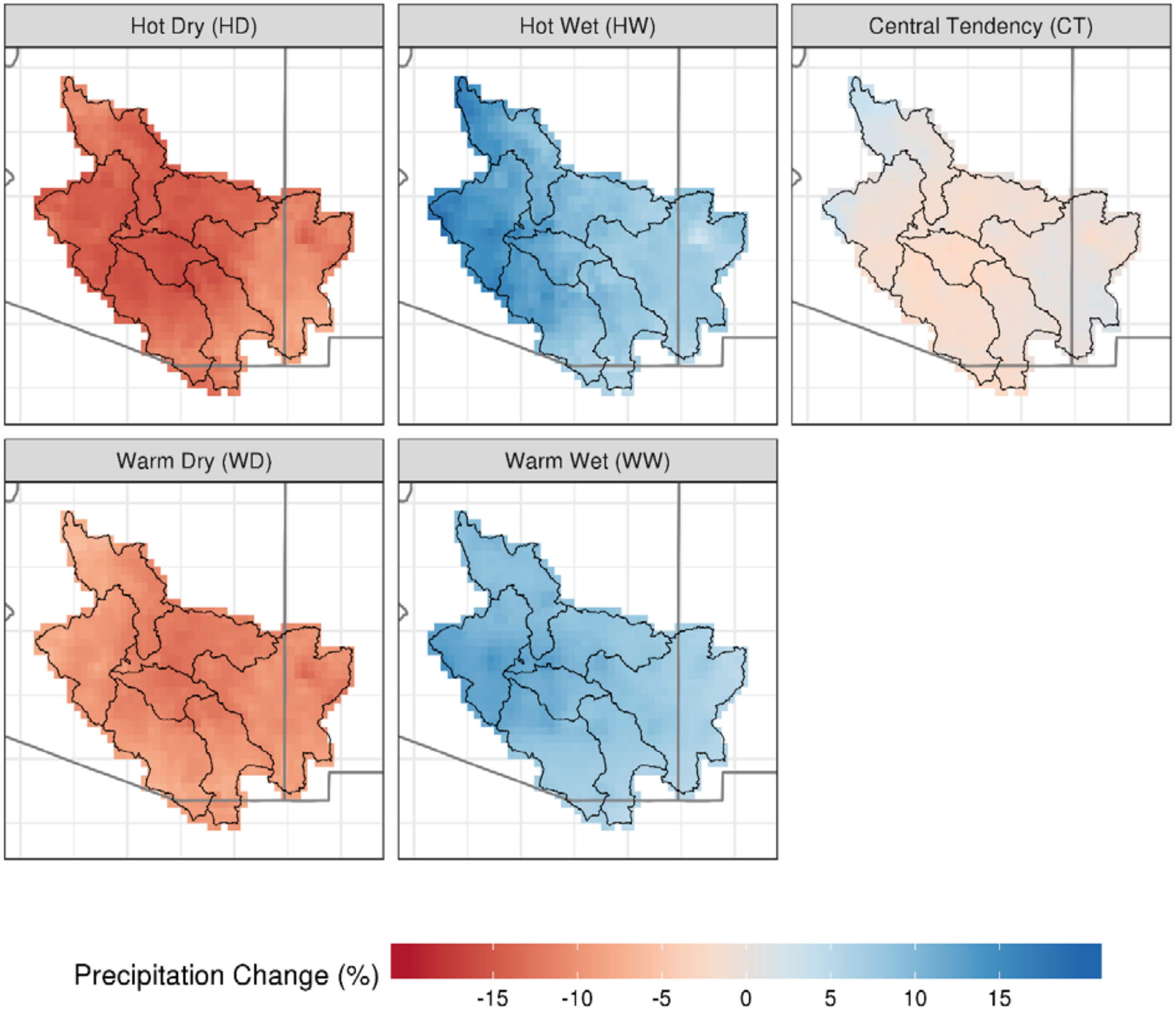


**Figure 8.—Change in mean annual precipitation (percent) from the baseline scenario.**

# CHAPTER 5. VIC HYDROLOGIC MODEL OVERVIEW

The VIC model has been widely used to evaluate hydrologic response to climate variability and change, including several analyses of large-scale watersheds in the western U.S. (e.g., Reclamation, 2011; Reclamation, 2016). The VIC model was selected for this basin study based on several criteria including consideration of the physical hydrologic processes represented by the model, availability of model inputs and parameter values over the basin study area, and consistency with previous and ongoing analyses of climate change impacts by Reclamation.

The VIC surface water hydrologic model provides estimates of historical and projected water balance variables. The VIC model (Liang et al., 1994; Liang et al., 1996; Nijssen et al., 1997) is a grid-based hydrologic model that solves the water balance at a spatial scale of 1/8° latitude/longitude (approximately 12 kilometers on a side). An overview schematic of the VIC model is given in Figure 9.

The VIC model contains a subgrid-scale parameterization of the infiltration process, which impacts the vertical distribution of soil moisture in, typically, a three-layer model grid cell (Liang et al., 1994). The VIC model also represents subgrid-scale vegetation variability using multiple vegetation types and properties per grid cell. Potential evapotranspiration is calculated using a Penman Monteith approach (e.g., Maidment (ed.), 1993). VIC also contains a subdaily (1-hour time step) snow energy balance model, illustrated by Figure 9b. (Cherkauer and Lettenmaier, 2003; Wigmosta et al., 1994; Andreadis et al., 2009).

The minimum VIC model input requirements include - gridded daily precipitation, maximum and minimum temperatures, and wind speed magnitude to simulate gridded daily state variables such as snow water equivalent and runoff (both surface and subsurface runoff). The WSRVBS utilizes baseline gridded observations developed by Maurer et al. (2002) for the period January 1950 to December 1999. The dataset is primarily based on observation stations that are part of the Co-Op Station Network, interpolated to a grid using the SYMAP algorithm (Shepard, 1984). The Maurer dataset only includes stations with more than 20 years of data during1949-2000. Additional model forcings that drive the water balance, such as solar (short-wave) and long-wave radiation, relative humidity, vapor pressure, and vapor pressure deficit, are calculated within the model using established empirical relationships.

The VIC outputs typically include grid cell moisture and energy states through time (i.e., soil moisture, snow water content, snowpack cold content) and water leaving the basin either as ET (evapotranspiration), baseflow, sublimation, or runoff; where the latter represents the combination of faster-response surface runoff and slower-response baseflow. Gridded surface runoff and baseflow are hydraulically routed to produce streamflow at selected locations (e.g., stream gages), using the model presented by Lohmann et al. (1996). A schematic of the VIC routing model is shown in Figure 9c. This setup requires specifying the coordinates of each streamflow location within the basin grid, identifying tributary grid cells and flow directions through these grid cells, and ultimately the fraction-area contribution from tributary grid cells to streamflow at the location of interest. Routed streamflow using this approach represents natural streamflow, that is, streamflow that would occur in the absence of water management (diversions, return flows, and surface reservoir storage as examples).

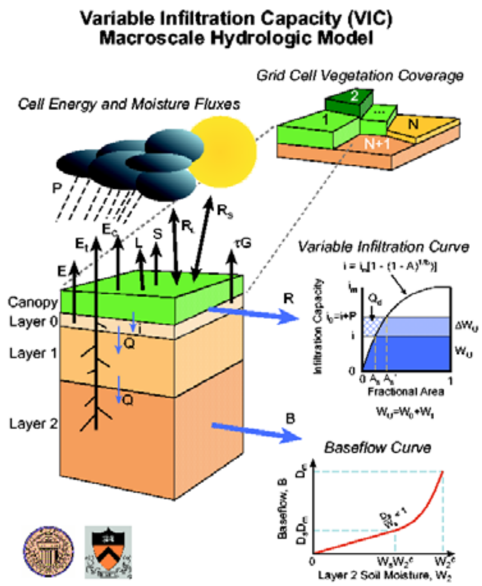


a)

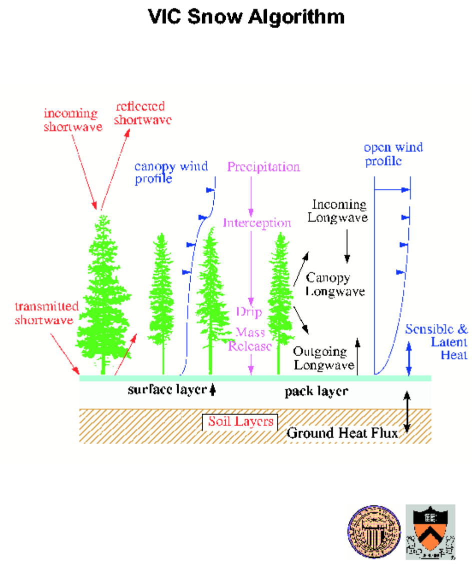


b)

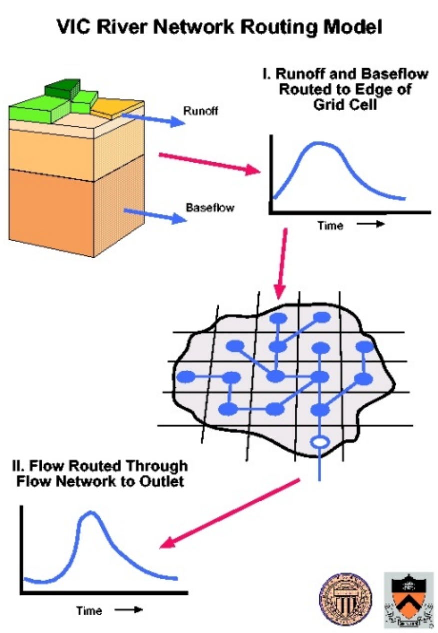


c)

**Figure 9.—Variable Infiltration Capacity Model schematics, including a) spatial discretization and overview, b) snow model algorithm, and c) routing model.**

(page intentionally left blank)

# CHAPTER 6. VIC HYDROLOGIC MODEL SIMULATIONS

The VIC model was used to generate HDe hydrology scenarios based on the baseline and associated HDe climate change scenarios. Simulated routed streamflows were developed at 16 stream locations (Figure 2; Table 2) for baseline conditions and the five HDe climate change scenarios.

Table 2.—Stream locations shown on the map in Figure 2.

| Name | Name |
|---|---|
| Agua Fria River | Salt River |
| Cave Creek | Santa Cruz Wash |
| Centennial Wash | Skunk Creek |
| Gila River | Star Wash |
| Hassayampa River | Trilby Wash |
| Jackrabbit Wash | Vekol Wash |
| New River | Waterman Wash |
| Queen Creek | Weekes Wash |

Monthly simulated streamflow results are shown in Figures 10 and 11 for the Gila and Hassayampa Rivers. In these figures, the average monthly simulated streamflow for the baseline and HDe scenarios is shown in the top plot. Below this, boxplots of the distribution of monthly simulated streamflow for each scenario is displayed. The median value is denoted by the red line in the boxplots. Appendix A contains figures for the other stream locations.

Generally, the baseline and central tendency streamflow results are similar. The warm-wet (WW) scenario produces the higher streamflow in the spring runoff season with the hot-wet (HW) scenario producing a second peak of streamflows in the summer and early fall months. The first peak of spring runoff is generally driven by snowmelt, rain and rain on snow events whereas the second peak is likely driven by the monsoon rainfall which is a characteristic phenomenon over the southwestern U.S. The smallest streamflows are usually seen in the hot-dry (HD) scenario. The boxplots show that the largest variation in monthly streamflow values occurring during the wetter scenarios (WW and HW) and the smallest variation in the dryer scenarios (HD and WD).

In addition, to support the groundwater modeling[2] efforts for the WSRVBS, transient streamflow change factors were also calculated for all stream locations for use in the groundwater model simulations using the climate change scenarios.

[2] The groundwater modeling task was conducted by a contractor under a separate agreement, and thus not included in this technical memorandum. The data described here was provided to the contractor upon request in support of the groundwater modeling efforts.

For each streamflow location, monthly streamflow for each projection used in producing the HDe scenarios was downloaded from the downscaled climate and hydrology projections website: [http://gdo-dcp.ucllnl.org/downscaled_cmip_projections/dcpInterface.html](http://gdo-dcp.ucllnl.org/downscaled_cmip_projections/dcpInterface.html). The appropriate projections were averaged in the five HDe scenarios and then a 30-year moving window for each month was used to calculate a monthly time-series of change factors for the period 2000-2099 relative to the historical period, 1950-1999. The factor was calculated as the mean of the 30 month values from the time-window divided by the mean of the 50 historical (1950-1999) monthly values.

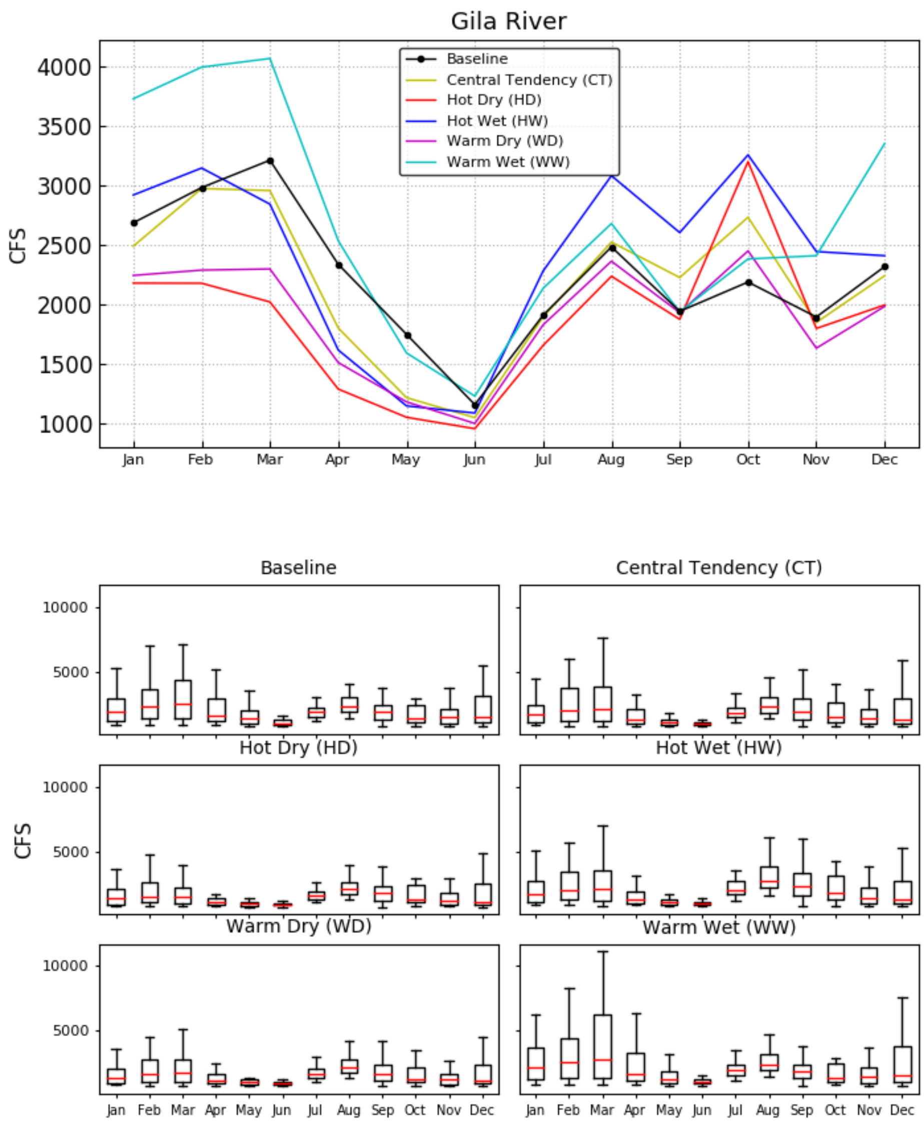


**Figure 10.—Monthly average (top) and boxplots (bottom) of simulated streamflow in cubic feet per second (CFS) for the baseline and five HDe climate change scenario simulations for the Gila River site (shown in Figure 1).**

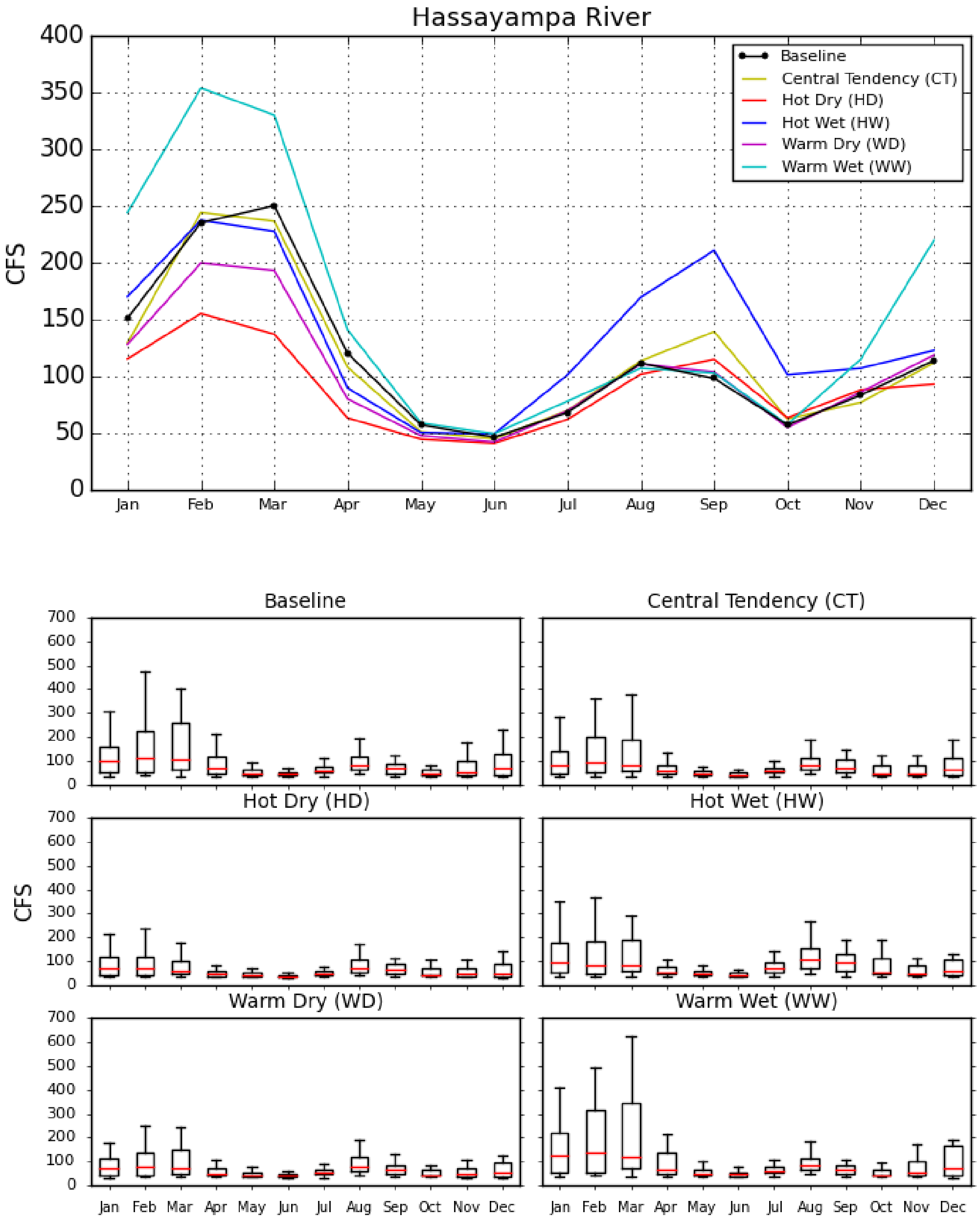


**Figure 11.—Monthly average (top) and boxplots (bottom) of simulated streamflow for the baseline and five HDe climate change scenario simulations for the Hassayampa River site (shown in Figure 1).**

(page intentionally left blank)

# CHAPTER 7. SAC-SMA HYDROLOGIC SIMULATIONS

SAC-SMA streamflow simulations for the Agua Fria, Verde, and Salt Rivers were produced and compared with VIC simulation results to explore the effects of using different models and parameterizations on simulated streamflow results.

## 7.1. Hydrologic Model Description

Hydrologic simulations were conducted for the Agua Fria, Salt, and Verde River Basins using a two coupled NWSRFS (National Weather Service River Forecasting System)[3] models. These models include the SAC-SMA (Sacramento Soil Moisture Accounting, Crawford and Linsley 1966) and the SNOW-17 (Snow Accumulation and Ablation Model, Anderson 1973). Calibrated SAC-SMA/SNOW-17 applications for the study region were obtained from the Colorado Basin River Forecast Center (CBRFC). The models use 1-hourly mean areal precipitation (MAP) and 6-hourly mean areal temperature (MAT) time-series as inputs for computing runoff time series. The SAC-SMA and SNOW-17 models are components of the NWSRFS' river forecast model that is used by CBRFC to produce river stage and river flow forecasts.

The SAC-SMA is the precipitation-runoff component of the NWSRFS river forecast model. The SAC-SMA is a lumped conceptual hydrology model that simulates the physical mechanisms driving water movement through the soil column— infiltration, percolation, storage, evapotranspiration, base flow, etc. The SAC-SMA model maintains system water balance via precipitation, evapotranspiration and changes in soil moisture storage.

The SNOW-17 snow accumulation and ablation model is a conceptual model in which each of the significant physical processes affecting snow accumulation, sublimation and snowmelt is mathematically represented. The model uses air temperature as the only index to energy exchange across the snow-air interface and it runs in conjunction with the SAC-SMA model.

---

[3] NWSRFS user manual documentation available from http://www.nws.noaa.gov/oh/hrl/nwsrfs/users_manual/htm/xrfsdocpdf.php. Accessed February, 2018.

Precipitation input to the SAC-SMA is first processed through SNOW-17. If precipitation is “typed” as rain, precipitation is directly input to SAC-SMA. If precipitation is “typed” as snow, SNOW-17 uses energy balance to partition the melt amount to be passed to SAC-SMA. For each watershed, the SAC-SMA model does a water balance calculation to estimate precipitation excess which is subsequently run through unit hydrographs to compute runoff time series (runoff hydrographs) at the watershed outlet. Runoff hydrographs produced for an upstream watershed are routed downstream using either hydrologic methods (empirical—e.g., Lag/K, Muskingum and the Layered Coefficient method) or hydraulic channel routing (energy and continuity or momentum equations—e.g., one-dimensional solution to the full St. Venant equations for unsteady flow). The Agua Fria, Salt, and Verde River applications used in this study use the Lag/K hydrologic method to route flows from upstream to downstream sections of the watersheds.

One hourly MAP and six hourly MAT time series were developed from the HDe projection sets for the future look-ahead period 2060s using the reference or base 50-year period, 1950-1999. The details of the weather generation are described in the next section.

## 7.2. Development of weather inputs using the HDe technique

The calibrated Agua Fria, Salt, and Verde River SAC-SMA/SNOW-17 applications include a base set of 1-hourly MAP and 6-hourly MAT time-series for each of the 34 elevation-based areas (Figure 12) for these streams covering the period October 1980 through September 2010. This base weather sequence is constructed from historical weather station observations and is used as the base climate condition in the hydrologic assessment, whereby this sequence of weather is input to the SAC-SMA/SNOW-17 models to generate an associated sequence of runoff.

To develop climate change scenario weather inputs using the HDe technique, two pre-processing steps were performed. First, 1-hourly MAP and 6-hourly MAT forcings covering the base period (10/1980 - 12/1999), for each watershed, were aggregated to monthly values of total precipitation and monthly average temperature. Second, gridded ($1/8^{th}$ degree) monthly precipitation and temperature values covering the watershed sub-basins (Figure 12) for each of the projections informing the climate change scenarios (see Chapter 4) were mapped and aggregated to the 34 elevation-based areas in the SAC-SMA/SNOW-17 applications. Following these pre-processing steps, the HDe technique as described in Chapter 4 was applied to derive the climate change scenarios.

## 7.3. Developing future potential evapotranspiration inputs for SAC-SMA

Surface hydrology models like the SAC-SMA simulate water balance via precipitation, evapotranspiration and changes in soil moisture storage. During simulation, the evapotranspiration (ET) rate from a landscape is constrained by potential evapotranspiration (PET). Potential evapotranspiration is the maximum amount of water that could be evaporated and transpired from a landscape at a given temperature if there were a sufficient supply of water. Some hydrology models compute PET internally as a function of weather inputs (e.g., the VIC model) while others like SAC-SMA require modelers to specify PET inputs. This SAC-SMA application obtained from CBRFC, like many other developed at National Weather Service River Forecast Centers, feature PET inputs that reflect historical climate conditions. Now under future climate conditions, it is expected with a warmer climate and increased moisture holding capacity, PET constraints on future ET rate will be elevated. To represent such an effect in this SAC-SMA simulation, the VIC model is used, offering internal PET calculation, and application of that model in several warming sensitivity analyses in order to develop a basis for PET input adjustment for SAC-SMA.

To adjust calibrated SAC-SMA monthly PET patterns, an approach used in an earlier Reclamation study (Reclamation 2010b) was used as summarized here. PET change factors were first estimated using the VIC model application for the Agua Fria, Salt, and Verde River watersheds. The VIC model uses the physically based Penman-Monteith formulation of PET. The objective for running the VIC model was to calculate the sensitivity of change in PET (for natural vegetation) with a 1°C change in temperature in order to adjust monthly SAC-SMA PET. Three VIC simulations were carried out to estimate the PET sensitivities. A base VIC run was done using the Maurer et al. (2002) daily weather forcings – precipitation, minimum temperature (Tmin), maximum temperature (Tmax), and wind speed. Two additional runs were done by perturbing the temperature fields to represent 1°C change in average temperature. The first temperature perturbation run involved increasing both Tmin and Tmax of the base case weather forcings (Maurer et al., 2002) by 1°C. The second temperature perturbation run was done by not changing Tmin, but increasing Tmax by 2 °C. These two sensitivities were then averaged and used to adjust the monthly PET in the SAC-SMA model.

## 7.4. Hydrologic modeling results

The SAC-SMA and VIC models were used to generate HDe hydrology scenarios based on the baseline and associated HDe climate change scenarios. Simulated routed streamflows were developed at three stream gage locations (Table 3; Figure 12) for baseline conditions and five HDe climate change scenarios.

Table 3.—Stream locations shown on the map in Figure 2.

| Stream Location | SAC-SMA Identifier | Contributing sub-basins |
|---|---|---|
| Agua Fria at Lake Pleasant | LKPA3 | 4 |
| Salt at Roosevelt Reservoir | RSVA3 | 12 |
| Verde at Bartlett Reservoir | BRTA3 | 18 |

Before discussing results, it is beneficial to summarize the relevant differences between the VIC and SAC-SMA models as used in this study. The VIC model application uses a gridded discretization of 1/8° resolution with a mostly informal calibration history primarily based on efforts at University of Washington. Additional calibration was deemed outside the scope of this study as it requires well vetted naturalized streamflow records and significant effort is necessary to derive such naturalized streamflows. The SAC-SMA model is based on lumped areas (called sub-basins here) which are significantly larger than the 1/8° VIC grid cells (see Figure 12), but has undergone formal calibration by the CBRFC. The VIC model computes PET internally, making it convenient for studies involving increasing temperatures, whereas the SAC-SMA model as applied requires direct input of PET. The VIC application historical period aligns perfectly with the historical period (1950-1999) of the GCM projections used in the HDe process, whereas SAC-SMA application historical period (1980-2010) only overlaps the GCM historical period by 20 years (1980-1999). The plots below (Figures 13-15) use VIC results based on 50 years (1950-1999), while the SAC-SMA results are based on 30 years (1980-2010).

Results (Figures 13-14) for streamflow at each site (see Figure 12) are presented for the baseline and HDe scenarios in three plots: mean monthly streamflow (top), boxplots of monthly streamflow (middle), and mean monthly streamflow ratio for each HDe scenario (bottom). This ratio is calculated by dividing scenario mean monthly value by the baseline mean monthly value for each month. Typically, results are interpreted in a relative sense compared to the baseline scenario, rather than the absolute magnitudes of the simulated streamflow for a given scenario.

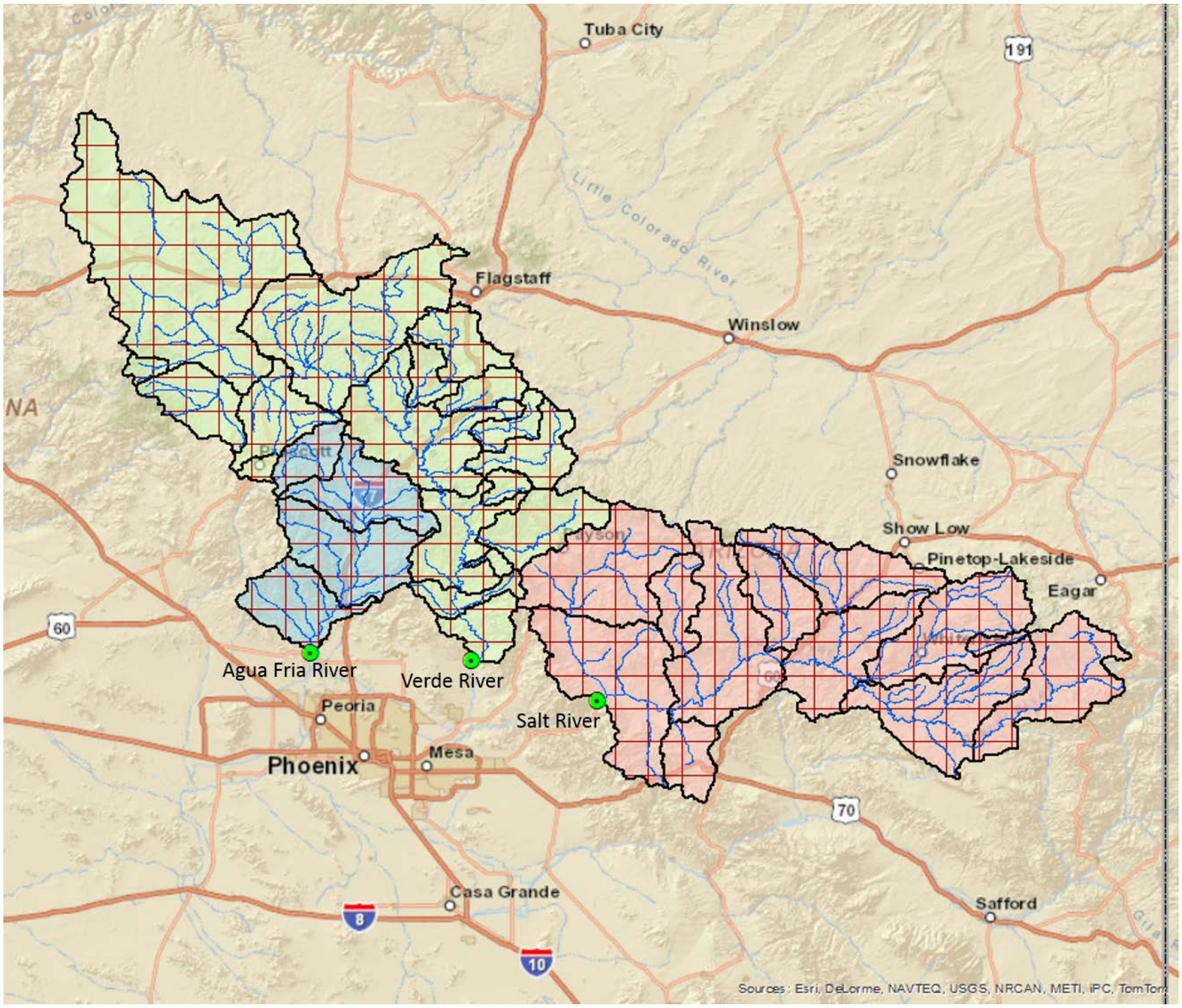


**Figure 12.—SAC-SMA sub-basins (black outline) and contributing streams (blue lines) to three sites on the Agua Fria, Salt, and Verde Rivers. VIC grid cells at 1/8° resolution (red lines) within the contributing areas are also shown.**

For this reason, monthly ratios of scenario values relative to baseline scenario values are often used as scaling factors to translate the climate change results to other models dependent on streamflow. Plots of ratios show how the VIC and SAC-SMA results may differ when used to adjust streamflow on a monthly basis for other models.

In general, the shape of the mean monthly streamflow traces (top plots) are similar between the SAC-SMA and VIC results for all sites, with SAC-SMA magnitudes being less for the Agua Fria and Verde sites. This translates to a larger range of ratio values (bottom plots), since the ratio is sensitive to smaller baseline values (denominator), especially for the Agua Fria which has much smaller streamflows than the Salt and Verde. For all three sites, the wetter scenarios (HW and WW) result in higher mean monthly streamflow, in the summer months for the HW scenario and in the winter months for the WW scenario. The boxplots (middle plots) show that the VIC streamflows have greater variability in most months compared to the SAC-SMA streamflows, especially for the Agua Fria and Verde Rivers. Some of this may be attributed to the longer simulation period (50 years) for VIC versus 30 years for the SAC-SMA simulations. Overall, SAC-SMA and VIC streamflow results are similar for the Salt River simulations.

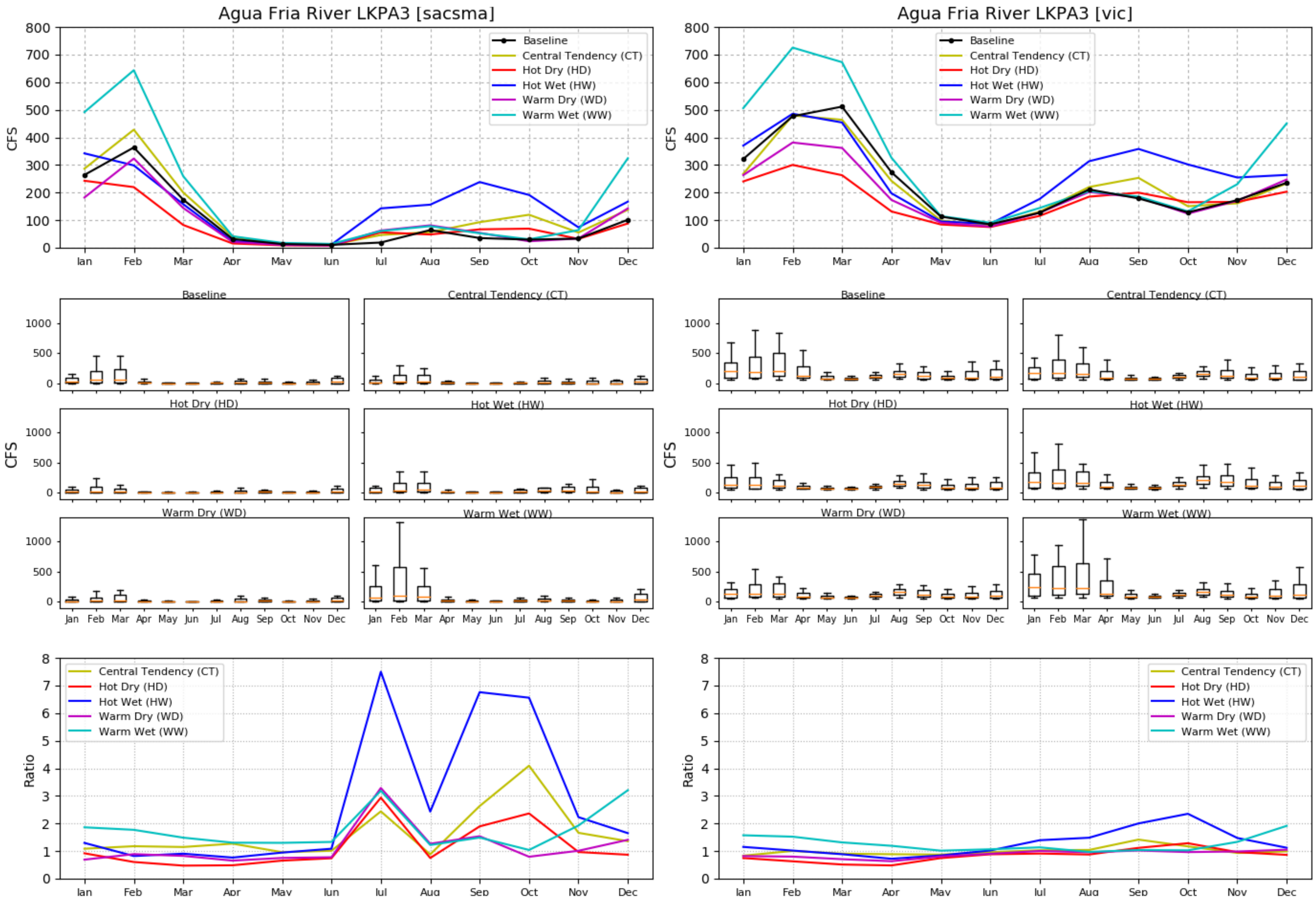


**Figure 13.—Monthly average (top) and boxplots (middle) of simulated streamflow and monthly ratios (bottom) for SAC-SMA (left panel) and VIC (right panel) simulations for the baseline and five HDe climate change scenario simulations for the Agua Fria River site (shown in Figure 12).**

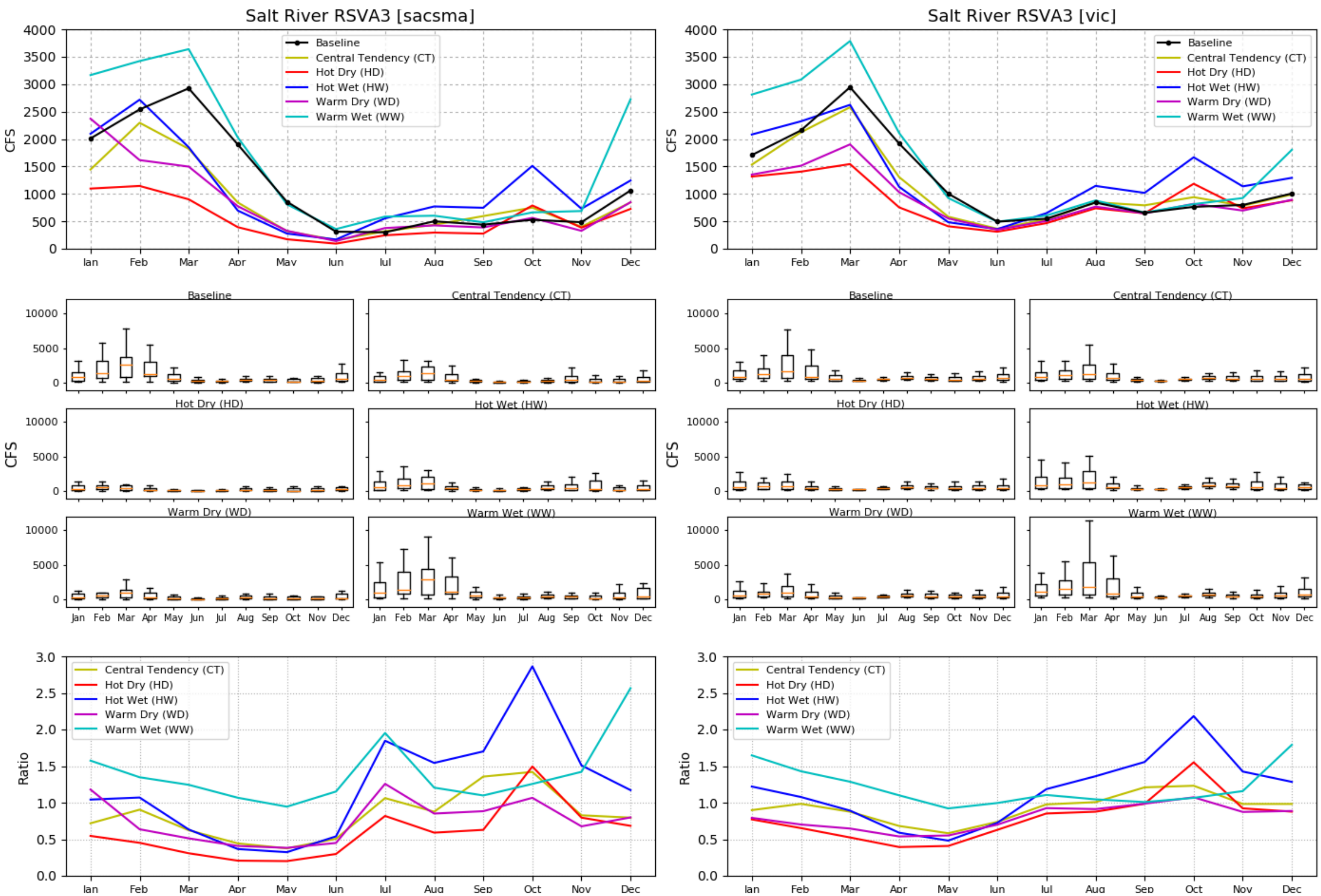


**Figure 14.—Monthly average (top) and boxplots (middle) of simulated streamflow and monthly ratios (bottom) for SAC-SMA (left panel) and VIC (right panel) simulations for the baseline and five HDe climate change scenario simulations for the Salt River site (shown in Figure 12).**

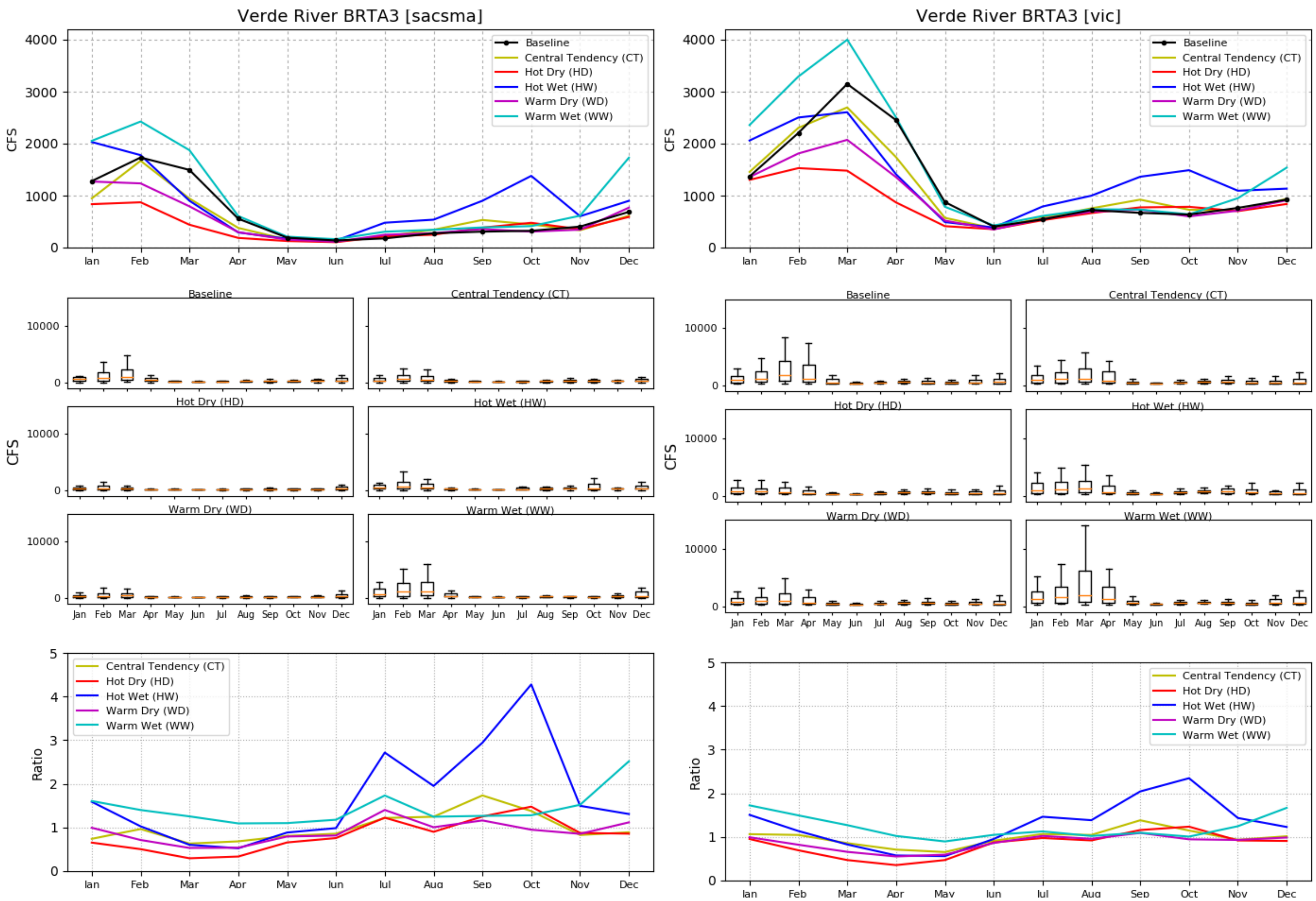


**Figure 15.—Monthly average (top) and boxplots (middle) of simulated streamflow and monthly ratios (bottom) for SAC-SMA (left panel) and VIC (right panel) simulations for the baseline and five HDe climate change scenario simulations for the Verde River site (shown in Figure 12).**

(page intentionally left blank)

# CHAPTER 8. IRRIGATION DEMANDS

Estimated agricultural irrigation demand under climate change scenarios for the study area are summarized here from a previous collaborative effort by Reclamation, Desert Research Institute (DRI) and the University of Idaho (Reclamation, 2015). This effort includes an analysis of the potential changes in crop irrigation demand in eight major river basins in the western U.S. when considering observed and projected impacts of climate change. The findings presented in that report were intended to be available for future basin-specific Basin Studies conducted under the Department of Interior's WaterSMART Program. Reclamation (2015) results are at the HUC8 sub-basin scale and the results for the HUC8 sub-basins (Figure 16) that fall within the WSRVBS study area were used.

It is important to recognize the differences between the HDe methodology used in this study for the hydrology analyses and that used in Reclamation (2014). These differences include:

1. Climate change scenarios were derived from a pool of 112 CMIP3 climate projections in Reclamation (2015), rather than 231 CMIP5 climate projections used in climate change scenarios for WSRVBS hydrology projections.

2. The entire Colorado River Basin is used in the HDe process for projection selections in Reclamation (2015). The WSRVBS study area is much smaller (Figure 2 and Figure 3).

3. In Reclamation (2015), climate change scenarios were defined by using projections falling within 5 different quadrants, four scenarios based on the 50th percentiles, and the Central scenario based on the 25th and 75th percentiles. WSRVBS climate change scenarios are developed by selecting the 10 individual climate projections that fall closest to the intersections of the 10th, 50th, and 90th percentiles of change (see Chapter 4).

4. The future time horizon from Reclamation (2015) is 2040-2069, rather than 2045-2074 used in WSRVBS.

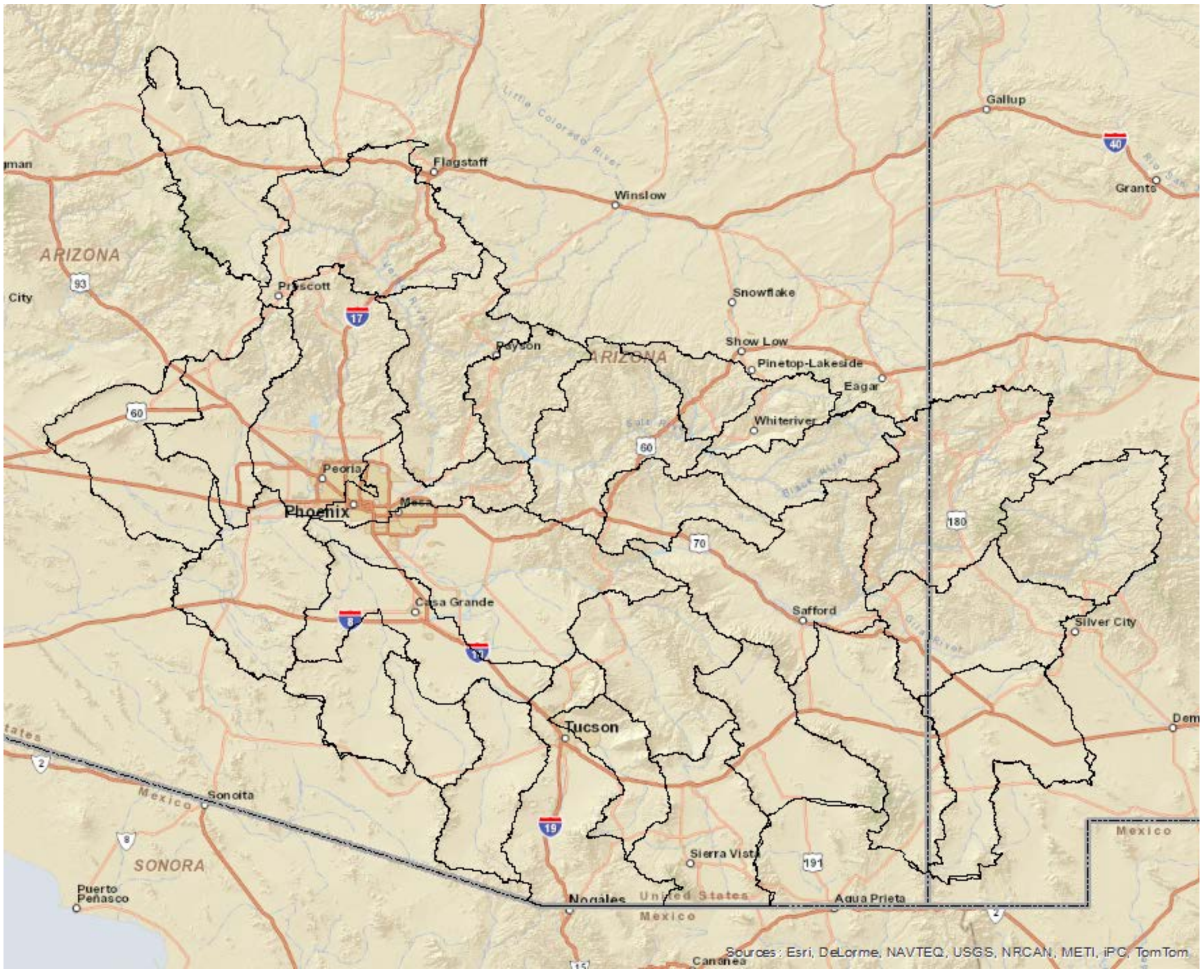


**Figure 16.—HUC8 sub-basins for which agricultural irrigation demand under climate change scenarios results are presented. Note that two HUC8 sub-basins are truncated at the US-Mexico border in this and subsequent maps—consistent with results presented in Reclamation, 2015.**

## 8.1. Background

The agricultural irrigation demand analysis (Reclamation, 2015) focused on crop demands, or crop net irrigation water requirement (NIWR). NIWR is equal to the total crop demand minus that amount of the crop demand that is met by precipitation, i.e. effective precipitation ($P_e$). NIWR does not include conveyance or on-farm losses. Crop water demand is a function of ET, which is the amount of water transpired by the crop plus the amount that evaporates from the plant and surrounding soil surfaces (Jensen et al., 1990).

In Reclamation (2015), current and future NIWR estimates for each HUC8 sub-basin were developed following methods established under Reclamation's West-wide Climate Risk Assessments (WWCRA). Brief descriptions of these methods follow and more detailed discussions are contained in Reclamation (2015).

The same Maurer et al. (2002) 1950-1999 climate data set used for current conditions in the hydrologic analyses was used for the demands analysis current conditions. However, the temperature and precipitation values used from this data set were adjusted based on historical observations from weather stations located near the irrigated crop areas to remove any biases that may exist between the gridded meteorological dataset (Maurer et al., 2002) and these point observations. Note, these adjustments were not done for the hydrologic analyses. The adjusted Maurer et al. (2002) and CMIP3 data sets were then used for the HDe climate change scenarios development process the same as for the hydrologic analyses.

## 8.2. Demands Methodology

Estimates of NIWR were developed using the ET Demands model, originally developed by the University of Idaho, Nevada Division of Water Resources, and DRI. Recent modifications to the model for WWCRA applications were made through a collaborative effort by Reclamation, DRI and the University of Idaho (Reclamation, 2015).

The ET Demands model is based on the Penman Monteith (PM) dual crop coefficient method, as described in the Food and Agriculture Organization (FAO) of the United Nations, FAO Irrigation and Drainage Paper 56 (Allen et. al, 1998). The American Society of Civil Engineers (ASCE) has adopted the FAO-56 PM equation as the standardized equation for calculating reference ET ($ET_o$) (ASCE, 2005). The short grass reference crop version of the PM equation was used to be consistent with other Reclamation work.

By using the PM dual crop coefficient method rather than a single crop coefficient approach, transpiration and evaporation are accounted for separately to better quantify evaporation from variable precipitation and simulated irrigation events. This also allows for accounting of winter soil moisture conditions, which can be a significant factor when estimating early irrigation season net irrigation water requirements (NIWR). The dual crop coefficient method provides a robust means for estimating NIWR based on continuous accounting of soil moisture balance.

The ET Demands model first calculates daily reference ET ($ET_o$) for each HUC8 sub-basin as a function of Tmax and Tmin from the 1950-1999 climate data set mentioned above. The PM equation variables of vapor pressure, solar radiation and wind speed are empirically estimated as described in Reclamation (2015) as per the methods recommended by ASCE (2005). Figure 17 is a schematic showing the basic parameters included in the PM equation.

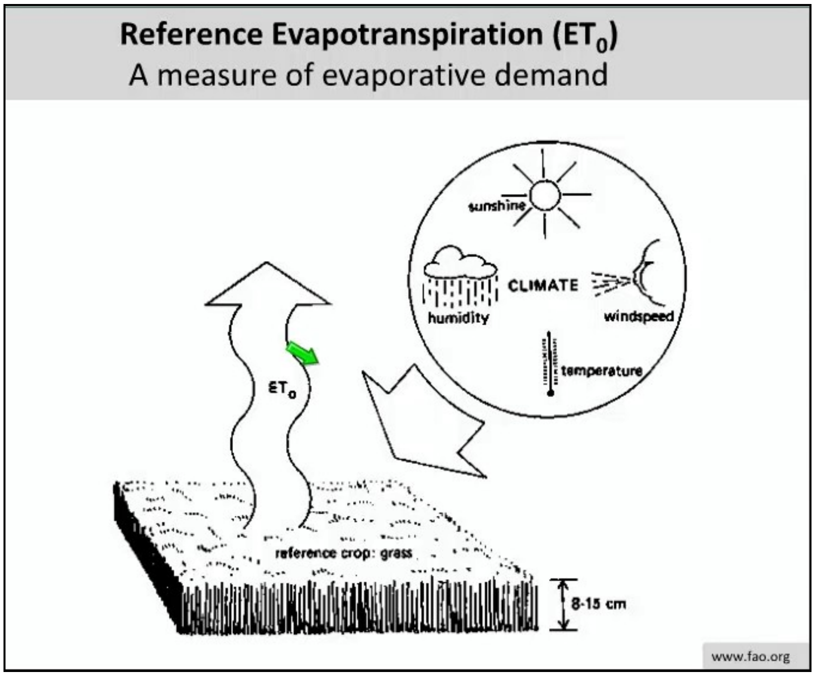


**Figure 17.—Reference evapotranspiration equation parameters schematic.**

Weighted average soil conditions (allowable water content and percent clay, silt and sand) for the irrigated lands in each HUC8 sub-basin were input to ET Demands. The soils information is based on data from the Natural Resources Conservation Service (NRCS) State Soil Geographic (STATSGO) database (USDA-NRCS, 1991). The soil parameters affect the estimation of irrigation scheduling, evaporation losses from soil, moisture holding capacity, deep percolation from root zones, antecedent soil moisture conditions, and runoff from precipitation.

Once daily $ET_o$ is calculated, the daily crop ET ($ET_c$) is then calculated as a function of the two primary crop coefficients and a crop stress coefficient. $ET_c$ for all crop types within a given HUC8 was estimated as follows:

$ET_c = (K_s K_{cb} + K_e) ET_o$ ;

where $ET_o$ is the ASCE-PM grass reference ET, $K_{cb}$ is the basal crop coefficient, Ke is the soil water evaporation coefficient, and Ks is the stress coefficient. $K_{cb}$ and $K_e$ are dimensionless and range from 0 to 1.4. Daily $K_{cb}$ values over a season, commonly referred to as the crop coefficient curve; represent impacts on crop ET from changes in vegetation phenology, which can vary from year to year depending on the start, duration, and termination of the growing season, all of which are dependent on temperature. $K_e$ is a function of the soil water balance in the upper 0.1 meter of the soil column since this zone is assumed to be the only layer supplying water for direct evaporation from the soil surface. $K_s$ ranges from 0 to 1, where 1 equates to no water stress, and is also dimensionless. A daily soil water balance for the simulated effective root zone is required and computed in

ET Demands to calculate $K_s$. In the case of computing the $ET_c$ and NIWR, $K_s$ is generally 1 but can be less than 1 in the winter if precipitation is low and winter surface cover is specified to be anything other than bare soil, such as mulch or grass. The dual crop coefficient concept is illustrated in the schematic shown in Figure 18.

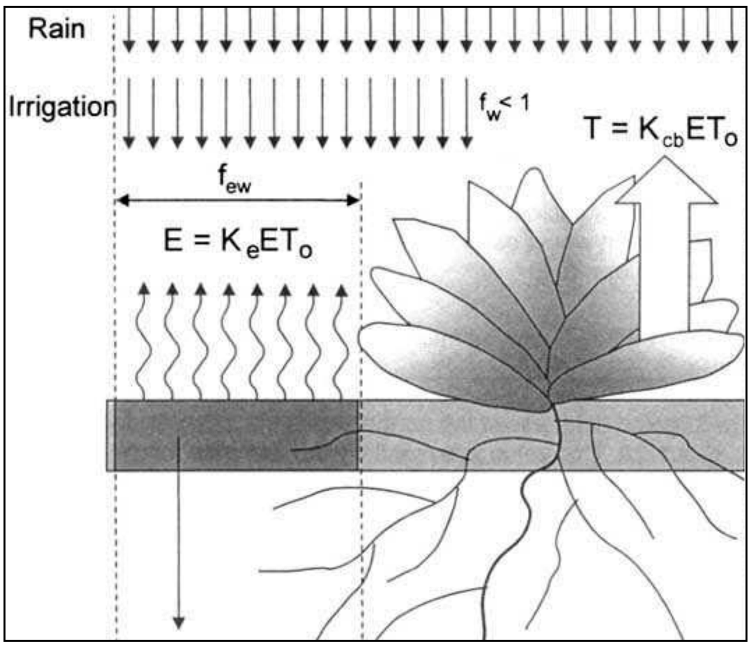


**Figure 18.—Dual crop coefficient evapotranspiration concept schematic.**

Values of $K_{cb}$ for a given crop vary seasonally and annually to simulate plant phenology as impacted by solar radiation, temperature, precipitation, and agricultural practice. Seasonal changes in vegetation cover and maturation are simulated in ET Demands by each crop specific $K_{cb}$ as a function of air temperature. This is done in terms of cumulative growing degree days (GDD). After planting of annuals or the emergence of perennials, the value of $K_{cb}$ gradually increases with increasing temperatures until the crop reaches full cover. Once this happens, and throughout the middle stage of the growing season, the $K_{cb}$ value is generally constant, or is reduced due to simulated cuttings and harvest. From the middle stage to the end of the growing season the $K_{cb}$ value reduces to simulate senescence. GDD is calculated in ET Demands by three different methods as described in Reclamation (2014). The GDD equations' constants were calibrated based on historical data (green-up or planting, timing of full cover, harvest, and termination dates).

Having the ability to simulate year to year variations in the timing of green-up or planting, timing of effective full cover, harvest, and termination, is necessary for integrating the effects of temperature on growing season length and crop growth and development, especially under changing climate scenarios.

The NIWR rate or depth is calculated in ET Demands by factoring in $P_e$ (NIWR = $ET_c - P_e$). $P_e$ is calculated as a function of daily precipitation (from the climate data set), antecedent soil moisture and precipitation runoff. Soil moisture is a function of moisture holding capacity of the weighted average soil type input to the model for each HUC8 sub-basin. Precipitation runoff is calculated based on daily precipitation using the NRCS curve number method (USDA-SCS, 1972).

Simulation of irrigation events by the ET Demands model occurs when the crop root zone moisture content drops to the crop specific maximum allowable depletion threshold. Irrigations are specified to fill the root zone by the difference between field capacity and the cumulative soil moisture depletion depth amount.

The NIWR and $ET_c$ rates for each crop within a given HUC8 sub-basin are multiplied by the ratio of the acres of the crop to total irrigated acres within the HUC8 sub-basin and all crop values are summed to calculate weighted average HUC8 sub-basin NIWR and $ET_c$ rates as shown in the equation below.

HUC8 sub-basin rate = $\sum_{i=1}^{i=n} crop\ ratio\ i * crop\ rate\ i$

The product of the weighted average NIWR rate and the total irrigated acreage yields the NIWR volume for each HUC8 sub-basin in acre-feet.

## 8.3. Historical Baseline Demands

The ET Demands model results for baseline conditions include $ET_o$, $ET_c$, and NIWR depth for each HUC8 sub-basin. For the purposes of this study, the historical baseline results presented consist of the mean annual values for 1950-1999. The results are presented graphically along with the mean annual values of the bias corrected T and P values that were input to the model. Annual average temperature, precipitation, $ET_o$, $ET_c$, and NIWR depth are shown respectively in the upper-left panels (Baseline) of Figures 19 through 23 and discussed below. (These figures also include future climate change scenario results that are discussed later.) The Appendix contains tabulated summaries of historical baseline and projected future estimates (discussed later) of annual average temperature, precipitation, $ET_o$, $ET_c$, and NIWR depth for each HUC8 sub-basin.

As shown in Figure 19, historical baseline mean annual temperature ranges from 53.1 degrees F at the higher elevations in the north and east to 73.1 degrees F in the southwest portions of the basin. The mean annual precipitation ranges from 6.7 inches in the southwestern portion of the basin to generally more precipitation in the northern portions, with a maximum of 19.4 inches. The respective basin-wide temperature and precipitation historical baseline annual averages are 63.7 degrees F and 14.7 inches.

These basin-wide values are based on temperature and precipitation values for each HUC8 sub-basin which are bias-corrected values from one 1/8º grid cell within each HUC8 sub-basin. These estimates for the entire basin were calculated using the ratios of sub-basin to basin irrigated acres as well. For these reasons, these basin-wide values differ from the observed baseline gridded (Maurer et al. 2002) basin-wide values of 59.3 degrees F and 15.9 inches reported in Table 1, which represents average values of all 1/8 degree grid cells within the basin.

Spatial distributions of historical baseline mean annual $ET_o$ and $ET_c$ are shown in Figures 21 and 22, respectively. ETo, which is primarily a function of temperature, solar radiation, wind speed and humidity, ranges from 59.2 inches in the northwestern portion of the basin to 79.2 inches in the southwestern portion of the basin. The basin-wide $ET_o$ historical baseline annual average is 69.1 inches.

$ET_c$, which is a function of $ET_o$ and the crop pattern (types and acres), ranges from 43.6 inches in the northern portion of the basin to 62.2 inches in the eastern portion of the basin. The basin-wide $ET_c$ historical baseline annual average is 50.1 inches.

NIWR depth, which is a function of $ET_c$ and effective precipitation, ranges from 32.8 inches in the northern portion of the basin to 51.0 inches in the eastern portion, as shown in Figure 23. The basin-wide NIWR depth historical baseline annual average is 38.5 inches.

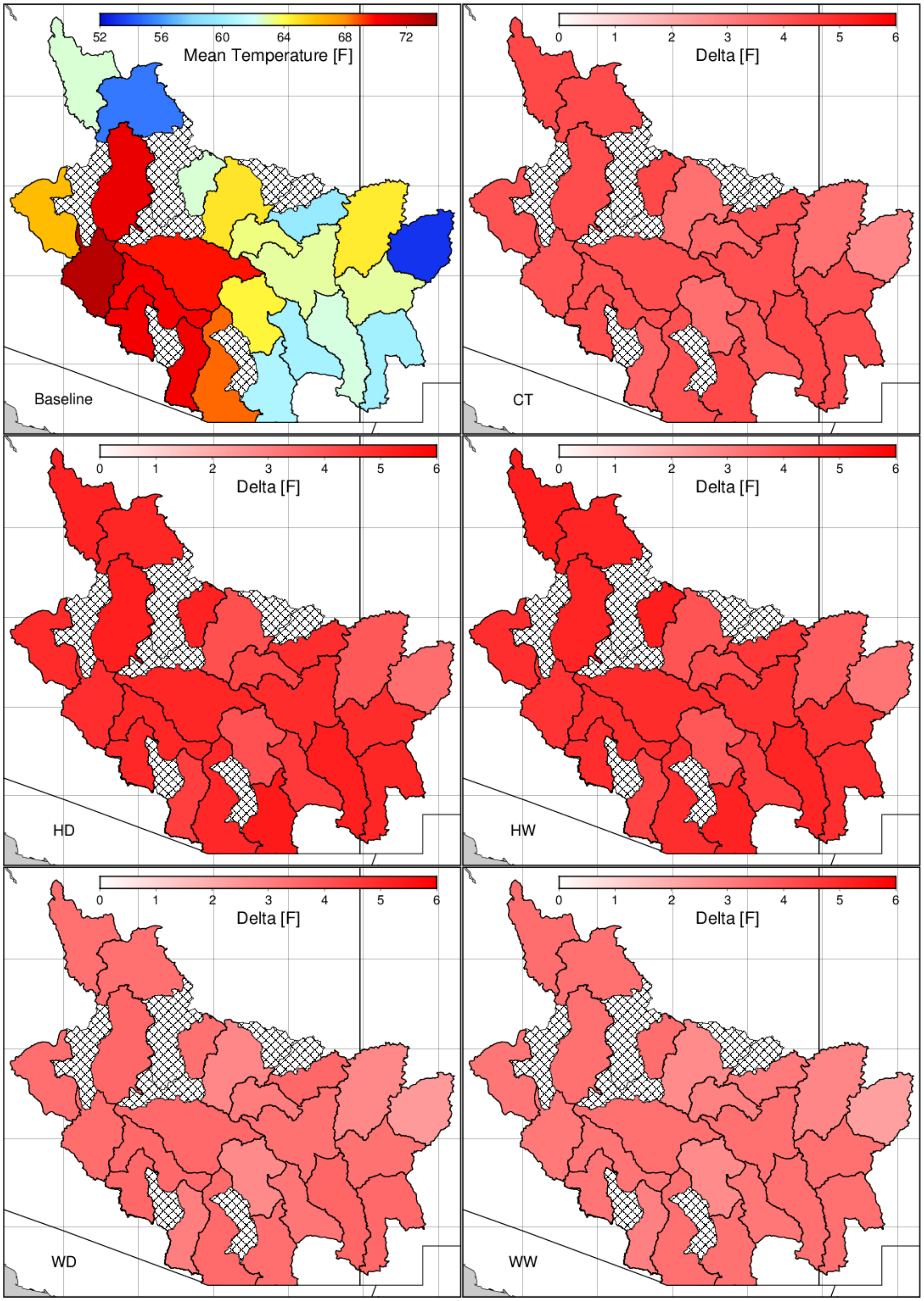


**Figure 19.—Spatial distribution of baseline temperature and projected temperature change for different climate scenarios for the 2040-2069 period. The cross-hatched pattern indicates no results available as no crops are likely grown on these HUC-8s.**

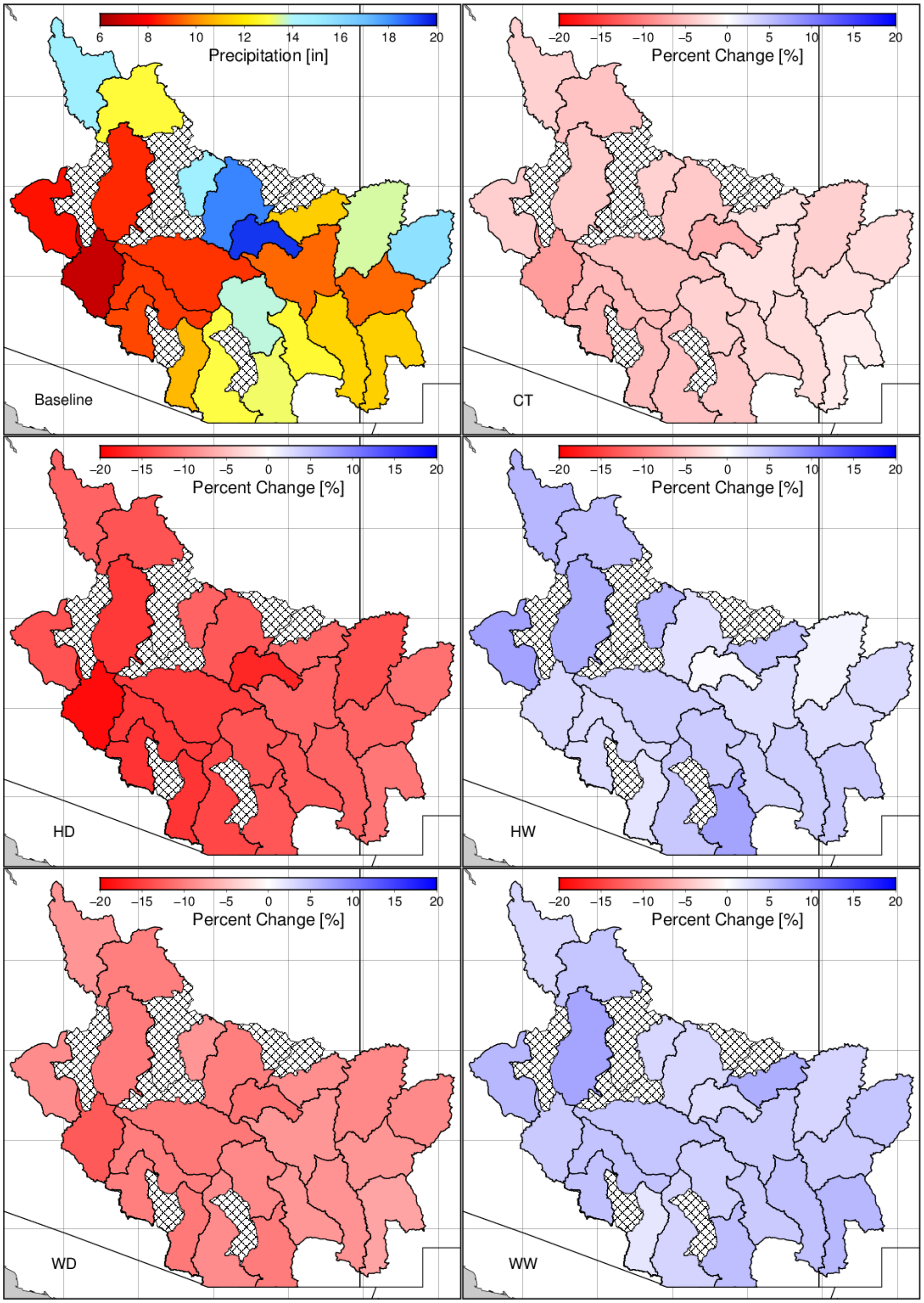


**Figure 20.—Spatial distribution of baseline precipitation and projected precipitation percent change for different climate scenarios for the 2050s (2040-2069 period).**

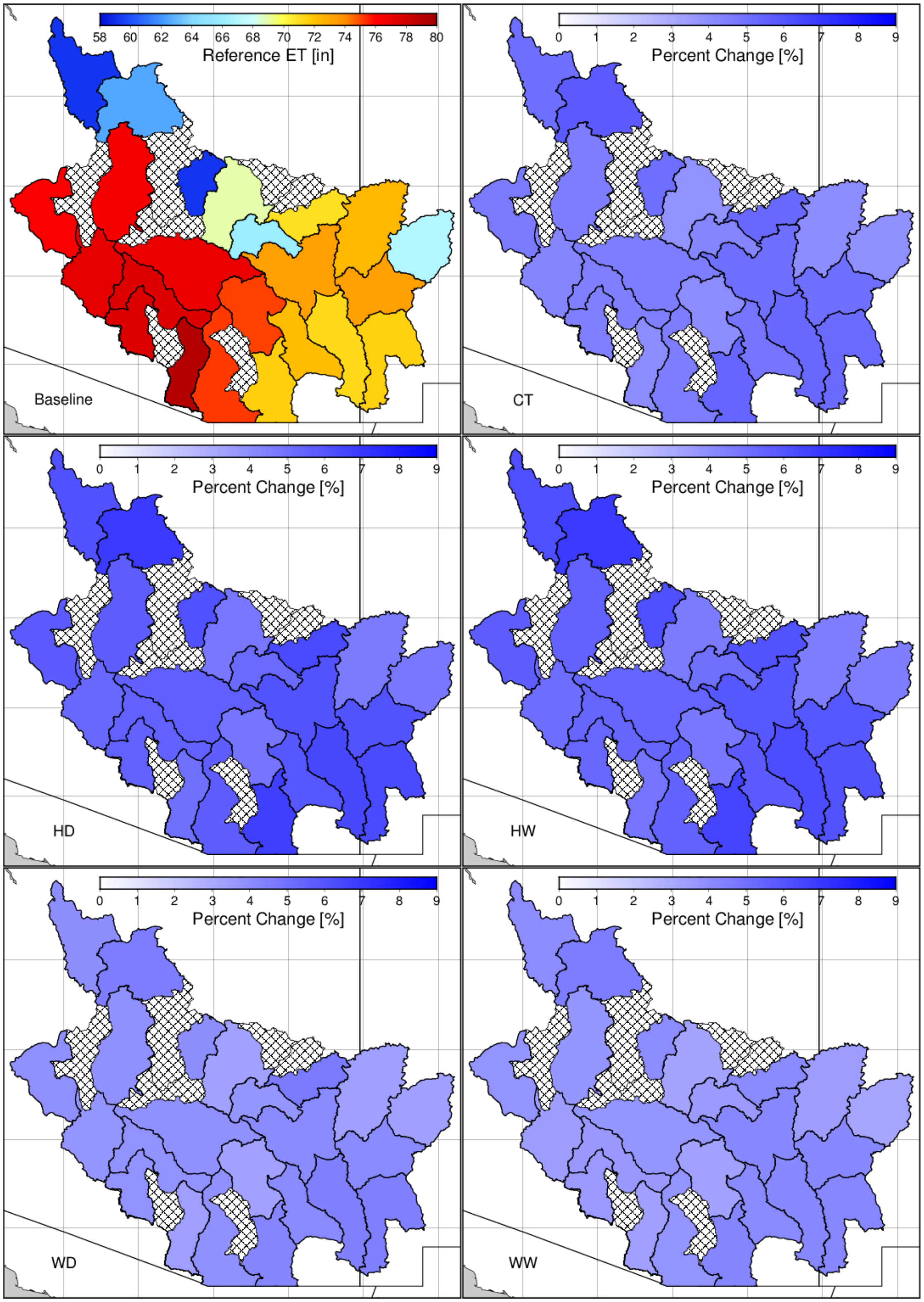


**Figure 21.—Spatial distribution of baseline reference evapotranspiration and projected evapotranspiration percent change for different climate scenarios for the 2050s (2040-2069 period).**

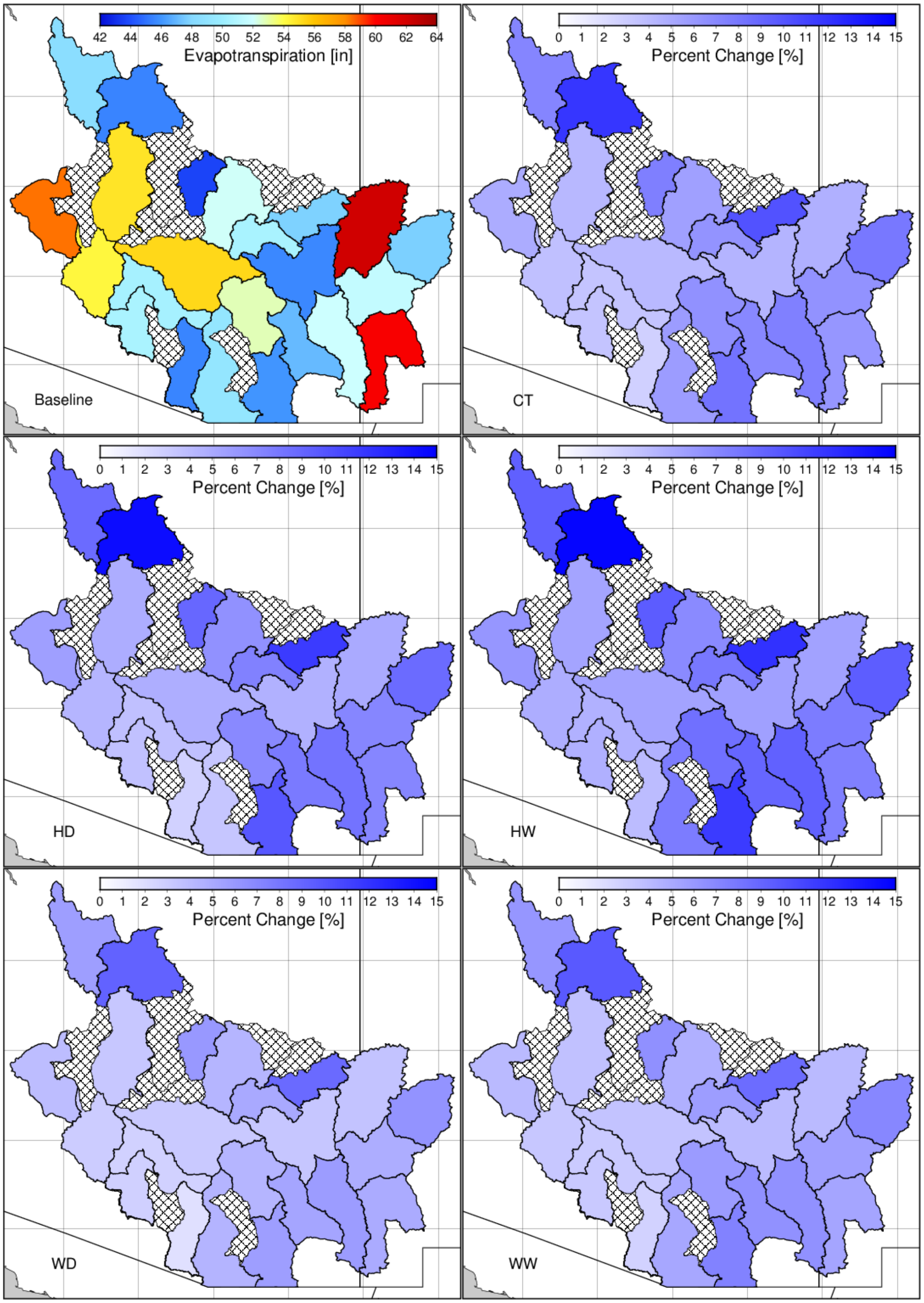


**Figure 22.—Spatial distribution of baseline crop evapotranspiration and projected evapotranspiration percent change for different climate scenarios for the 2050s (2040-2069 period).**

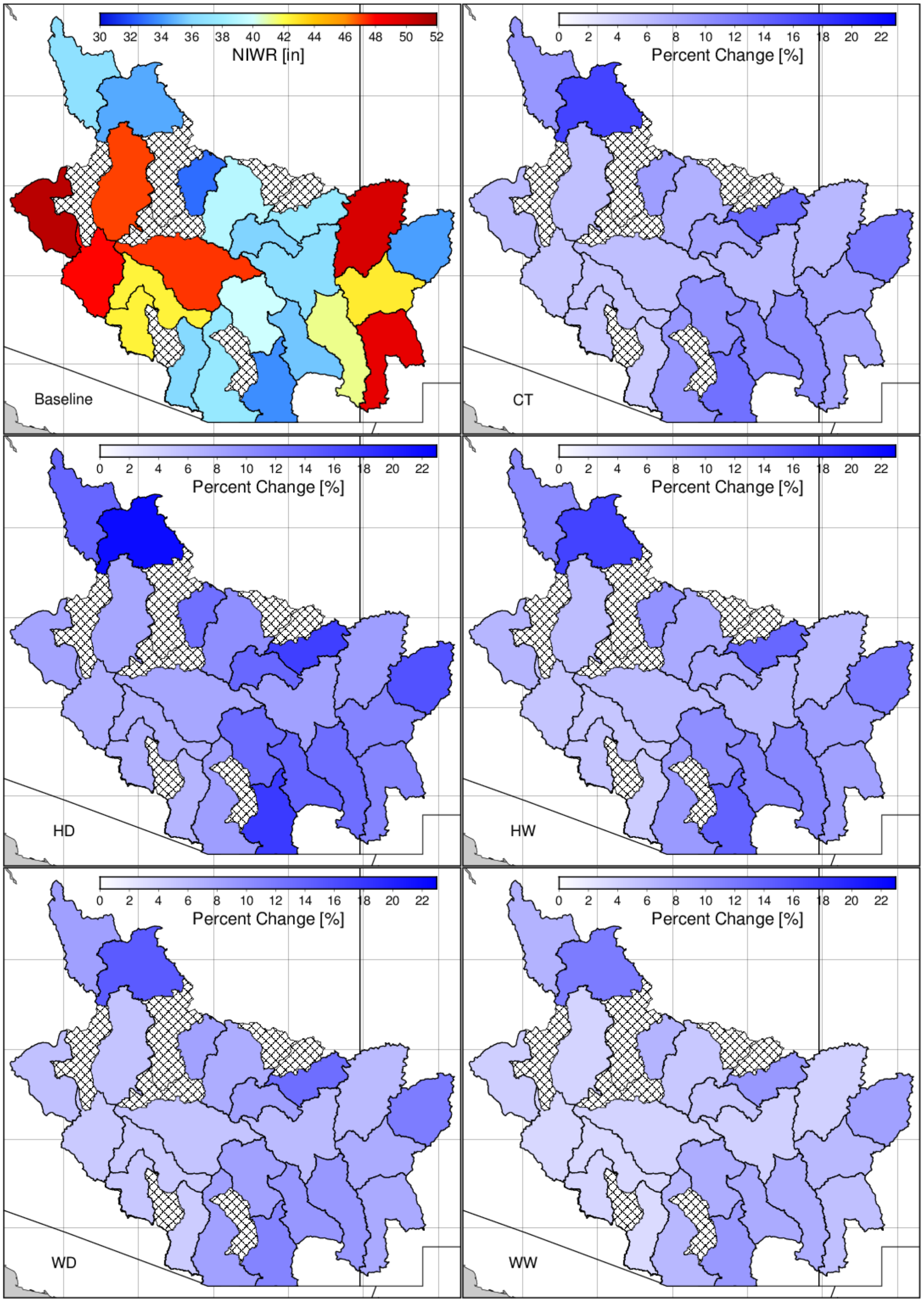


**Figure 23.—Spatial distribution of baseline net irrigation water requirements (NIWR) and projected NIWR percent change for different climate scenarios for the 2050s (2040-2069 period).**

## 8.4. Future Demands

The WSRVBS utilizes one future time period for analysis of climate change impacts (2060s), compared with three future time periods (2020s, 2050s, 2080s) used in the WWCRA analysis (Reclamation, 2015). Here, results are presented for the 2050s future time period (2040-2069) from the WWCRA and is closest is time frame to the 2060s WSRVBS planning horizon.

A single growth scenario or cropping pattern for 2005 conditions (Reclamation, 2015) was used in conjunction with five scenarios of future climate to encompass a range of potential future irrigation water demands. In the discussion of Historical Baseline Demands, the ET Demands model is described as using basal crop coefficient ($K_{cb}$) curves which are developed as a function of GDD. For this study, the $K_{cb}$ curves for annual crops are developed using baseline (historical) temperatures, while perennial $K_{cb}$ curves are developed using future projected temperatures.

It is acknowledged that actual $K_{cb}$ curves for annual crops under future conditions will likely vary. Changes in future farming practice of annual crops, such as potential earlier planting, development, and harvest are uncertain under warming climatic conditions. These potential changes will depend on future crop cultivars, water availability, and economics. For these reasons, 'static phenology' annual crop $K_{cb}$ curves were simulated for future periods, where historical baseline temperatures were used for simulating planting, crop development and harvest dates using the GDD approach previously described. In effect, all scenarios and time periods have identical seasonal $K_{cb}$ curve shapes for each annual crop, and only exhibit differences in daily $ET_c$ magnitudes due to daily $ET_o$ and precipitation differences. A detailed discussion on this 'static phenology' approach is included in Reclamation (2015).

The future irrigation demands results cover mean annual precipitation, temperature, $ET_o$, $ET_c$, and NIWR. The future $ET_o$, $ET_c$ and NIWR sub-basin and basin total estimates were calculated using the same methods as for the historical baseline values. Specifically, the NIWR depth and $ET_c$ rates for each crop within a given HUC8 sub-basin are multiplied by the ratio of the acres of the crop to total irrigated acres within the HUC8 sub-basin and all crop values are summed to calculate weighted average HUC8 sub-basin NIWR depth and $ET_c$ rates. And $ET_o$, $ET_c$ and NIWR depth estimates for the entire basin were calculated using the ratios of sub-basin to basin irrigated acres.

The results are summarized below and in figures (Figures 19-23) showing predicted changes from historical baseline values. Predicted changes are presented as the difference from historical baseline mean values for temperature, and percent change from baseline mean values for all other results. Appendix B contains tabulated summaries of the projected future estimates of annual average T, P, $ET_o$, $ET_c$, and NIWR depth for each HUC8 sub-basin. And again, the five future scenarios are hot-dry (HD), hot-wet (HW), central tendency (CT), warm-dry (WD) and warm-wet (WW).

Figure 19 shows the spatial distribution of projected average temperature change for the different climate scenarios. Increased temperatures are shown for all scenarios with slightly larger projected average temperature changes in the western portion of the basin for all scenarios. Depending on the scenario, basin-wide annual average temperature changes range from 2.2 to 5.4 degrees Fahrenheit with the central tendency future scenario basin-wide annual average estimate of 67.5 degrees increasing 3.8 degrees F from the baseline value of 63.7 degrees F.

Figure 20 shows the spatial distribution of projected precipitation percent change for the different scenarios. Depending on the scenario, precipitation percent changes range from -19.1% to 7.2%. The central tendency future scenario basin-wide annual average estimate of 14.1 inches is 0.6 inches less than the baseline value of 14.7 inches.

Figure 21 shows the spatial distribution of projected $ET_o$ percent change for the different climate scenarios. Depending on the scenario, basin-wide average $ET_o$ percent changes range from 3.2% to 6.9% with the central tendency future scenario basin-wide annual average estimate increasing 3.1 inches from the baseline value of 69.1 inches.

Figure 22 shows the spatial distribution of projected $ET_c$ percent change for the different climate scenarios. Spatial differences in the distribution of projected percent change in $ET_c$ are due to differences in $ET_o$, crop types and historical baseline $ET_c$. Depending on the scenario, basin-wide average $ET_c$ percent changes range from 1.8% to 14.7% with the central tendency future scenario basin-wide annual average estimate of 53.3 inches increasing 3.2 inches from the baseline value of 50.1 inches.

Figure 23 shows the spatial distribution of projected NIWR depth percent change for the different climate scenarios. Spatial differences in the distribution of projected percent change in NIWR depth are a function of $ET_c$ and precipitation. Depending on the scenario, basin-wide average NIWR depth percent changes range from 3.2% to 22.0% with the central tendency future scenario basin-wide annual average estimate of 41.8 inches increasing 3.3 inches from the baseline value of 38.5 inches.

# CHAPTER 9. SUMMARY

Climate change scenarios for the West Salt River Valley Basin Study hydrologic analyses were developed based on CMIP5 projections using the ensemble informed hybrid delta (HDe) method. Five climate change scenarios were derived using the future period defined by the 30-year range, 2045-2074, and the historical period of record (50 years), 1950-1999. Table 1 summarizes projected precipitation and temperature changes for these five scenarios. All five scenarios indicate warmer mean annual basin wide temperatures than the historical (1950-1999) value of 59.3 °F, ranging from an increase of 2.8 to 6.9 °F. Changes in projected mean annual basin wide precipitation range from -12.9 to +10.0 percent change from the historical value of 15.9 inches.

The VIC surface water hydrologic model was subsequently used to generate five HDe hydrology scenarios based on the associated HDe climate change scenarios. Simulated routed streamflows were developed at 16 stream locations (Figure 2, Table 2) for historical baseline conditions and the five HDe climate change scenarios. Monthly streamflow results for the stream locations are shown in Figure 10 and 11 and in Appendix A. Generally, the warm-wet (WW) scenario produces the largest streamflow in the winter and spring months with the hot-wet (HW) scenario producing the largest streamflows in the summer and early fall months. The smallest streamflows are usually seen in the hot-dry (HD) scenario. The baseline and central tendency streamflow results are generally similar.

SAC-SMA streamflow simulations for the Agua Fria, Verde, and Salt Rivers for five HDe hydrology scenarios were produced and compared with VIC simulation results to explore the effects of using different models and parameterizations on simulated streamflow results. In general, the shape of the mean monthly streamflow traces (Figures 13-15) are similar between the SAC-SMA and VIC results. The VIC streamflows have greater variability in most months compared to the SAC-SMA streamflows.

Estimated agricultural irrigation demands under climate change scenarios for the study area are summarized here from a previous effort (Reclamation, 2014) that is based on CMIP3 projections. Results from this work for the HUC8 sub-basins (Figure 16) that fall within the WSRVBS study area are presented.

Results from five HDe-based demand scenarios are presented using the future period defined by the 30-year range, 2040-2069, and the historical period of record (50 years), 1950-1999. All five scenarios indicate warmer mean annual basin wide temperatures than the historical, ranging from an increase of 2.2 to 5.4 °F. Changes in projected mean annual basin wide precipitation range from -19.1

to +7.2 percent change from the historical value of 14.7 inches.  The basin-wide average NIWR depth percent changes range from 3.2% to 22.0%.

# CHAPTER 10. UNCERTAINTY

The information presented in this report was peer reviewed in accordance with the Bureau of Reclamation and Department of the Interior polices. This report is intended to inform and support planning for the future by identifying potential future scenarios. The analyses provided in this report reflect the use of best available datasets and methodologies at the time of the study.

## 10.1. GCMs and Climate Downscaling

Water resources studies are developed to evaluate potential future scenarios to assess risks and potential actions that can be taken to minimize impacts, including supply and demand imbalances. These types of studies support a proactive approach to water resources management, using the best available science and information to develop scenarios of future conditions within the watershed. This positions communities to take steps now to mitigate the impacts of future water supply management issues, including water shortages, impacts of droughts and floods, variations in water supply, and changing water demands for water for new or different uses.

Because every water resources planning study requires the study partners to make assumptions about future conditions, addressing the uncertainties in those assumptions is an essential component of the planning process. For example, there are uncertainties associated with the characterization of future water supply and demand, demographics, environmental and other policies, economic projections, climate conditions, and land use, to name a few. Moreover, projections are often developed using modeling techniques that themselves are only potential representations of a particular process or variable, and therefore, introduce additional uncertainties into characterizations of the future. The cumulative effect of these interacting uncertainties is not yet well known in the scientific community and are not presented within this study. However, by recognizing this at each process step, uncertainties are adjusted for and reduced when possible, to allow Reclamation and its stakeholders to use the best available science to create a range of possible future risks that can be used to help identify appropriate adaptation strategies, which is fundamental to the planning process. Importantly, scenarios of future conditions should not be interpreted as a prediction of the future, nor is the goal of any water resources planning study to focus on a singular future. Rather the goal is to plan for a range of possible conditions, thereby providing decision support tools for water managers.

Of significant interest are projections of future climate, which ultimately drive many assumptions of water supplies and demands through their influence on the water cycle. Projections of future climate are developed using the scientific communities' best assessment of potential future conditions as characterized by global climate models (GCMs). GCM projections are based upon initial model states, assumptions of future greenhouse gases in the atmosphere, and internal as well as external forcings, such as solar radiation and volcanic activity to name just a few. Changes in land surface, atmosphere, and ocean dynamics, as well as how such changes are best modeled in GCMs continue to be areas of active research. Depending on these and other uncertainties, projected future conditions, such as the magnitude of temperature and precipitation changes, may vary.

Observed climatic data and GCM simulations show warming trends over recent decades. However, the degree to which the magnitude of GCM simulated warming agrees with historic observations[3] varies based on the data, methods, and time periods used for making such comparisons. Some recent studies have found that models have simulated higher rates of temperature increases relative to observations (Santer et al., 2014a, 2014b); another study has shown that current warming is within a range of model simulations (Lin et al., 2016); and yet other studies, have shown the observed and projected warming rates to be similar (Richardson et al., 2016) The evaluation and refinement of GCM performance is an ongoing area of research and includes methods to characterize model outputs and observations, and how measurement errors, internal variability, and model forcings can be improved to enhance future performance (Santer et al., 1014b).

Further, it is important to recognize that these models perform better at global rather than regional or watershed level scales. Accordingly, techniques must be employed to localize or "downscale" GCM output for applications such as basin-specific water resources planning studies. These downscaled projections of climate are used as inputs to hydrologic models to produce projected streamflows, which are then used to assess impacts to the water resource system in question. Uncertainties at each of the steps necessary to translate GCM output to water resources impacts can be characterized and adjusted for, yet uncertainties remain in the downscaling process that can result in variations depending on the modeling technique used.

Ultimately, future conditions at any particular time or place cannot be known exactly, given the current scientific understanding of potential future conditions. Likewise, it is important to recognize that the risks and impacts are the result of collective changes at a given location. Warming and increased carbon dioxide may increase plant water use efficiency, lengthen the agricultural growing season, but may also have adverse effects on snowpack and water availability. These complex interactions underscore the importance of using a planning approach that identifies future risks to water resources systems based on a range of plausible future conditions, and working with stakeholders to evaluate options that minimize potential impacts in ways most suitable for all stakeholders involved.

## 10.2. Hydrologic Modeling

An important result in research on the hydrologic impacts of climate change is that the portrayal of climate change impacts depends on the decisions made on the selection, configuration, and calibration of hydrologic models (Wilby 2005; Miller et al. 2012; Vano et al. 2014; Mendoza et al. 2015). In one of the earliest studies, Wilby (2005) demonstrated that parameter uncertainties have a large impact on the portrayal of climate change impacts. Subsequent work has demonstrated that the portrayal of climate change impacts also depends on the choice of hydrologic models and on specific decisions made in model calibration (Miller et al. 2012; Vano et al. 2014; Mendoza et al., 2015). For a variety of reasons, hydrologic model calibration often receives inadequate attention in climate change impact assessments, with potential first-order effects on the estimation of future hydrologic responses.

The uncertainties in hydrologic modeling stem from both algorithmic simplifications of hydrologic theory and data limitations (Clark et al. 2016). Considerations of parsimony may compel modelers to neglect specific processes (e.g., groundwater-surface water interactions, carbon fertilization). Moreover, data limitations constrain the extent that it is possible to adequately capture the details of the landscape, and especially, define appropriate model parameter values. Specifically, inter-model differences occur because different modelers have made model development decisions in different ways, as manifested in different spatial discretizations, process parameterizations, model parameter values, and time-stepping schemes (Clark et al. 2011). It is now possible to use multiple hypothesis-modeling frameworks to deliberately and systematically characterize uncertainties in physically motivated hydrologic models (Clark et al. 2015a; Clark et al. 2015b), and such work will be important to improve the realism of the portrayal of climate risk.

The problem confronting practitioners and decision-makers is that the projection uncertainty space (i.e., the combined uncertainty arising from uncertainties present at each step in the analysis) has expanded as research reveals a fuller range of uncertainties associated with the identified modeling steps. It is important to acknowledge that our current analytical approach provides only a limited view of the uncertainty space. For example, the trend toward using multiple hydrologic models rather than a single model (the standard approach for many prior studies, as well as this one) has confirmed that a single hydrologic model selection erroneously narrows the final projection uncertainty space by failing to represent the hydrologic sensitivities that would be estimated through different modeling choices. As the impact assessment community continues to formulate strategies toward reducing projection uncertainty, it is nonetheless critical now to gain a better understanding the full extent and sources of uncertainty, which likely are more significant than the present approach assumes.

## 10.3. Demands

There are numerous uncertainties and limitations in modeling $ET_o$, $ET_c$, and NIWR. One source of uncertainty is associated with underlying assumptions in modeling; for example, static cropping patterns and farming practices. This study uses data from the USDA crop land data layer and OWRB water rights data as the sources for quantifying the types of irrigated crops grown in the basin. It is assumed these crop types and quantities do not change in the modeling. Obviously, increases or decreases in the overall amounts irrigated areas would result in respective changes in demands. Changes in crop choice may significantly affect future agricultural demands given the variability in water demand for different crop types.

Another source of uncertainty is the weighted average soil conditions used in the estimation of NIWR. Precipitation runoff and soil water holding capacity are a function of soil type and soil types can vary significantly even within a single irrigated parcel of land. The degree of uncertainty in the method used depends on the variability of soil types within each HUC8 sub-basin for which a weighted average soil type was calculated as described in Reclamation (2014).

Climatic data used in this basin study analysis were limited to daily maximum and minimum temperatures and daily precipitation; therefore, solar radiation, humidity, and windspeed were approximated for baseline and future time periods using empirical approaches. Solar radiation was simulated for baseline and future periods based on empirical relationships of differences between daily maximum and minimum air temperatures, where maximum air temperature generally decreases during cloud cover, and minimum temperature is increased due to increased downward emission of long wave radiation by clouds at night. Integration of potential changes in solar radiation, and evaluating the potential impact of such changes on irrigation water demands was not addressed in this analysis.

Historical agricultural weather station data were used to estimate the spatial distribution of baseline and projected mean monthly dewpoint depression and windspeed. Given the uncertainties and limited availability in future projections of humidity and windspeed, mean monthly dewpoint depression and windspeed were considered static for future periods. While there is considerable uncertainty in projecting future reference ET, estimation of reference ET for historical periods using assumptions outlined above was shown to be robust when compared to agricultural weather station estimated reference ET.

An important limitation in the application of the ET Demands model for this assessment is the lack of consideration as to how $CO_2$ potentially impacts crop development and water use. The impact of increased $CO_2$ on crop transpiration, water use efficiency, and yield is of particular interest and is probably one of the largest uncertainties. Recent studies have described how elevated $CO_2$

concentrations may reduce stomatal aperture, transpiration, and crop production processes (Kruijt et al. 2008 and Islam et al. 2012). However, estimating $CO_2$-induced changes on irrigation demands remains an extremely difficult task because of plant dependency, adaptation, unknown non-linear near-surface boundary-layer feedbacks from reduced transpiration and resulting increased leaf temperatures and vapor pressure deficits, uncertainties of increased leaf area index, stomatal and aerodynamic resistances, and plant-dependent stomatal sensitivities (i.e., C3 versus C4 plants). For these reasons, this study focused on major change factors and considerations such as physically based reference ET estimation, temperature-dependent growing seasons and crop development, bare soil evaporation, and non-growing-season soil moisture accounting for better representation of monthly and annual net irrigation water requirements. Addressing the impacts of $CO_2$ on irrigation water demands is currently, and will be, the focus of further Reclamation studies.

(page intentionally left blank)

# CHAPTER 11. REFERENCES

Allen, R.G., L.S. Pereira, D. Raes, and M. Smith. 1998. "Crop Evapotranspiration: Guidelines for Computing Crop Water Requirements," FAO Irrigation and Drainage Paper 56, Food and Agriculture Organization of the United Nations, Rome, 300 p.

Anderson, E. A. 1973. "National Weather Service River Forecast System— Snow Accumulation and Ablation Model," NOAA Technical Memorandum NWS Hydro-17, Dept. of Commerce, Silver Spring, Maryland.

Andreadis K., P. Storck, and D.P. Lettenmaier. 2009. Modeling snow accumulation and ablation processes in forested environments, *Water Resources Research*, 45, W05429, doi:10.1029/2008WR007042.

ASCE-EWRI (Environmental and Water Resources Institute of the American Society of Civil Engineers). 2005. The ASCE Standardized Reference Evapotranspiration Equation, Report 0-7844-0805-X, ASCE Task Committee on Standardization of Reference Evapotranspiration, Reston, Virginia., American Soc. Civil Engineers.

Cherkauer K.A., L.C. Bowling, D.P. Lettenmaier. 2003. Variable Infiltration Capacity (VIC) cold land process model updates. *Global Planetary Change*, 38(1–2):151–159.

Clark, M. P., D. Kavetski, and F. Fenicia, 2011: Pursuing the method of multiple working hypotheses for hydrological modeling. Water Resources Research, 47, doi: 10.1029/2010WR009827.

Clark, M. P., B. Nijssen, J. Lundquist, D. Kavetski, D. Rupp, R. Woods, E. Gutmann, A. Wood, L. Brekke, J. Arnold, D. Gochis, and R. Rasmussen, West-Wide Climate Risk Assessments: Hydroclimate Projections 134 2015a: A unified approach to process-based hydrologic modeling. Part 1: Modeling concept. Water Resources Research, 51, doi: 10.1002/2015WR017198.

Clark, M. P., B. Nijssen, J. Lundquist, D. Kavetski, D. Rupp, R. Woods, E. Gutmann, A. Wood, D. Gochis, R. Rasmussen, D. Tarboton, V. Mahat, G. Flerchinger, and D. Marks, 2015b: A unified approach for process-based hydrologic modeling: Part 2. Model implementation and example applications. Water Resources Research, 51, doi: 10.1002/2015WR017200.

Clark, M. P., B. Schaefli, S. J. Schymanski, L. Samaniego, C. H. Luce, B. M. Jackson, J. E. Freer, J. R. Arnold, R. Dan Moore, E. Istanbulluoglu, and S. Ceola, 2016: Improving the theoretical underpinnings of process-based hydrologic models. Water Resources Research, doi: 10.1002/2015WR017910.

Crawford, N., and R. Linsley 1966. "Digital Simulation in Hydrology: Stanford Watershed Model IV," Stanford University, Dept. of Civil Engineering Tech. Report 39.

Hamlet, A.F., M.M. Elsner, G.S. Mauger, S.Y. Lee, I. Tohver, and R.A. Norheim. 2013. An overview of the Columbia Basin Climate Change Scenarios Project: Approach, methods, and summary of key results. *Atmosphere-ocean* 51(4): 392-415.

Intergovernmental Panel on Climate Change (IPCC), 2000. Emissions Scenarios. Special Report of the Intergovernmental Panel on Climate Change, Nebojsa Nakicenovic and Rob Swart (eds.), Cambridge University Press, Cambridge, United Kingdom, and New York, New York, USA, 570 p.

Intergovernmental Panel on Climate Change (IPCC). 2007. Climate Change 2007: Synthesis Report. Contribution of Working Groups I, II and III to the Fourth Assessment Report of the Intergovernmental Panel on Climate Change [Core Writing Team, Pachauri, R.K and Reisinger, A. (eds.)]. IPCC, Geneva, Switzerland, 104 pp.

Knutti R. and J. Sedlacek. 2012. Robustness and uncertainties in the new CMIP5 climate model projections. *Nature Climate Change,* 3:369–373.

Liang X., Lettenmaier D.P.,Wood E.F., and S.J. Burges. 1994. A simple hydrologically based model of land surface water and energy fluxes for GCMs. *Journal of Geophysical Research,* 99(D7): 14,415–14,428

Liang X., Wood E.F., and D.P. Lettenmaier. 1996. Surface soil moisture parameterization of the VIC-2L model: evaluation and modifications. *Global Planetary Change*, 13:195–206.

Lin M, Huybers P 2016. Revisiting Whether Recent Surface Temperature Trends Agree with the CMIP5 Ensemble. Journal of Climate, 29, 8673–8687.

Lohmann, D., R. Nolte-Holube, and E. Raschke. 1996. A large-scale horizontal routing model to be coupled to land surface parameterization schemes. *Tellus*, 48 A, pp. 708–72.

Maidment, D.R. (ed.). 1993. *Handbook of Hydrology*, McGraw-Hill, New York, New York, 1424 pp.

Maurer, E.P., A.W. Wood, J.C. Adam, D.P. Lettenmaier, and B. Nijssen. 2002. "A Long-Term Hydrologically-Based Data Set of Land Surface Fluxes and States for the Conterminous United States," *Journal of Climate* 15(22):3237–3251.

Meehl, G. A., C. Covey, T. Delworth, M. Latif, B. McAvaney, J. F. B. Mitchell, R. J. Stouffer, and K. E. Taylor. 2007. The WCRP CMIP3 multi-model dataset: A new era in climate change research, *Bulletin of the American Meteorological Society*, 88, 1383-1394.

Mendoza, P. A., M. P. Clark, N. Mizukami, A. J. Newman, M. Barlage, E. D. Gutmann, R. M. Rasmussen, B. Rajagopalan, L. D. Brekke, and J. R. Arnold, 2015: Effects of hydrologic model choice and calibration on the portrayal of climate change impacts. Journal of Hydrometeorology, 16, 762-780.

Miller, W. P., R. A. Butler, T. Piechota, J. Prairie, K. Grantz, and G. DeRosa, 2012: Water management decisions using multiple hydrologic models within the San Juan River basin under changing climate conditions. Journal of Water Resources Planning and Management, 138, 412-420.

Nijssen B.N., D.P. Lettenmaier, X. Liang, S.W. Wetzel, and E.F. Wood. 1997. Streamflow simulation for continental-scale river basins. *Water Resoures Research*, 33(4):711–724.

Reclamation (Bureau of Reclamation). 2010a. *Climate Change and Hydrology Scenarios for Oklahoma Yield Studies.* Technical Memorandum No. 86-68210-2010-01. Technical Service Center, Denver, Colorado, April 2010.

Reclamation (Bureau of Reclamation). 2010b. *Climate Change Analysis for the St. Mary and Milk River Systems in Montana.* Technical Memorandum No. 86-68210-2010-04. Technical Service Center, Denver, Colorado, August 2010.

Reclamation (Bureau of Reclamation). 2011. *West-wide Climate Risk Assessments: Bias-Corrected and Spatially Downscaled Surface Water Projections. Technical Memorandum No. 86-68210-2011-01*, Reclamation Technical Service Center, Denver, Colorado. 122 pp. March 2011.

Reclamation (Bureau of Reclamation), 2012. Colorado River Basin Water Supply and Demand Study, Executive Summary, 34 p.

Reclamation (Bureau of Reclamation), 2013. Literature Synthesis on Climate Change Implications for Water and Environmental Resources Third Edition. Technical Memorandum 86-68210-2013-06. Prepared by Technical Service Center, Denver, CO.

Reclamation (Bureau of Reclamation), 2015. "West-Wide Climate Risk Assessments: Bias-Corrected and Spatially Downscaled Irrigation and Open Water Demand Projections."

Reclamation (Bureau of Reclamation), 2016. "West-Wide Climate Risk Assessments: Hydroclimate Projections." Technical Memorandum No. 86-68210-01.

Rosenberg, N.J. 1987. Climate of the Great Plains Region of the United States. Great Plains Quarterly. Paper 344. http://digitalcommons.unl.edu/greatplainsquarterly/344.

Richardson M, Cowtan K, Hawkins E, Stolpe MB, 2016. Reconciled climate response estimates from climate models and the energy budget of Earth. Nature Climate Change, 6, 931–935.

Santer, B.D., Solomon, S., Pallotta, G., Mears, C., Po-Chedley, S., Fu, Q., Wentz, F., Zou, C.Z., Painter, J., Cvijanovic, I. and Bonfils, C., 2017. Comparing tropospheric warming in climate models and satellite data. Journal of Climate, 30(1), pp.373-392.

Santer, B.D., Fyfe, J.C., Pallotta, G., Flato, G.M., Meehl, G.A., England, M.H., Hawkins, E., Mann, M.E., Painter, J.F., Bonfils, C., Evijanovic, I., Mears, C., Wentz, F.J., Po-Chedley, S., Fu, Q., Zou, C.: 2017. Causes of differences in model and satellite tropospheric warming rates, Nature Geosciences, DOI: 10.1038/NGEO2973.

Shepard D.S. 1984. *Computer mapping: the SYMAP interpolation algorithm.* In: Willmott GL, Reidel CJ (eds) Spatial statistics and Models Gaille, pp 133–145.

USDA-NRCS (United States Department of Agriculture, Natural Resources Conservation Service). 1991. “State Soil Geographic (STATSGO) Data Base Data use information,” United States Department of Agriculture Natural Resources Conservation Service, National Soil Survey Center, Miscellaneous Publication number 1492.

USDA-SCS (United States Department of Agriculture, Soil Conservation Service). 1972. “National Engineering Handbook,” Section 4, Table 10.1.

Vano, J. A., B. Udall, D. R. Cayan, J. T. Overpeck, L. D. Brekke, T. Das, H. C. Hartmann, H. G. Hidalgo, M. Hoerling, and G. J. McCabe, 2014: Understanding uncertainties in future Colorado River streamflow. Bulletin of the American Meteorological Society, 95, 59-78.

Wilby, R. L., 2005: Uncertainty in water resource model parameters used for climate change impact assessment. Hydrological Processes, 19, 3201-3219.

Wigmosta, M.S., L.W. Vail, and D.P. Lettenmaier. 1994. A distributed hydrology vegetation model for complex terrain, *Water Resources Research*, 30:1665–1679.

# APPENDIX A. VIC SIMULATED STREAMFLOW GRAPHICS

(page intentionally left blank)

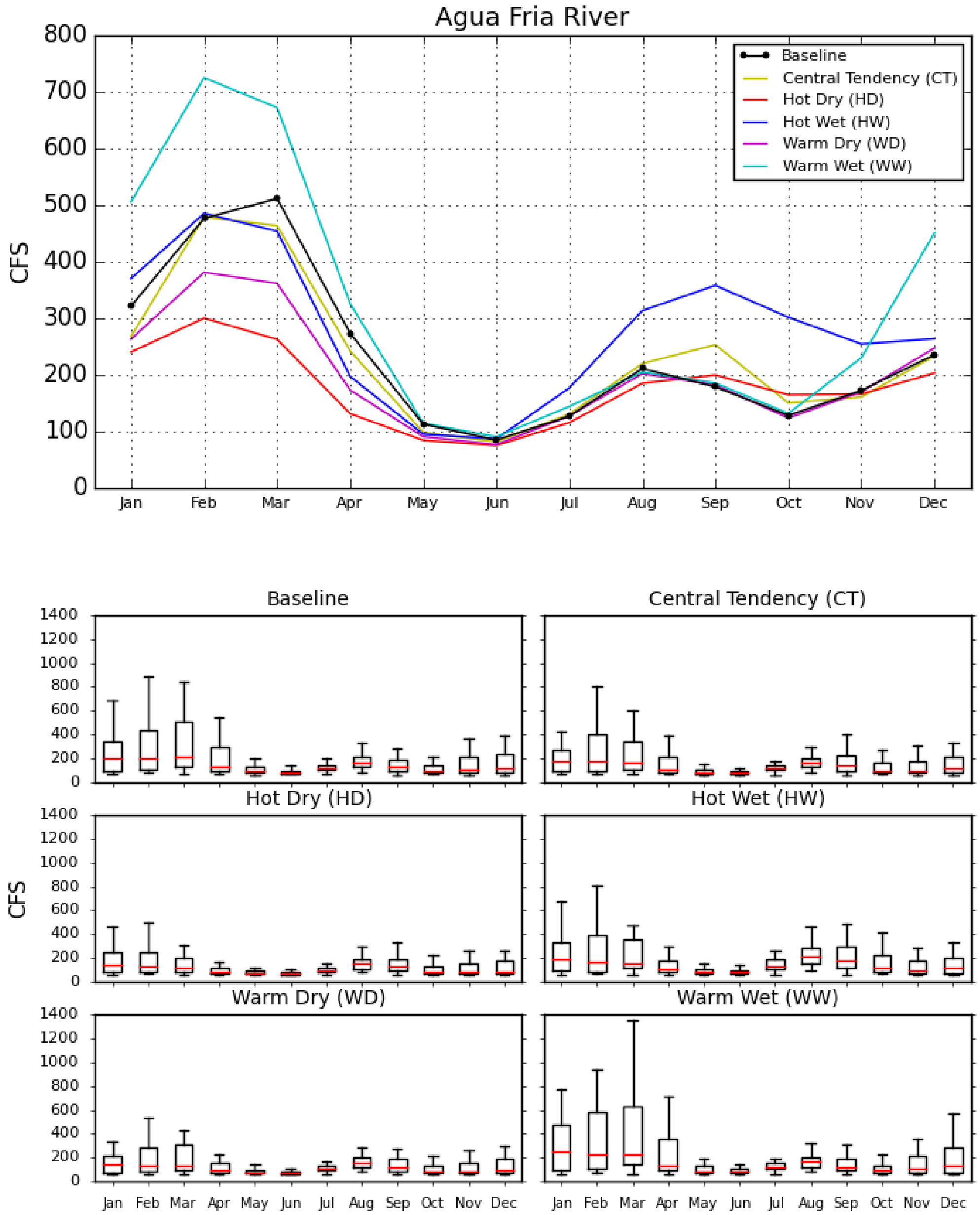


**Figure A1.—Monthly averages of streamflow for the baseline and five HDe climate change scenario simulations for the Agua Fria River site shown in Figure 1.**

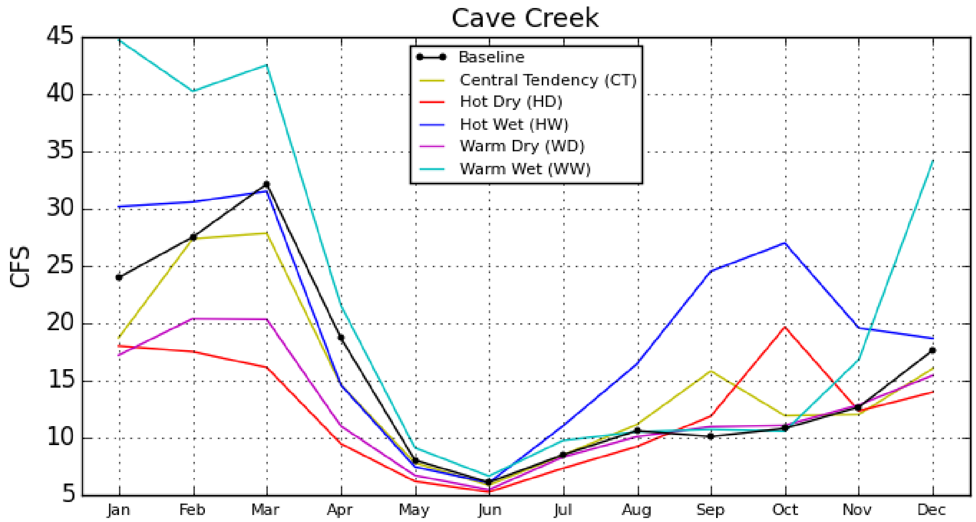


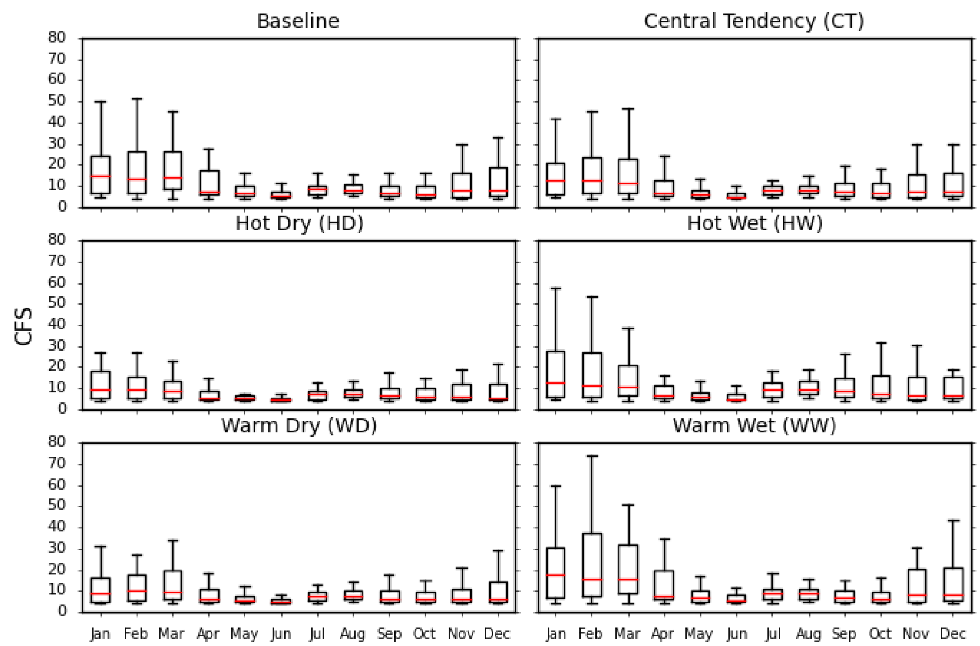


**Figure A2.—Monthly averages of streamflow for the baseline and five HDe climate change scenario simulations for the Cave Creek site shown in Figure 1.**

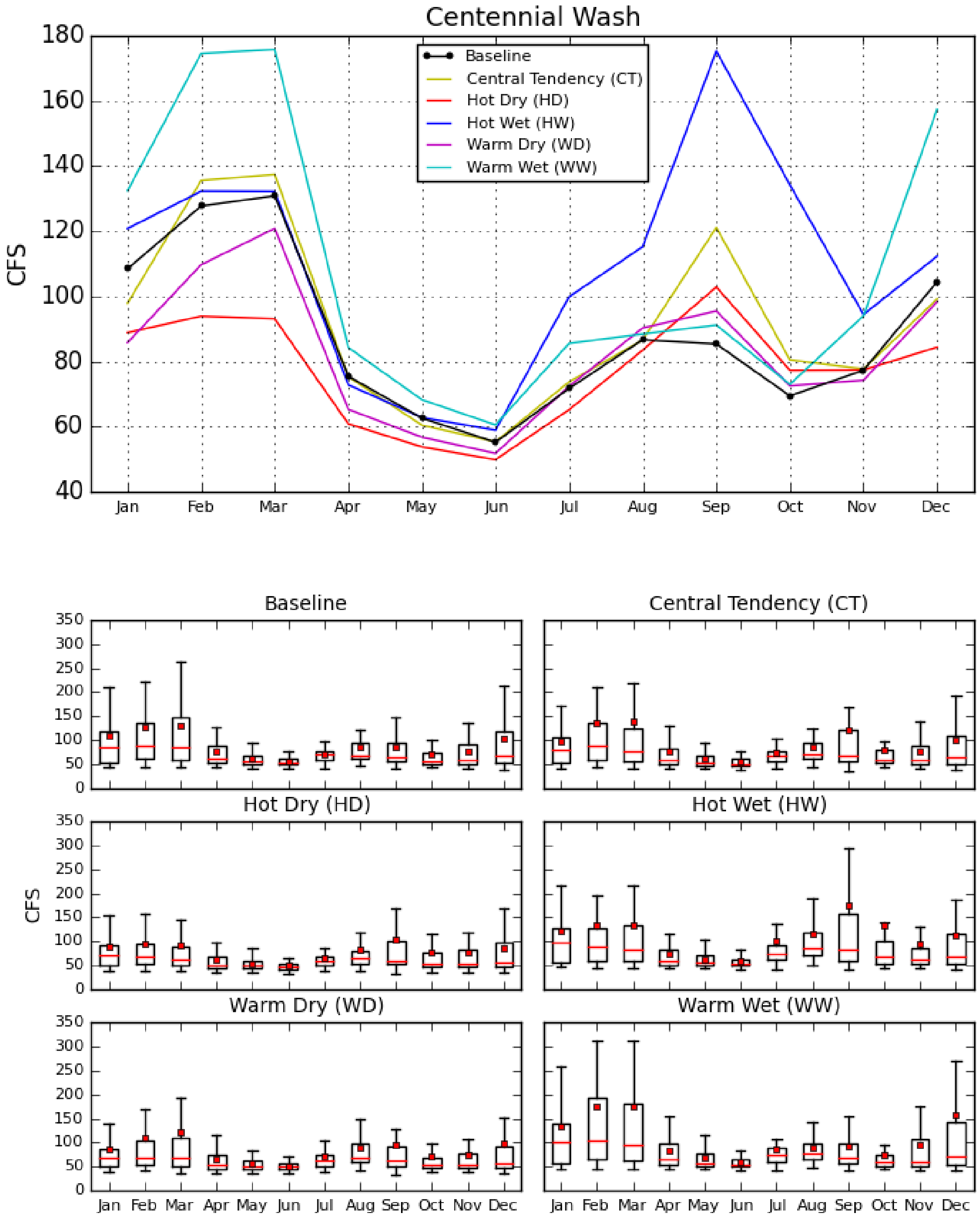


**Figure A3.—Monthly averages of streamflow for the baseline and five HDe climate change scenario simulations for the Centennial Wash site shown in Figure 1.**

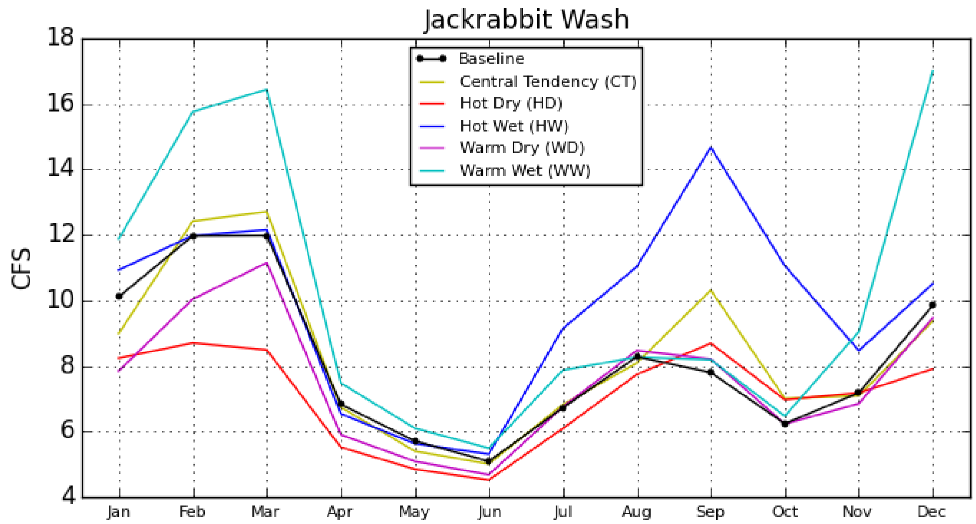


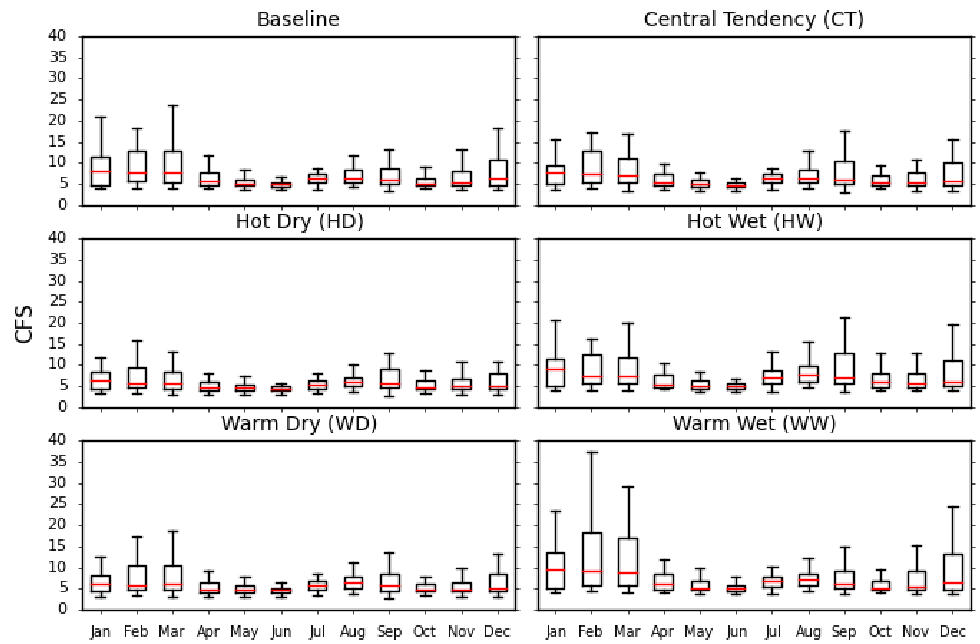


**Figure A4.—Monthly averages of streamflow for the baseline and five HDe climate change scenario simulations for the Jackrabbit Wash site shown in Figure 1.**

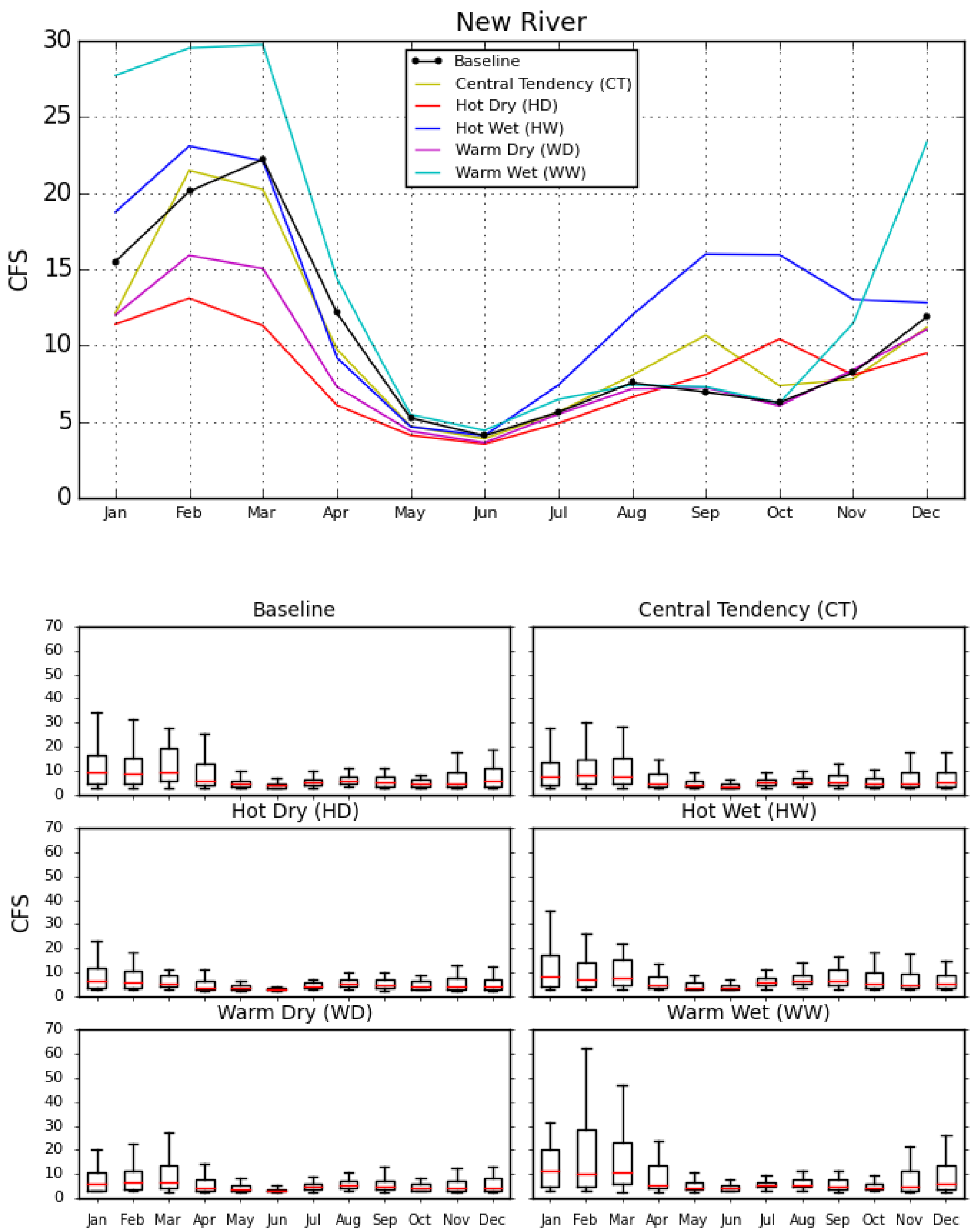


**Figure A5.—Monthly averages of streamflow for the baseline and five HDe climate change scenario simulations for the New River site shown in Figure 1.**

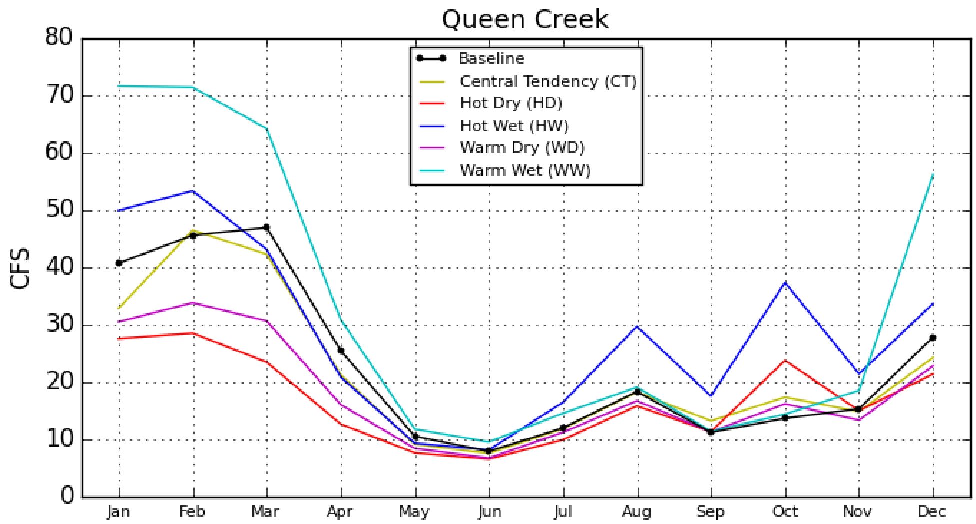


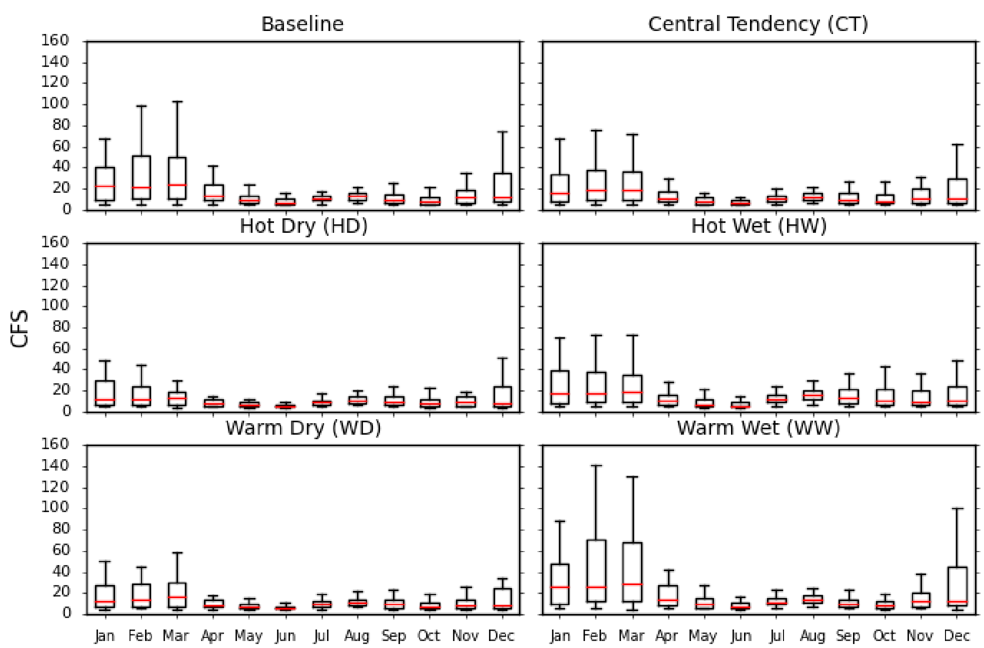


**Figure A6.—Monthly averages of streamflow for the baseline and five HDe climate change scenario simulations for the Queen Creek site shown in Figure 1.**

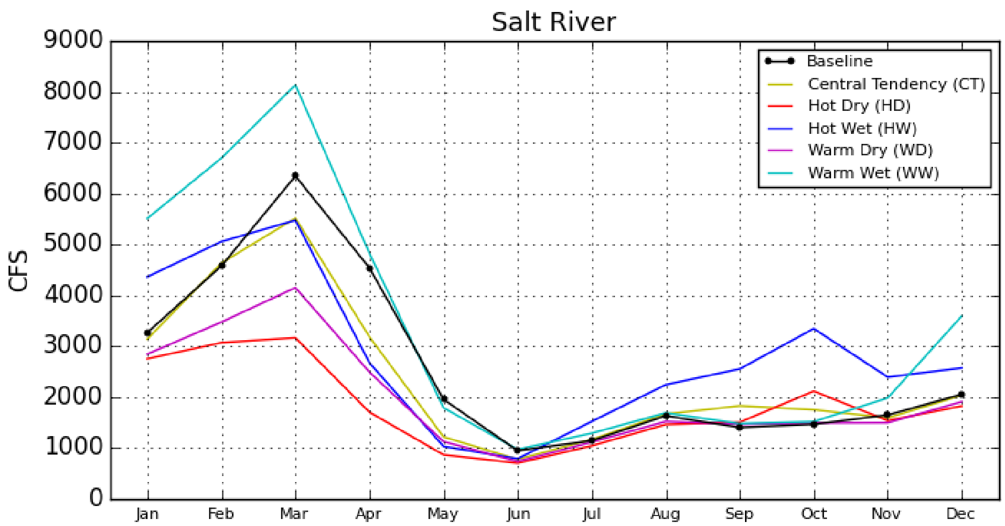


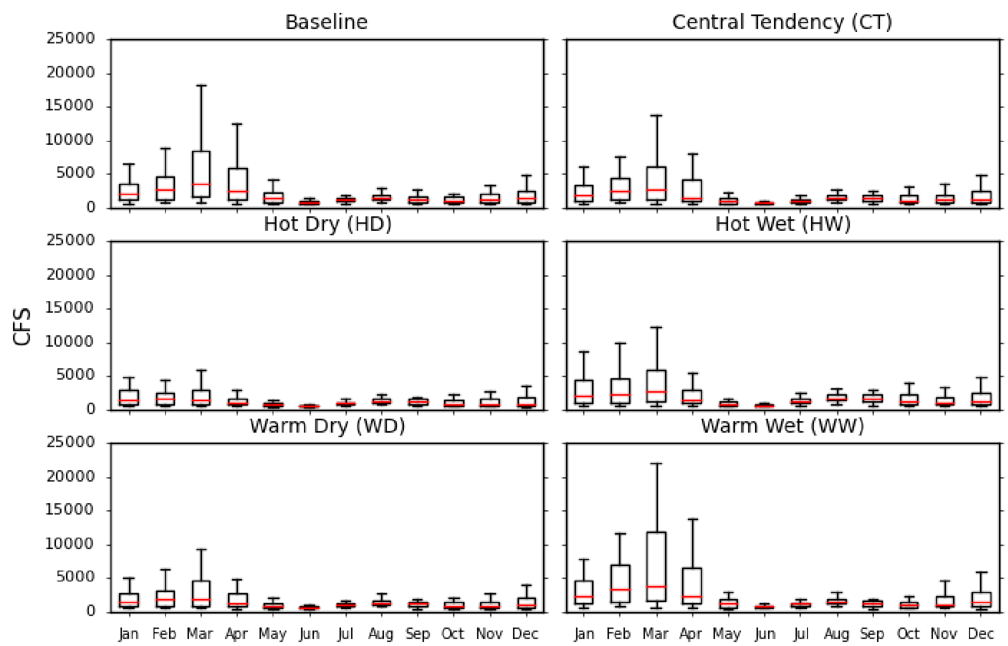


**Figure A7.—Monthly averages of streamflow for the baseline and five HDe climate change scenario simulations for the Salt River site shown in Figure 1.**

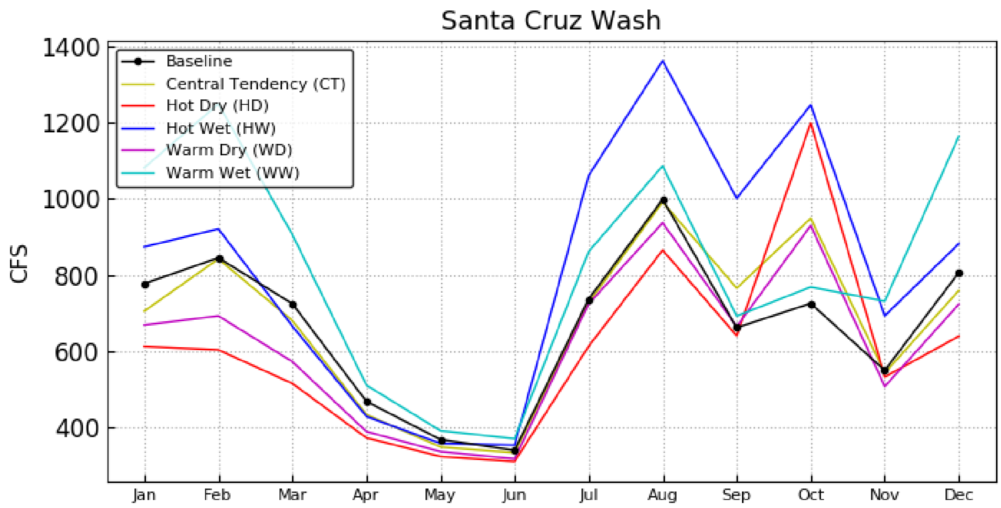


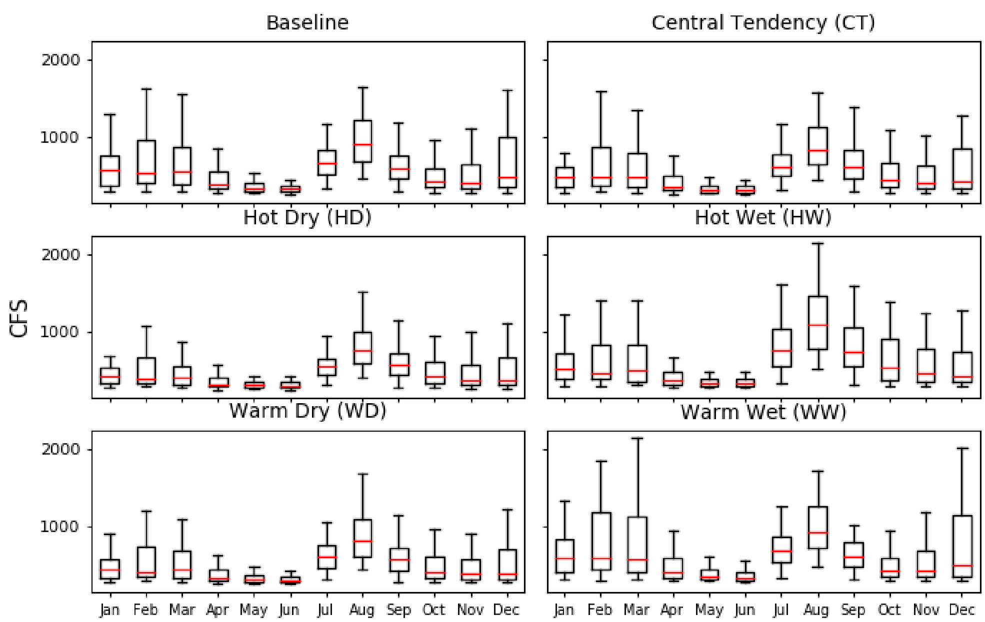


**Figure A8.—Monthly averages of streamflow for the baseline and five HDe climate change scenario simulations for the Santa Cruz Wash site shown in Figure 1.**

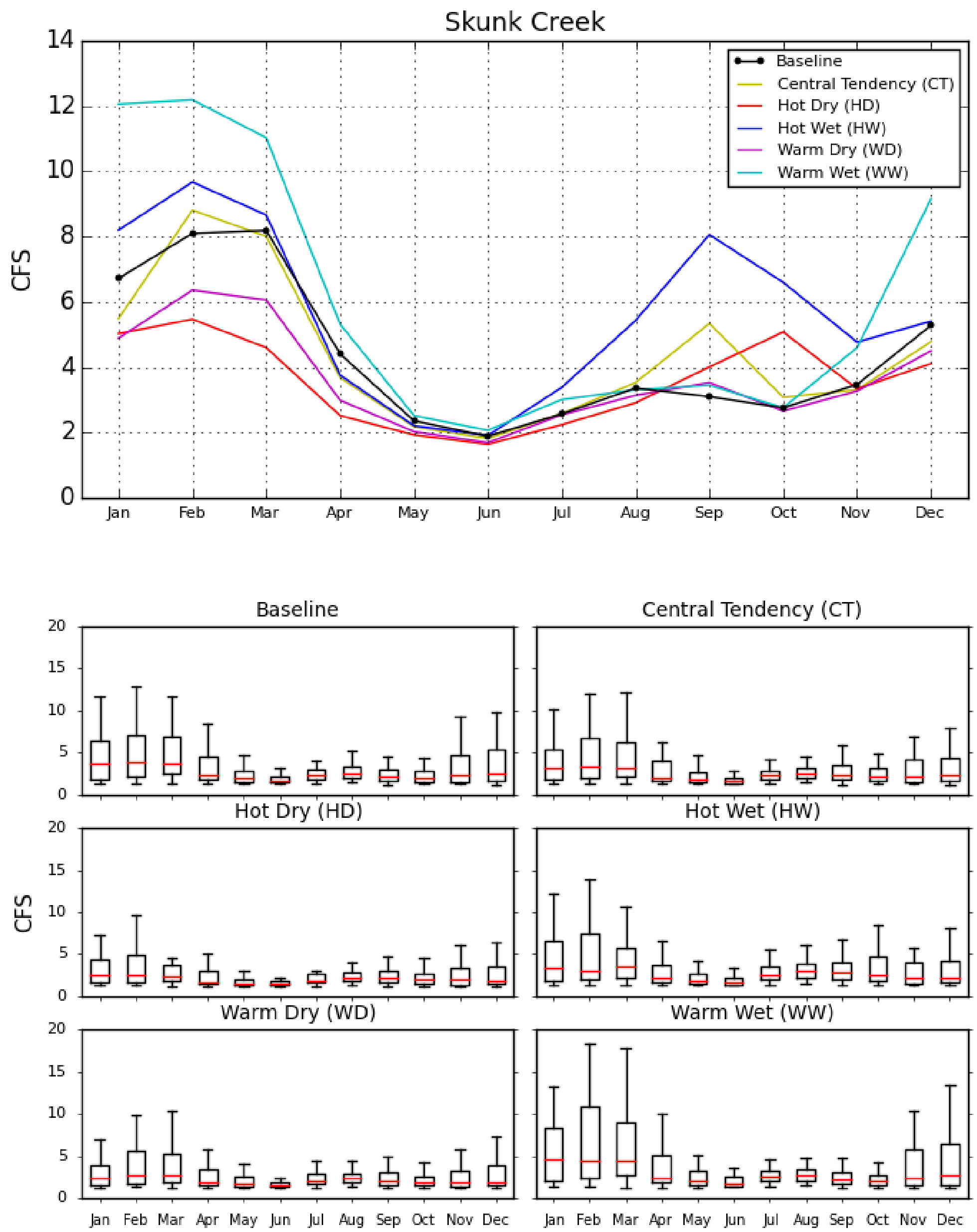


**Figure A9.—Monthly averages of streamflow for the baseline and five HDe climate change scenario simulations for the Skunk Creek site shown in Figure 1.**

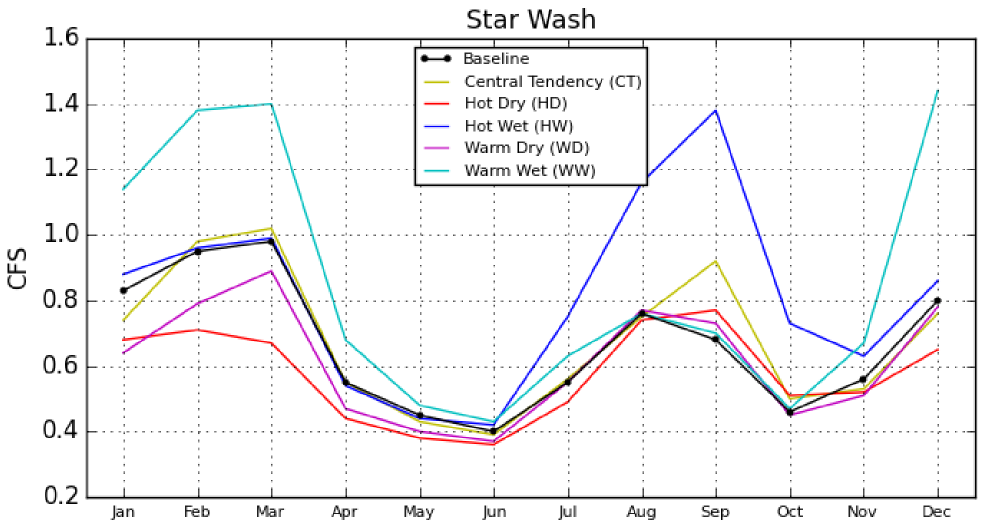


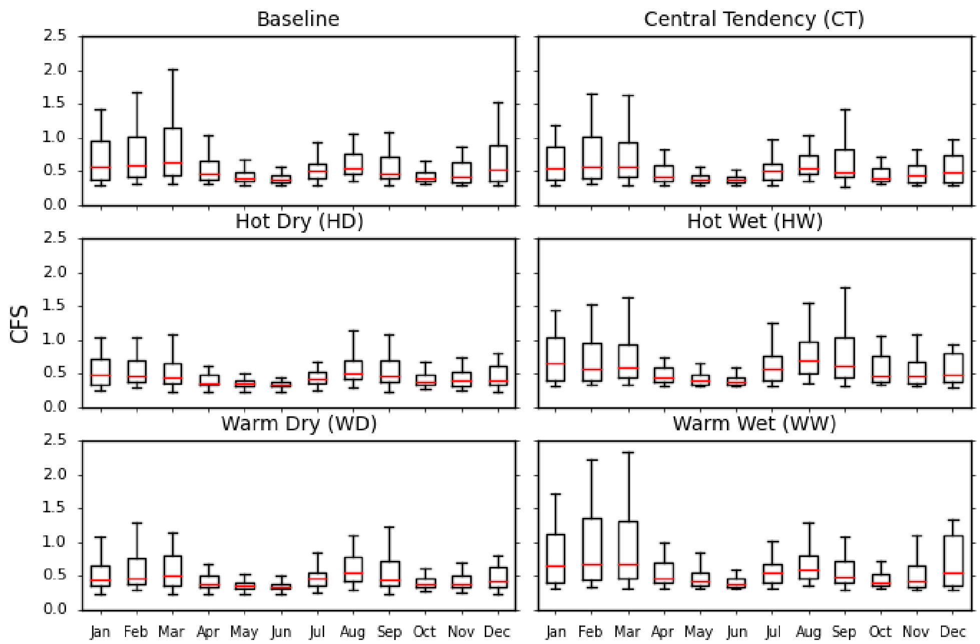


**Figure A10.—Monthly averages of streamflow for the baseline and five HDe climate change scenario simulations for the Star Wash site shown in Figure 1.**

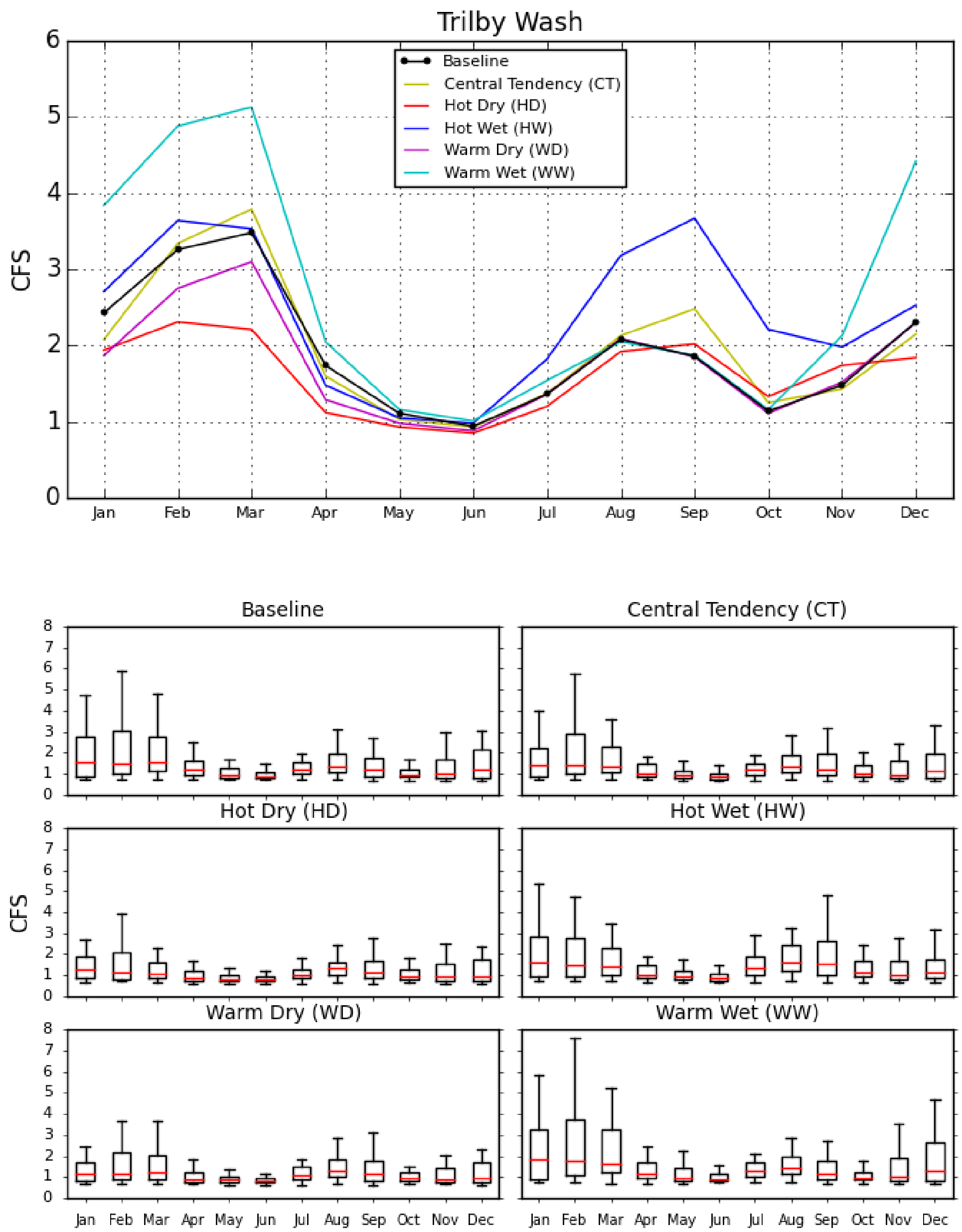


**Figure A11.—Monthly averages of streamflow for the baseline and five HDe climate change scenario simulations for the Trilby Wash site shown in Figure 1.**

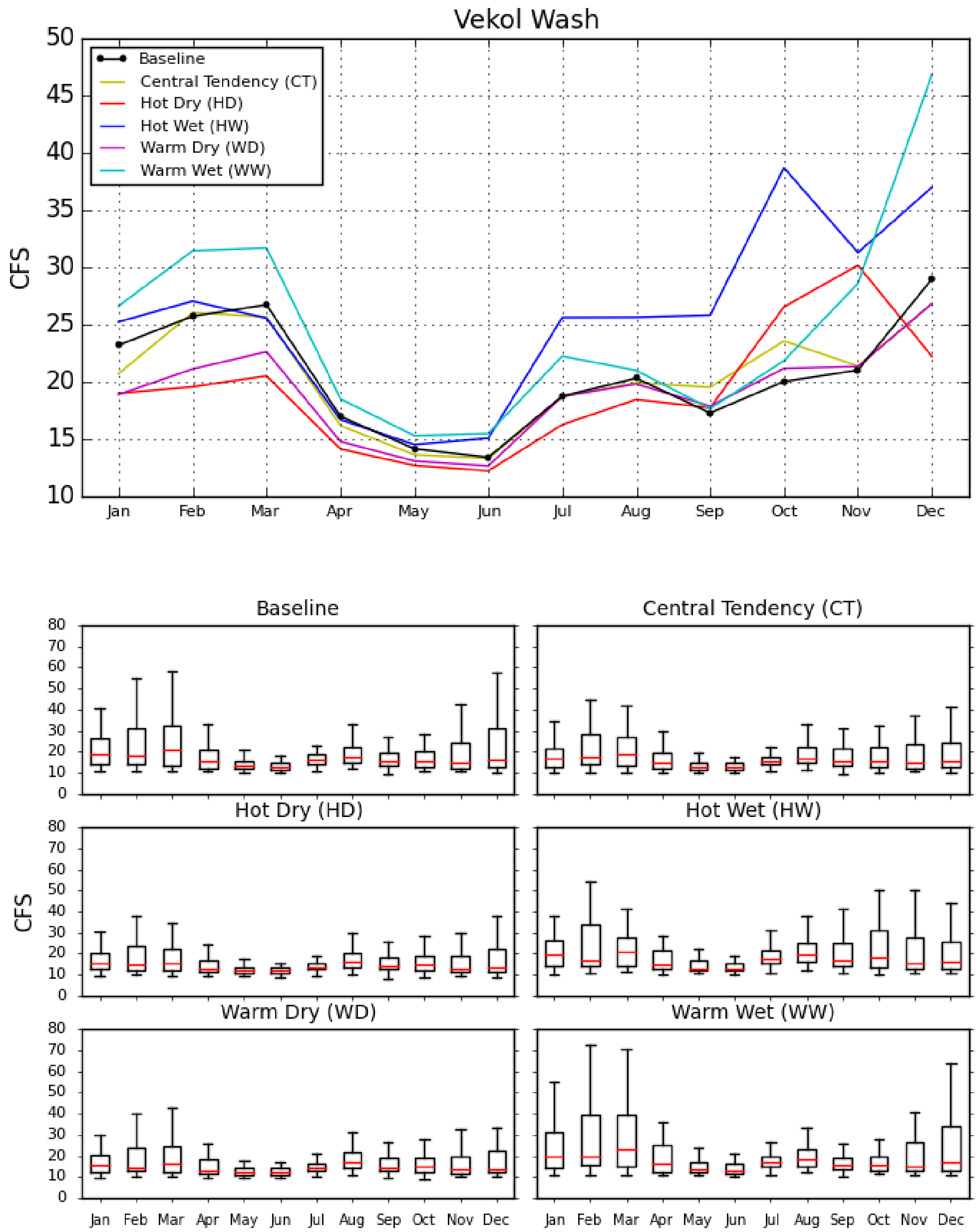


**Figure A12.—Monthly averages of streamflow for the baseline and five HDe climate change scenario simulations for the Vekol Wash site shown in Figure 1.**

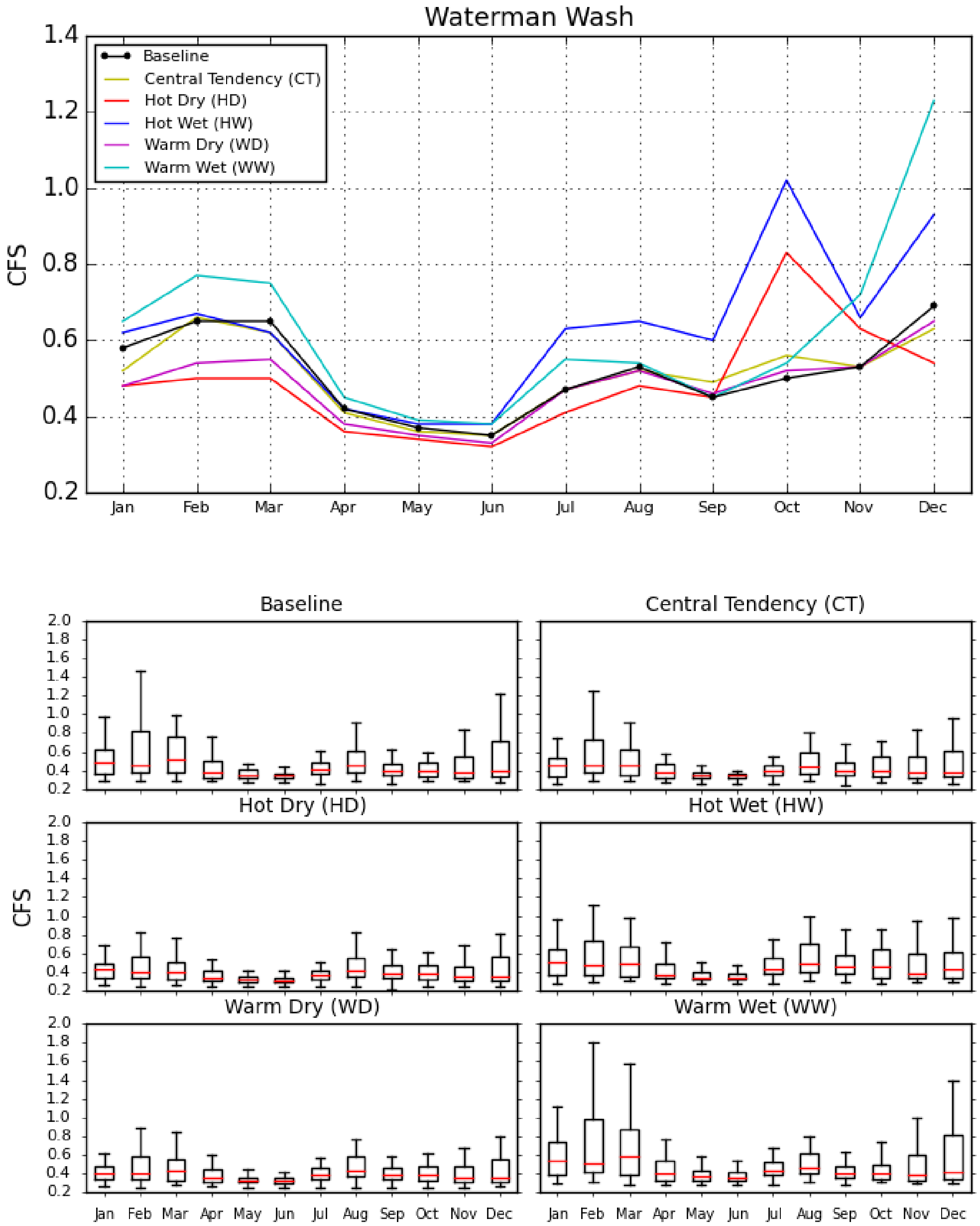


**Figure A13.—Monthly averages of streamflow for the baseline and five HDe climate change scenario simulations for the Waterman Wash site shown in Figure 1.**

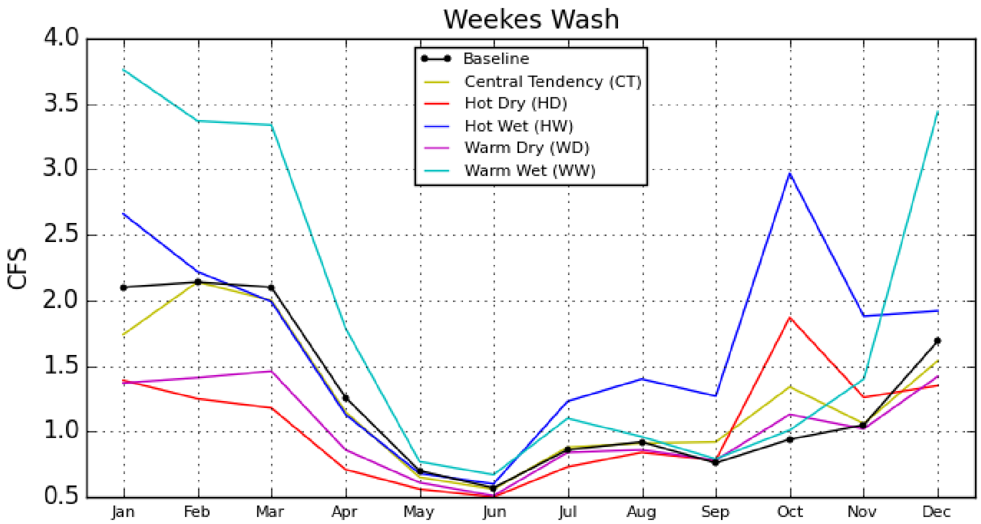


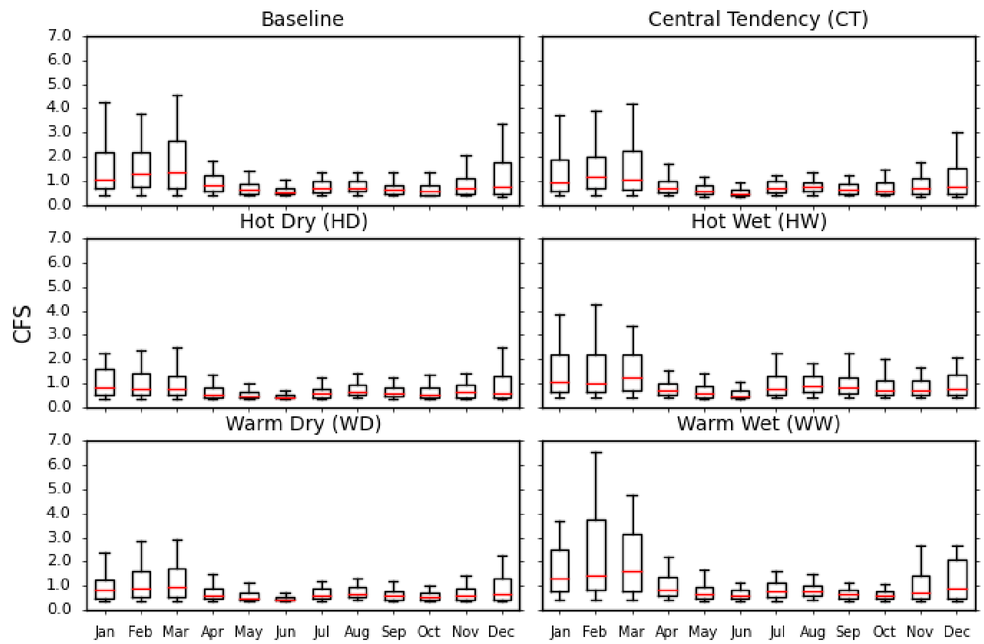


**Figure A14.—Monthly averages of streamflow for the baseline and five HDe climate change scenario simulations for the Weekes Wash site shown in Figure 1.**

# Appendix B. Demands Summary Tables

Table B-1.—Summary of HUC8 Sub-basin Average Annual Historical Baseline and Projected Future Temperatures and Projected Future Average Annual Change in Temperature

| HUC8 | Average Annual Temperature (°F) | | | | | | Change in Temperature (°F) | | | | |
|---|---|---|---|---|---|---|---|---|---|---|---|
| Sub-basin | Baseline | WD | WW | HD | HW | CT | WD | WW | HD | HW | CT |
| 15040001 | 53.1 | 55.5 | 55.4 | 56.5 | 56.4 | 56.0 | 2.4 | 2.2 | 3.4 | 3.3 | 2.8 |
| 15040002 | 63.0 | 66.4 | 66.4 | 68.0 | 67.8 | 67.1 | 3.3 | 3.3 | 5.0 | 4.8 | 4.1 |
| 15040003 | 60.3 | 63.8 | 63.6 | 65.4 | 65.2 | 64.5 | 3.5 | 3.3 | 5.1 | 4.9 | 4.2 |
| 15040004 | 64.7 | 67.5 | 67.5 | 68.6 | 68.5 | 68.0 | 2.8 | 2.9 | 3.9 | 3.8 | 3.4 |
| 15040005 | 63.0 | 66.4 | 66.4 | 68.0 | 67.8 | 67.1 | 3.3 | 3.3 | 5.0 | 4.8 | 4.1 |
| 15040006 | 62.3 | 65.9 | 65.7 | 67.6 | 67.4 | 66.6 | 3.6 | 3.3 | 5.3 | 5.1 | 4.3 |
| 15040007 | 63.4 | 66.4 | 66.3 | 67.8 | 67.6 | 67.0 | 3.1 | 3.0 | 4.4 | 4.2 | 3.6 |
| 15050100 | 69.8 | 73.3 | 73.1 | 74.9 | 74.7 | 73.9 | 3.5 | 3.4 | 5.1 | 5.0 | 4.2 |
| 15050201 | 60.4 | 63.7 | 63.7 | 65.1 | 65.0 | 64.3 | 3.2 | 3.2 | 4.7 | 4.5 | 3.8 |
| 15050202 | 60.8 | 64.2 | 64.1 | 66.1 | 66.0 | 65.0 | 3.4 | 3.3 | 5.4 | 5.2 | 4.3 |
| 15050203 | 64.3 | 67.1 | 67.1 | 68.4 | 68.3 | 67.7 | 2.8 | 2.7 | 4.1 | 3.9 | 3.4 |
| 15050301 | 68.6 | 72.1 | 71.9 | 73.7 | 73.5 | 72.7 | 3.5 | 3.3 | 5.1 | 4.9 | 4.1 |
| 15050303 | 70.3 | 73.9 | 73.6 | 75.4 | 75.3 | 74.5 | 3.5 | 3.3 | 5.1 | 5.0 | 4.1 |
| 15050304 | 70.6 | 73.6 | 73.6 | 75.1 | 75.0 | 74.2 | 3.0 | 3.0 | 4.5 | 4.4 | 3.7 |
| 15050306 | 70.5 | 74.0 | 73.7 | 75.6 | 75.4 | 74.6 | 3.6 | 3.3 | 5.1 | 4.9 | 4.1 |
| 15060101 | 59.6 | 63.2 | 62.7 | 64.5 | 64.3 | 63.7 | 3.6 | 3.1 | 4.9 | 4.7 | 4.1 |
| 15060103 | 64.9 | 67.7 | 67.6 | 69.0 | 68.9 | 68.2 | 2.8 | 2.7 | 4.1 | 4.0 | 3.4 |
| 15060105 | 62.5 | 65.8 | 65.9 | 67.7 | 67.8 | 66.8 | 3.4 | 3.4 | 5.2 | 5.3 | 4.3 |
| 15060201 | 62.5 | 65.8 | 65.9 | 67.7 | 67.8 | 66.8 | 3.4 | 3.4 | 5.2 | 5.3 | 4.3 |
| 15060202 | 55.2 | 58.5 | 58.5 | 60.3 | 60.3 | 59.4 | 3.4 | 3.3 | 5.1 | 5.1 | 4.2 |
| 15070101 | 73.1 | 76.5 | 76.3 | 78.0 | 77.9 | 77.1 | 3.4 | 3.2 | 4.9 | 4.8 | 4.0 |
| 15070102 | 71.0 | 74.5 | 74.3 | 76.2 | 76.1 | 75.2 | 3.6 | 3.4 | 5.3 | 5.1 | 4.2 |
| 15070104 | 66.3 | 69.7 | 69.5 | 71.3 | 71.2 | 70.4 | 3.4 | 3.2 | 5.0 | 4.9 | 4.0 |
| Total Basin | 63.7 | 66.9 | 66.8 | 68.4 | 68.3 | 67.5 | 3.2 | 3.1 | 4.6 | 4.5 | 3.8 |
| Maximum | 73.1 | 76.5 | 76.3 | 78.0 | 77.9 | 77.1 | 3.6 | 3.4 | 5.4 | 5.3 | 4.3 |
| Minimum | 53.1 | 55.5 | 55.4 | 56.5 | 56.4 | 56.0 | 2.4 | 2.2 | 3.4 | 3.3 | 2.8 |

Table B-2.—Summary of HUC8 Sub-basin Average Annual Historical Baseline and Projected Future Precipitation, Projected Future Average Annual Change in Precipitation and Percent Change in Precipitation

| HUC8 | Average Annual Precipitation (inches) | | | | | | Change in Precipitation (inches) | | | | | Percent Change in Precipitation (%) | | | | |
|---|---|---|---|---|---|---|---|---|---|---|---|---|---|---|---|---|
| Sub-basin | Baseline | WD | WW | HD | HW | CT | WD | WW | HD | HW | CT | WD | WW | HD | HW | CT |
| 15040001 | 15.6 | 14.1 | 16.3 | 13.8 | 16.0 | 15.1 | -1.4 | 0.7 | -1.7 | 0.4 | -0.4 | -9.1% | 4.6% | -11.2% | 2.8% | -2.8% |
| 15040002 | 9.4 | 8.7 | 9.8 | 8.3 | 9.7 | 9.2 | -0.8 | 0.4 | -1.1 | 0.3 | -0.2 | -8.3% | 4.1% | -12.1% | 2.7% | -2.4% |
| 15040003 | 11.3 | 10.5 | 11.9 | 10.1 | 11.8 | 11.1 | -0.8 | 0.6 | -1.2 | 0.5 | -0.2 | -7.1% | 5.6% | -10.7% | 4.1% | -1.4% |
| 15040004 | 13.5 | 12.2 | 13.9 | 11.7 | 13.6 | 13.0 | -1.3 | 0.4 | -1.9 | 0.1 | -0.5 | -9.4% | 3.3% | -13.7% | 0.9% | -3.7% |
| 15040005 | 9.4 | 8.7 | 9.8 | 8.3 | 9.7 | 9.2 | -0.8 | 0.4 | -1.1 | 0.3 | -0.2 | -8.3% | 4.1% | -12.1% | 2.7% | -2.4% |
| 15040006 | 11.4 | 10.4 | 12.0 | 10.0 | 11.8 | 11.1 | -1.0 | 0.6 | -1.4 | 0.4 | -0.3 | -8.6% | 4.9% | -12.2% | 3.8% | -2.6% |
| 15040007 | 19.4 | 17.3 | 19.9 | 16.1 | 19.5 | 18.2 | -2.1 | 0.5 | -3.3 | 0.1 | -1.2 | -11.0% | 2.7% | -17.0% | 0.4% | -6.2% |
| 15050100 | 8.7 | 7.8 | 9.1 | 7.4 | 9.0 | 8.3 | -0.9 | 0.4 | -1.3 | 0.3 | -0.4 | -10.6% | 4.5% | -15.3% | 4.0% | -4.9% |
| 15050201 | 12.7 | 11.7 | 13.3 | 11.1 | 13.2 | 12.3 | -1.0 | 0.5 | -1.6 | 0.4 | -0.4 | -8.2% | 4.2% | -12.8% | 3.5% | -3.2% |
| 15050202 | 13.2 | 11.8 | 13.8 | 11.4 | 14.1 | 12.6 | -1.4 | 0.7 | -1.7 | 0.9 | -0.6 | -10.3% | 5.0% | -13.2% | 7.1% | -4.3% |
| 15050203 | 13.8 | 12.5 | 14.3 | 12.0 | 14.4 | 13.3 | -1.3 | 0.5 | -1.9 | 0.6 | -0.5 | -9.2% | 3.6% | -13.4% | 4.1% | -3.6% |
| 15050301 | 12.9 | 11.8 | 13.4 | 11.1 | 13.5 | 12.3 | -1.2 | 0.4 | -1.9 | 0.6 | -0.6 | -9.0% | 3.4% | -14.4% | 4.3% | -4.9% |
| 15050303 | 8.8 | 7.9 | 9.2 | 7.4 | 9.0 | 8.3 | -0.9 | 0.4 | -1.4 | 0.3 | -0.5 | -10.2% | 4.7% | -15.6% | 2.9% | -5.5% |
| 15050304 | 10.8 | 9.6 | 11.0 | 9.1 | 11.0 | 10.2 | -1.1 | 0.2 | -1.7 | 0.2 | -0.6 | -10.6% | 2.0% | -15.8% | 2.1% | -5.3% |
| 15050306 | 9.0 | 8.1 | 9.4 | 7.5 | 9.2 | 8.5 | -0.9 | 0.4 | -1.4 | 0.3 | -0.5 | -10.1% | 4.8% | -16.0% | 2.9% | -5.9% |
| 15060101 | 11.2 | 10.2 | 12.0 | 9.9 | 11.8 | 11.0 | -1.0 | 0.7 | -1.3 | 0.5 | -0.3 | -8.9% | 6.3% | -12.0% | 4.5% | -2.2% |
| 15060103 | 18.3 | 16.4 | 18.8 | 15.9 | 18.7 | 17.5 | -1.8 | 0.6 | -2.4 | 0.4 | -0.8 | -10.1% | 3.1% | -13.1% | 2.3% | -4.2% |
| 15060105 | 14.8 | 13.5 | 15.2 | 13.0 | 15.6 | 14.2 | -1.2 | 0.5 | -1.8 | 0.8 | -0.5 | -8.3% | 3.1% | -12.3% | 5.7% | -3.6% |
| 15060201 | 14.8 | 13.5 | 15.2 | 13.0 | 15.6 | 14.2 | -1.2 | 0.5 | -1.8 | 0.8 | -0.5 | -8.3% | 3.1% | -12.3% | 5.7% | -3.6% |
| 15060202 | 12.8 | 11.5 | 13.4 | 11.1 | 13.5 | 12.2 | -1.3 | 0.6 | -1.7 | 0.7 | -0.6 | -10.2% | 4.6% | -13.4% | 5.2% | -4.7% |
| 15070101 | 6.7 | 5.9 | 7.0 | 5.4 | 6.9 | 6.2 | -0.9 | 0.3 | -1.3 | 0.2 | -0.5 | -12.9% | 4.1% | -19.1% | 3.0% | -7.7% |
| 15070102 | 8.6 | 7.7 | 9.2 | 7.2 | 9.1 | 8.2 | -0.9 | 0.6 | -1.3 | 0.5 | -0.4 | -10.4% | 7.1% | -15.6% | 6.3% | -4.1% |
| 15070104 | 8.2 | 7.5 | 8.7 | 7.1 | 8.8 | 7.9 | -0.7 | 0.5 | -1.1 | 0.6 | -0.3 | -9.0% | 5.6% | -13.6% | 7.2% | -3.9% |
| Total Basin | 14.7 | 13.3 | 15.2 | 12.7 | 15.2 | 14.1 | -1.4 | 0.5 | -2.0 | 0.5 | -0.6 | -9.6% | 3.6% | -13.3% | 3.2% | -4.1% |
| Maximum | 19.4 | 17.3 | 19.9 | 16.1 | 19.5 | 18.2 | -0.7 | 0.7 | -1.1 | 0.9 | -0.2 | -7.1% | 7.1% | -10.7% | 7.2% | -1.4% |
| Minimum | 6.7 | 5.9 | 7.0 | 5.4 | 6.9 | 6.2 | -2.1 | 0.2 | -3.3 | 0.1 | -1.2 | -12.9% | 2.0% | -19.1% | 0.4% | -7.7% |

Table B-3.—Summary of HUC8 Sub-basin Average Annual Historical Baseline and Projected Future Reference Evapotranspiration (ET), Projected Future Average Annual Change in Reference ET and Percent Change in Reference ET

| HUC8 | Average Annual Reference ET (inches) | | | | | | Change in Reference ET (inches) | | | | | Percent Change in Reference ET (%) | | | | |
|---|---|---|---|---|---|---|---|---|---|---|---|---|---|---|---|---|
| Sub-basin | Baseline | WD | WW | HD | HW | CT | WD | WW | HD | HW | CT | WD | WW | HD | HW | CT |
| 15040001 | 66.9 | 69.2 | 69.0 | 70.1 | 69.9 | 69.5 | 2.3 | 2.1 | 3.2 | 3.0 | 2.6 | 3.4% | 3.2% | 4.8% | 4.5% | 4.0% |
| 15040002 | 73.4 | 76.4 | 76.4 | 77.9 | 77.7 | 77.1 | 3.0 | 3.0 | 4.5 | 4.4 | 3.7 | 4.1% | 4.2% | 6.1% | 5.9% | 5.1% |
| 15040003 | 71.6 | 74.7 | 74.6 | 76.1 | 75.9 | 75.3 | 3.2 | 3.0 | 4.5 | 4.4 | 3.7 | 4.4% | 4.2% | 6.3% | 6.1% | 5.2% |
| 15040004 | 72.4 | 74.9 | 74.9 | 75.8 | 75.7 | 75.4 | 2.4 | 2.5 | 3.4 | 3.3 | 2.9 | 3.4% | 3.4% | 4.7% | 4.5% | 4.0% |
| 15040005 | 73.4 | 76.4 | 76.4 | 77.9 | 77.7 | 77.1 | 3.0 | 3.0 | 4.5 | 4.4 | 3.7 | 4.1% | 4.2% | 6.1% | 5.9% | 5.1% |
| 15040006 | 71.3 | 74.4 | 74.2 | 75.9 | 75.7 | 75.0 | 3.2 | 3.0 | 4.6 | 4.5 | 3.8 | 4.5% | 4.2% | 6.5% | 6.3% | 5.3% |
| 15040007 | 65.9 | 68.4 | 68.3 | 69.4 | 69.3 | 68.8 | 2.4 | 2.4 | 3.5 | 3.3 | 2.8 | 3.7% | 3.6% | 5.3% | 5.0% | 4.3% |
| 15050100 | 76.9 | 80.0 | 79.8 | 81.3 | 81.2 | 80.5 | 3.0 | 2.9 | 4.3 | 4.2 | 3.5 | 3.9% | 3.8% | 5.6% | 5.5% | 4.6% |
| 15050201 | 72.3 | 75.2 | 75.3 | 76.6 | 76.4 | 75.8 | 3.0 | 3.0 | 4.3 | 4.2 | 3.5 | 4.1% | 4.1% | 5.9% | 5.8% | 4.9% |
| 15050202 | 71.6 | 74.7 | 74.7 | 76.5 | 76.3 | 75.5 | 3.1 | 3.1 | 4.9 | 4.7 | 3.9 | 4.3% | 4.3% | 6.8% | 6.6% | 5.4% |
| 15050203 | 75.1 | 77.6 | 77.6 | 78.8 | 78.6 | 78.2 | 2.5 | 2.5 | 3.7 | 3.5 | 3.1 | 3.3% | 3.3% | 4.9% | 4.7% | 4.1% |
| 15050301 | 75.2 | 78.2 | 78.0 | 79.5 | 79.3 | 78.7 | 3.0 | 2.8 | 4.3 | 4.1 | 3.4 | 3.9% | 3.8% | 5.7% | 5.5% | 4.6% |
| 15050303 | 77.6 | 80.6 | 80.4 | 81.9 | 81.8 | 81.1 | 3.0 | 2.8 | 4.3 | 4.2 | 3.5 | 3.9% | 3.6% | 5.6% | 5.4% | 4.5% |
| 15050304 | 79.2 | 81.9 | 81.9 | 83.2 | 83.1 | 82.4 | 2.7 | 2.7 | 4.0 | 3.9 | 3.2 | 3.4% | 3.4% | 5.0% | 4.9% | 4.0% |
| 15050306 | 77.7 | 80.7 | 80.5 | 81.9 | 81.8 | 81.2 | 3.0 | 2.8 | 4.3 | 4.2 | 3.5 | 3.9% | 3.6% | 5.5% | 5.4% | 4.5% |
| 15060101 | 71.0 | 74.3 | 73.9 | 75.6 | 75.4 | 74.8 | 3.3 | 2.9 | 4.6 | 4.3 | 3.8 | 4.7% | 4.1% | 6.4% | 6.1% | 5.3% |
| 15060103 | 68.9 | 71.2 | 71.1 | 72.2 | 72.1 | 71.6 | 2.3 | 2.2 | 3.3 | 3.2 | 2.7 | 3.3% | 3.2% | 4.8% | 4.7% | 3.9% |
| 15060105 | 59.2 | 61.5 | 61.6 | 62.8 | 62.9 | 62.2 | 2.4 | 2.4 | 3.6 | 3.7 | 3.0 | 4.0% | 4.1% | 6.2% | 6.2% | 5.1% |
| 15060201 | 59.2 | 61.5 | 61.6 | 62.8 | 62.9 | 62.2 | 2.4 | 2.4 | 3.6 | 3.7 | 3.0 | 4.0% | 4.1% | 6.2% | 6.2% | 5.1% |
| 15060202 | 62.5 | 65.4 | 65.4 | 66.8 | 66.8 | 66.1 | 2.9 | 2.9 | 4.3 | 4.3 | 3.6 | 4.6% | 4.6% | 6.9% | 6.9% | 5.8% |
| 15070101 | 77.2 | 80.1 | 79.9 | 81.3 | 81.2 | 80.6 | 2.9 | 2.6 | 4.1 | 4.0 | 3.3 | 3.7% | 3.4% | 5.3% | 5.2% | 4.3% |
| 15070102 | 76.4 | 79.3 | 79.2 | 80.7 | 80.6 | 79.8 | 3.0 | 2.8 | 4.4 | 4.2 | 3.5 | 3.9% | 3.7% | 5.7% | 5.5% | 4.5% |
| 15070104 | 76.2 | 79.3 | 79.1 | 80.6 | 80.6 | 79.8 | 3.0 | 2.9 | 4.4 | 4.3 | 3.6 | 4.0% | 3.8% | 5.8% | 5.7% | 4.7% |
| Total Basin | 69.1 | 71.8 | 71.7 | 73.0 | 72.9 | 72.3 | 2.6 | 2.6 | 3.8 | 3.7 | 3.1 | 3.8% | 3.7% | 5.5% | 5.4% | 4.5% |
| Maximum | 79.2 | 81.9 | 81.9 | 83.2 | 83.1 | 82.4 | 3.3 | 3.1 | 4.9 | 4.7 | 3.9 | 4.7% | 4.6% | 6.9% | 6.9% | 5.8% |
| Minimum | 59.2 | 61.5 | 61.6 | 62.8 | 62.9 | 62.2 | 2.3 | 2.1 | 3.2 | 3.0 | 2.6 | 3.3% | 3.2% | 4.7% | 4.5% | 3.9% |

Table B-4.—Summary of HUC8 Sub-basin Average Annual Historical Baseline and Projected Future Crop Evapotranspiration (ET), Projected Future Average Annual Change in Crop ET and Percent Change in Crop ET

| HUC8 | Average Annual Crop ET (inches) | | | | | | Change in Crop ET (inches) | | | | | Percent Change in Crop ET (%) | | | | |
|---|---|---|---|---|---|---|---|---|---|---|---|---|---|---|---|---|
| Sub-basin | Baseline | WD | WW | HD | HW | CT | WD | WW | HD | HW | CT | WD | WW | HD | HW | CT |
| 15040001 | 47.7 | 50.8 | 51.1 | 51.9 | 52.3 | 51.5 | 3.0 | 3.4 | 4.1 | 4.5 | 3.8 | 6.4% | 7.1% | 8.7% | 9.5% | 7.9% |
| 15040002 | 51.6 | 54.1 | 54.5 | 55.3 | 55.5 | 54.9 | 2.5 | 2.9 | 3.7 | 4.0 | 3.3 | 4.8% | 5.6% | 7.1% | 7.7% | 6.4% |
| 15040003 | 60.3 | 63.3 | 63.5 | 64.6 | 64.9 | 64.1 | 3.0 | 3.2 | 4.3 | 4.5 | 3.7 | 5.0% | 5.3% | 7.1% | 7.5% | 6.2% |
| 15040004 | 62.2 | 64.4 | 64.7 | 65.3 | 65.6 | 65.0 | 2.2 | 2.5 | 3.1 | 3.4 | 2.9 | 3.5% | 4.0% | 5.0% | 5.5% | 4.6% |
| 15040005 | 45.6 | 47.1 | 47.4 | 47.7 | 48.2 | 47.6 | 1.5 | 1.8 | 2.1 | 2.6 | 2.0 | 3.3% | 4.0% | 4.6% | 5.6% | 4.4% |
| 15040006 | 52.0 | 55.0 | 55.3 | 56.3 | 56.8 | 55.9 | 3.0 | 3.4 | 4.3 | 4.8 | 3.9 | 5.8% | 6.4% | 8.3% | 9.3% | 7.5% |
| 15040007 | 50.5 | 53.1 | 53.4 | 54.3 | 54.5 | 53.7 | 2.6 | 2.9 | 3.7 | 4.0 | 3.2 | 5.1% | 5.8% | 7.4% | 8.0% | 6.4% |
| 15050100 | 55.3 | 57.1 | 57.3 | 57.9 | 58.3 | 57.6 | 1.8 | 2.0 | 2.6 | 3.0 | 2.3 | 3.2% | 3.5% | 4.8% | 5.4% | 4.1% |
| 15050201 | 47.1 | 49.6 | 50.1 | 50.7 | 51.3 | 50.4 | 2.5 | 3.0 | 3.7 | 4.2 | 3.3 | 5.3% | 6.5% | 7.8% | 9.0% | 7.0% |
| 15050202 | 46.0 | 48.6 | 49.4 | 50.5 | 51.3 | 49.7 | 2.6 | 3.4 | 4.5 | 5.3 | 3.8 | 5.7% | 7.4% | 9.9% | 11.5% | 8.2% |
| 15050203 | 52.8 | 55.1 | 55.9 | 56.4 | 57.2 | 56.2 | 2.3 | 3.1 | 3.7 | 4.4 | 3.4 | 4.4% | 5.9% | 6.9% | 8.4% | 6.5% |
| 15050301 | 49.2 | 51.4 | 51.8 | 50.9 | 53.0 | 52.1 | 2.2 | 2.5 | 1.7 | 3.8 | 2.9 | 4.4% | 5.2% | 3.4% | 7.7% | 5.8% |
| 15050303 | 50.4 | 51.8 | 52.0 | 52.3 | 52.7 | 52.2 | 1.4 | 1.6 | 1.9 | 2.3 | 1.8 | 2.7% | 3.1% | 3.7% | 4.6% | 3.5% |
| 15050304 | 45.5 | 46.3 | 46.7 | 46.8 | 47.3 | 46.8 | 0.8 | 1.2 | 1.2 | 1.8 | 1.3 | 1.8% | 2.7% | 2.7% | 3.9% | 2.8% |
| 15050306 | 50.6 | 51.9 | 52.2 | 52.4 | 52.9 | 52.3 | 1.4 | 1.6 | 1.9 | 2.3 | 1.8 | 2.8% | 3.2% | 3.7% | 4.6% | 3.5% |
| 15060101 | 47.8 | 52.0 | 51.9 | 53.3 | 53.6 | 52.6 | 4.2 | 4.1 | 5.5 | 5.8 | 4.9 | 8.8% | 8.7% | 11.5% | 12.1% | 10.2% |
| 15060103 | 52.1 | 54.3 | 54.5 | 55.4 | 55.6 | 55.0 | 2.3 | 2.4 | 3.4 | 3.6 | 2.9 | 4.3% | 4.7% | 6.4% | 6.9% | 5.6% |
| 15060105 | 43.6 | 46.3 | 46.5 | 47.5 | 47.8 | 46.9 | 2.6 | 2.9 | 3.9 | 4.2 | 3.3 | 6.1% | 6.6% | 9.0% | 9.6% | 7.5% |
| 15060201 | 48.5 | 51.2 | 51.5 | 52.7 | 53.0 | 51.9 | 2.8 | 3.0 | 4.2 | 4.5 | 3.5 | 5.7% | 6.2% | 8.7% | 9.3% | 7.2% |
| 15060202 | 45.5 | 49.7 | 49.9 | 52.0 | 52.2 | 50.9 | 4.2 | 4.4 | 6.5 | 6.7 | 5.4 | 9.3% | 9.7% | 14.3% | 14.7% | 11.8% |
| 15070101 | 54.2 | 55.9 | 56.0 | 56.6 | 56.9 | 56.3 | 1.6 | 1.8 | 2.4 | 2.6 | 2.0 | 3.0% | 3.3% | 4.3% | 4.8% | 3.7% |
| 15070102 | 54.9 | 56.7 | 56.9 | 57.5 | 57.8 | 57.2 | 1.8 | 2.0 | 2.6 | 2.9 | 2.3 | 3.3% | 3.7% | 4.8% | 5.3% | 4.2% |
| 15070104 | 58.4 | 60.7 | 60.8 | 61.7 | 62.0 | 61.3 | 2.3 | 2.4 | 3.3 | 3.6 | 2.9 | 3.9% | 4.0% | 5.7% | 6.2% | 4.9% |
| Total Basin | 50.1 | 52.6 | 52.8 | 53.7 | 54.1 | 53.3 | 2.5 | 2.8 | 3.6 | 4.0 | 3.2 | 5.1% | 5.5% | 7.3% | 8.0% | 6.4% |
| Maximum | 62.2 | 64.4 | 64.7 | 65.3 | 65.6 | 65.0 | 4.2 | 4.4 | 6.5 | 6.7 | 5.4 | 9.3% | 9.7% | 14.3% | 14.7% | 11.8% |
| Minimum | 43.6 | 46.3 | 46.5 | 46.8 | 47.3 | 46.8 | 0.8 | 1.2 | 1.2 | 1.8 | 1.3 | 1.8% | 2.7% | 2.7% | 3.9% | 2.8% |

Table B-5.—Summary of HUC8 Sub-basin Average Annual Historical Baseline and Projected Future Net Irrigation Water Requirement (NIWR) Depth, Projected Future Average Annual Change in NIWR Depth and Percent Change in NIWR Depth

| HUC8 | Average Annual NIWR Depth (inches) | | | | | | Change in NIWR Depth (inches) | | | | | Percent Change in NIWR Depth (%) | | | | |
|---|---|---|---|---|---|---|---|---|---|---|---|---|---|---|---|---|
| Sub-basin | Baseline | WD | WW | HD | HW | CT | WD | WW | HD | HW | CT | WD | WW | HD | HW | CT |
| 15040001 | 34.3 | 38.3 | 37.2 | 39.6 | 38.4 | 38.4 | 4.0 | 2.9 | 5.3 | 4.1 | 4.1 | 11.7% | 8.4% | 15.6% | 12.0% | 11.9% |
| 15040002 | 42.7 | 45.8 | 45.3 | 47.4 | 46.4 | 46.1 | 3.2 | 2.7 | 4.7 | 3.7 | 3.5 | 7.4% | 6.2% | 11.1% | 8.8% | 8.1% |
| 15040003 | 49.1 | 52.9 | 51.9 | 54.5 | 53.3 | 53.1 | 3.8 | 2.8 | 5.4 | 4.2 | 3.9 | 7.6% | 5.7% | 11.0% | 8.5% | 8.0% |
| 15040004 | 49.9 | 53.0 | 52.0 | 54.3 | 53.1 | 53.1 | 3.1 | 2.1 | 4.4 | 3.2 | 3.2 | 6.1% | 4.2% | 8.8% | 6.3% | 6.4% |
| 15040005 | 36.6 | 38.8 | 38.2 | 39.7 | 39.0 | 38.9 | 2.2 | 1.6 | 3.1 | 2.3 | 2.3 | 6.1% | 4.3% | 8.5% | 6.4% | 6.2% |
| 15040006 | 41.3 | 45.1 | 44.3 | 46.6 | 45.7 | 45.5 | 3.8 | 3.0 | 5.4 | 4.5 | 4.2 | 9.3% | 7.3% | 13.0% | 10.8% | 10.3% |
| 15040007 | 35.9 | 38.9 | 37.7 | 40.7 | 38.6 | 38.9 | 3.0 | 1.9 | 4.9 | 2.8 | 3.0 | 8.4% | 5.3% | 13.6% | 7.8% | 8.4% |
| 15050100 | 47.3 | 49.8 | 49.1 | 51.0 | 50.1 | 50.0 | 2.5 | 1.9 | 3.8 | 2.8 | 2.7 | 5.3% | 3.9% | 7.9% | 6.0% | 5.8% |
| 15050201 | 35.4 | 38.8 | 38.1 | 40.4 | 39.3 | 39.1 | 3.3 | 2.7 | 5.0 | 3.9 | 3.7 | 9.4% | 7.5% | 14.0% | 10.9% | 10.5% |
| 15050202 | 33.8 | 37.5 | 36.9 | 39.8 | 38.5 | 38.1 | 3.7 | 3.1 | 6.0 | 4.7 | 4.3 | 11.1% | 9.2% | 17.8% | 14.0% | 12.8% |
| 15050203 | 40.0 | 43.4 | 43.0 | 45.3 | 44.1 | 43.9 | 3.4 | 3.0 | 5.3 | 4.1 | 3.9 | 8.5% | 7.4% | 13.2% | 10.2% | 9.7% |
| 15050301 | 37.5 | 40.7 | 40.0 | 40.8 | 41.0 | 41.1 | 3.2 | 2.4 | 3.3 | 3.4 | 3.5 | 8.5% | 6.4% | 8.7% | 9.1% | 9.4% |
| 15050303 | 42.4 | 44.5 | 43.9 | 45.4 | 44.6 | 44.6 | 2.1 | 1.5 | 3.1 | 2.2 | 2.2 | 4.9% | 3.5% | 7.2% | 5.2% | 5.2% |
| 15050304 | 36.0 | 37.7 | 37.2 | 38.4 | 37.7 | 37.7 | 1.7 | 1.2 | 2.4 | 1.7 | 1.7 | 4.6% | 3.2% | 6.7% | 4.6% | 4.7% |
| 15050306 | 42.4 | 44.5 | 43.9 | 45.3 | 44.7 | 44.5 | 2.1 | 1.6 | 3.0 | 2.3 | 2.2 | 5.0% | 3.7% | 7.0% | 5.4% | 5.1% |
| 15060101 | 37.6 | 42.5 | 41.0 | 44.1 | 42.7 | 42.6 | 4.9 | 3.5 | 6.5 | 5.2 | 5.0 | 13.1% | 9.3% | 17.3% | 13.8% | 13.4% |
| 15060103 | 39.1 | 42.0 | 41.0 | 43.0 | 42.1 | 41.8 | 2.9 | 1.9 | 4.0 | 3.0 | 2.8 | 7.4% | 5.0% | 10.1% | 7.6% | 7.1% |
| 15060105 | 32.8 | 35.6 | 35.1 | 37.1 | 36.1 | 35.7 | 2.8 | 2.2 | 4.2 | 3.2 | 2.9 | 8.4% | 6.8% | 12.9% | 9.9% | 8.8% |
| 15060201 | 36.8 | 40.0 | 39.3 | 41.9 | 40.6 | 40.2 | 3.2 | 2.5 | 5.1 | 3.8 | 3.4 | 8.6% | 6.9% | 13.8% | 10.4% | 9.4% |
| 15060202 | 34.6 | 39.7 | 38.7 | 42.2 | 40.5 | 40.4 | 5.1 | 4.1 | 7.6 | 5.9 | 5.8 | 14.8% | 11.8% | 22.0% | 17.0% | 16.9% |
| 15070101 | 48.0 | 50.2 | 49.6 | 51.4 | 50.5 | 50.4 | 2.3 | 1.7 | 3.4 | 2.5 | 2.5 | 4.8% | 3.5% | 7.2% | 5.2% | 5.1% |
| 15070102 | 47.1 | 49.6 | 48.9 | 50.8 | 49.9 | 49.8 | 2.5 | 1.8 | 3.7 | 2.8 | 2.7 | 5.4% | 3.9% | 7.9% | 5.9% | 5.6% |
| 15070104 | 51.0 | 53.8 | 53.2 | 55.2 | 54.4 | 54.1 | 2.8 | 2.2 | 4.2 | 3.4 | 3.1 | 5.6% | 4.3% | 8.2% | 6.6% | 6.1% |
| Total Basin | 38.5 | 41.7 | 40.8 | 43.0 | 42.0 | 41.8 | 3.2 | 2.3 | 4.5 | 3.4 | 3.3 | 8.3% | 6.0% | 11.7% | 8.9% | 8.5% |
| Maximum | 51.0 | 53.8 | 53.2 | 55.2 | 54.4 | 54.1 | 5.1 | 4.1 | 7.6 | 5.9 | 5.8 | 14.8% | 11.8% | 22.0% | 17.0% | 16.9% |
| Minimum | 32.8 | 35.6 | 35.1 | 37.1 | 36.1 | 35.7 | 1.7 | 1.2 | 2.4 | 1.7 | 1.7 | 4.6% | 3.2% | 6.7% | 4.6% | 4.7% |